PREDICTION OF LARGE EARTHQUAKES USING PATTERN RECOGNITION METHOD AND CHAOS THEORY

BY

FOLASADE LUCIA ADEREMI

Matric No. 70611

B.Sc (Hons.) Physics (Ibadan), M.Sc. Physics (Lagos)

A Thesis in the Department of Physics Submitted to the Faculty of Science in partial fulfillment of the requirements for the Degree of

DOCTOR OF PHILOSOPIIY

of the

UNIVERSITY OF IBADAN

MAY 2014

ABSTRACT

The prediction of Large Earthquakes (LE) constitutes a global challenge. Several methods of earthquake prediction including Pattern Recognition (PR) have been proposed but sometimes produce patterns that are not suitable. Occurrence of earthquakes is always assumed to be random when these methods produce unreliable pattern. The fact that these patterns considered to be random could be chaotic (predictable but difficult) has not been investigated. This study was designed to use chaos theory to investigate patterns of occurrence of earthquakes where PR method gives unreliable pattern.

Earthquake data (1899-2009) of the Circum-Pacific seismic zone were extracted from the catalogue of Advanced National Seismic System (USA). The zone is the source of 90% of the world's earthquakes and the one with most recorded data. The zone was divided into five regions [Rl(Lat 55° to 67° ; Long -170° to -145°), R2(Lat 32° to 44° ; Long 134° to 148°), R3(Lat 39° to 50° ; Long 140° to 157°), R4(Lat -42° to -29° ; Long -80° to -66°), R5(Lat 48° to 54° ; Long -179° to -160°)] based on the pattern of occurrence of small earthquakes. Events in each region were divided into constant time intervals and annular width of 100 km for the investigation of temporal and spatial distribution of the earthquakes respectively. The PR method was applied to the data in each time interval and annular width, and the pattern monitored using seismic b-values and the locations of the maximum seismic energy. The b-values were determined from Gutenberg-Richter law using the linear curve fitting method, while the locations of the maximum seismic energy were determined using Compicat program. Using chaos theory, the phase space plots of the seismic activities were constructed to determine the space clustering of the seismic events associated with LE. The Lyapunov Exponent (LEX) and its spectrum were obtained using Wolf and Sprott procedures to provide a picture of the system's dynamics and determine whether it is random or chaotic.

The temporal and spatial variations of the b-values for all the regions were oscillatory but with variable periods, indicating unreliable patterns. The pattern of propagation of the maximum seismic energy was non-linear and appeared to be geometrically fractal. The phase space was densely filled with scattered points (chaotic trajectory) which showed that the occurrence of earthquakes had chaotic characteristics. The LEX was positive for all the regions, indicating the chaotic nature of the earthquakes occurrence. This was highest for R3 (LEX = 2.688) and lowest for R4 (LEX = 0.688). The LEX spectrum behaved asymptotically prior to the occurrence of the LE.

Chaos theory showed that unreliable pattern from Pattern Recognition method was chaotic. The asymptotic behaviour of the Lyapunov Exponent spectrum could be used as a precursor in seismic hazard management. Chaos theory should be incorporated into Pattern Recognition method for effective prediction of large earthquakes.

Keywords: Large Earthquake Prediction, Pattern Recognition, Chaos theory.

Word count: 469

CERTIFICATION

I certify that this work was carried out by Mrs. Folasade Lucia Aderemi in the Department of Physics, University of Ibadan

______________________________ ______________________

Dr. O.I. POPOOLA **DATE**

B.Sc (Hons.), M.Sc., Ph.D (Ibadan)
Senior Lecturer
Department of Physics
University of Ibadan

DEDICATION

This work is dedicated to the Almighty God, the source of all blessing.

ACKNOWLEDGEMENT

My special thanks and appreciation goes to the source and sustainer of my life, the Almighty God, my present help in time of trouble, for grace, strength and resources to complete this programme.

I appreciate with deep sincerity the support and guidance given to me by my supervisor, Dr. O.I. Popoola, for his painstaking efforts in making this research work a reality. Without his selfless counsel and encouragement the success of this work would have been impossible, your understanding and support is very highly appreciated. Thank you sir.

My profound appreciation goes to my beloved husband Caleb Olayiwola Aderemi for the encouragement, understanding, prayer and supports in all ramifications, ML there are many men of valour, but you excel all. To my wonderful children Princess Mercy and my two great men Oluwadamilare and Emmanuel, thank you for the understanding, words of encouragements and your prayers through out the duration of this programme.

I also want to acknowledge the concern and encouragement of the following people; the head of department, Dr. F.O. Ogundare, Prof I. P. Farai, Dr. A.T. Bolarinwa, Dr. J.A. Adegoke, Dr. E.F. Nymphas, Dr. E.O. Ogunsola, Dr. Bola Popoola, RCCG KEC brethren and all other lecturers in the department of Physics, I say thank you all.

Finally, I acknowledge the following organizations for their assistance; The Abdus Salam International Centre for Theoretical Physics Triseste, Italy.. Institute of Geophysics and Planetary Physics, Los Angeles U.S.A and International Institute of Earthquake Prediction, Theory and Mathematical Geophysics, Moscow RUSSIAN FEDERATION for CompiCat software. Advanced National Seismic System (ANSS), Northern California Earthquake Data Centre, USA, for earthquake catalogue.

TABLE OF CONTENTS

LIST OF TABLES

LIST OF FIGURES

CHAPTER ONE

INTRODUCTION

1.1 Meaning of Earthquake

Earthquake is defined as a sudden release of accumulated strain energy in a confined region of the Earth interior or along a fault or fracture in the earth's crust. Earthquakes are natural disaster that can not be controlled; it can be described as an experiment performed by nature. No earthquake has ever been directly observed.

The sudden movement within the crust or mantle creates concentric shock waves or seismic waves that move out from that point. This point of initial rupture is called its focus or hypocenter. Since this is often deep below the surface and difficult to map, the location of the earthquake is often referred to as the point on the Earth surface directly above the focus, this point is called the epicentre. If the epicentre is located near the sea then it can cause the creation of Tsunami waves. Earthquakes are measured with seismographs; the record of a seismograph is known as seismogram (Doyle, 1995; Yeats et al, 1997).

1.2 Earthquakes and Myth

Earthquakes have been around since the beginning of man and many different religions and cultures had their own way of explaining why earthquakes occur. Ancient societies often developed religious, diverse legends, myths and stories and animistic explanations of how and why earthquakes occur.

The ancient Greeks believed that their god Atlas was condemned by Zeus the king of the gods to bear the Earth on his shoulders. To ease this burden, Atlas sometimes shifted the world from one shoulder to the other, when he does the Earth shook or quakes, hence an earthquake.

The Hindus, who lived in India, believed that eight giant elephants gathered in a circle held the earth on their heads. An earthquake would happen when one of the elephants lowered its head out of weariness and shook it.

People in China explained earthquakes by saying that the Great Dragon, who lived deep inside the Earth, shook the ground when annoyed. According to Russian tales, a giant god travelled through the snow-covered fields by dogsled. The ground shook whenever the dogs scratched at their fleas. The Norse attributed earthquakes to subterranean writhing of the imprisoned god Loki in his vain attempt to avoid venom dripping from a serpent’s tooth.

The Maimas, an ancient Peruvian tribe, believed that earthquakes were caused by the footsteps of their god when he walked the earth to count the number of people on the earth, and to make the god's task easier, Maimas custom was to run out of their houses and shout, "I'm here, I'm here!" each time an earthquake occurred and whether they knew it or not, this was a wise course of action, since their houses were frail and could potentially have collapsed upon them.

The Japanese blamed earthquakes on a giant namazu, or catfish that lived underground or lived in the mud under the earth. Although its destructive activities were kept in check by a god named Kashima, sometimes Kashima would be distracted and the catfish would be free for a while to move about and cause earthquakes.

Hellenic mythology attributed the phenomenon to Poseidon, the god of the sea, perhaps because of the association of seismic shaking with tsunamis, which are common in the north-eastern Mediterranean.

Earthquakes were also connected with the movements of animals e.g. a mole or an elephant in India, an ox in Turkey, a hog in Mongolia, and a tortoise in Native America (Davison, 1978; Paige, 1999; Riper and Bowdoin, 2002; Hyndman and Hyndman, 2009 and USGS, 2010).

1.3 Earthquake and Science

Though the destructive force of earthquakes has stimulated human inquiry and curiosity since ancient times, the scientific study of earthquakes is relatively a recent development. Despite rapid progress in the latter part of the twentieth century, the study of earthquakes, like the science of many other complex natural systems, is still in the stage of exploration and discovery. Earthquakes occur as a result of different processes that are still not entirely described and understood (Peresan et al, 2007). An attempt to apply theory of dynamical systems to the analysis of earthquake behaviour in the solid Earth is limited because the response of rocks to stresses can be highly nonlinear. Moreover, because earthquake source regions are inaccessible and opaque, the state of the lithosphere at seismogenic depths simply cannot be observed by any direct means (Kossobokov, 2009).

Much remains to be learned about the physics and geology of earthquakes and many key questions remain to be answered. A comprehensive theory of earthquake that adequately describes the dynamical interactions among faults, physics of seismogenic process, as well as the basic or universal features of earthquake-like phenomena does not yet exist. The need for such a theory is the focus of basic research in solid earth (Sauber and Dwonska, 1999; Kanamori and Brodsky, 2004).

1.4 The Challenge of Earthquake Prediction

Because earthquakes can cause so much destruction, seismologists have looked for ways of predicting them so that people can move to safety before disaster strikes by proposing several methods of prediction such as seismic gap hypothesis, immediate alert, and pattern recognition. Unfortunately, no reliable system of earthquake prediction has yet been developed because no two quakes follow identical patterns (Worth, 2005).

Not all natural catastrophes are so apparently unpredictable like earthquake. The onset of some natural disaster can be predicted to some degree for instance, storms approaches, fire grow, flood migrate after large rainfalls but earthquakes occur almost suddenly without advance warning such that a perfectly normal day can be turn into disaster within seconds, Despite the global effort that has gone into the investigation of earthquakes, it still strike without any apparent or obvious warning, therefore earthquake prediction is still a global challenge because; The hypocenters of earthquakes are inaccessible and the state of the lithosphere at seismogenic depth can not be observed directly hence no earthquake has ever being observed directly (Kossobokov, 2009). The earth crust where most earthquakes occur is highly heterogeneous in distribution of strength and stored elastic strain energy. No satisfactory theory of earthquake source process exists at present (Geller 1997). Application of dynamics theory is limited because response of rocks to stress is highly complex and non linear. The interaction of faults is highly complex and non linear. The relationship is complex and may differ in seismogenic zones (Biagi, 1999). Laboratory and experimental models are conducted on a limited scale and do not replicate the complex and heterogeneous conditions of the problem or phenomenon in situ. Determining history of earthquakes is difficult in some areas because the historic record of such area is short compared with the average time between major earthquakes (Michael, 1999a). Because little is known about the physics of faulting many attempts to predict earthquakes have searched for precursors (Stein and Wysession, 2003).

Several precursors have been proposed such as: Foreshocks in Haicheng China (Suyehiro et al., 1964; IASPEI 1994); Seismic cycle (Fedotov, 1968); Seismic Doughnut (Mogi, 1969; 1979; 1981); Seismic quiescence; several cases in Japan (Gutenberg and Richter, 1965; IASPEI 1994); Radon concentration and temperature decrease in groundwater; Izu-Oshima-Kinkai 14/01/1978 M7.0 (Wakita et al, 1980; IASPEI 1994); Groundwater rise in well; Kettleman Hills, Californian M6.1 04/08/1985 (Roeloffs and Langbein, 1994; Roeloffs and Quilty, 1997).

However these precursors do not reproduce themselves (Scholz, 1990; Wyss, 1991 and Campbell, 1998). Lack of consistency in seismic precursors and inability to predict earthquake has made many seismologists to conclude that earthquake occurrence is stochastic and its prediction is a Gambler's fallacy (Geller, 1997).

The precursors were unrelated to earthquakes just like the beating of tom-tom drums and restoration of the sun after an eclipse are unrelated (Geller, 1999). The differing in observations completely implies that earthquake behaviour is random (Michael, 1999b). Occurrence of earthquakes is random, efforts at achieving deterministic prediction seem unwarranted (Geller et al, 1997; Michael, 1999b; Saegusa, 1999). Given that years of effort have led to no accepted precursors, there is no valid precursor (Michael, 1999a; Main, 1996, 1999).

An earthquake do not know how big it will become and from the canonical sandpile model, the earth is in a state of self organized criticality (SOC), hence earthquakes of any size can occur randomly anywhere at any time (Scholz, 1990).

For earthquake to be predicted or predictable there is a need to develop a physics based theory of the seismogenesis, nucleation and precursory process of the earthquake. The dynamic nature of earthquake must be clearly understood in a scientific method and manner, not just by speculation. There is the need to know and not assumed whether the occurrence of earthquake is periodic, chaotic or random in space and time.

1.5 Justification for Research

Earthquakes are natural disasters, the prediction of which constitutes a global challenge, especially Large Earthquakes, which are the most destructive. Several methods of earthquake prediction including Pattern Recognition, which is relatively new, have been proposed but sometimes these produce patterns that are not suitable for prediction (Wyss, 1997a; 1997b). Occurrence of earthquakes is always assumed to be random when these methods produce unreliable pattern (Geller, 1999; Michael, 1999b; Scholz, 1990 and Worth, 2005). The fact that these patterns considered to be random could be chaotic (predictable but difficult) has not been investigated. Also in previous works on pattern recognition, determination of b-values (a seismotectonic parameter) were mainly based on the use of surface wave magnitude (Ms) and body wave magnitude (Mb) which have the disadvantage of saturation instead of moment magnitude (Mw) that does not saturate.

Also, propagation trend of maximum radiated energy of earthquakes in a region were not investigated and chaos theory have not been applied to earthquake occurrence pattern.

1.6 Aim of the Research .

This study was designed to use chaos theory to investigate patterns of occurrence of earthquakes where Pattern Recognition method gives unreliable pattern.

1.7 Objectives of the Research

1) Identification of large earthquakes globally.

2) Modification of existing procedure for better result.

3) Determination of the pattern of seismotectonic parameters.

4) Investigating the phase space trajectory.

5) Investigating the divergence or convergence of its trajectory by determining the Lyapunov exponent.

CHAPTER TWO
LITERATURE REVIEW

2.1 The Structure of the Earth

The structure of the earth is divided into chemical or mechanical layers

Chemically, Earth can be divided into the crust, upper mantle, lower mantle, outer core, and inner core.

Mechanically; it can be divided into lithosphere, asthenosphere, mesosphere, outer core, and the inner core (Figure 2.1a and Figure 2.1b).

2.1.1 The Crust

The crust lies above the mantle and is the earth's hard outer shell, the surface on which we are living. In relation to the other layers, the crust is much thinner. It floats upon the softer, denser mantle. The crust is made up of solid material but these material is not everywhere the same, they are divisible into Oceanic and Continental crusts. The Oceanic crust underlies the ocean basins (5–10 km thick) and are composed of dense heavy rocks, like basalt (mafic; iron magnesium silicate rocks). The Continental crust is less dense and thicker than the Oceanic crust (about 30 km thick). It is mainly made up of light material composed of felsic, sodium potassium aluminium silicate rocks, like granite (Jordan, 1978; Herndon, 1980 and Wegener 1966; Jordan, 1979; Herndon, 2005).

2.1.2 The Mantle

The mantle begins about 10 km below the oceanic crust and about 30 km below the continental crust. It is divided into the upper mantle and the lower mantle. The Mantle extends to a depth of 2,890 km, making it the thickest layer of the Earth and makes up nearly 80 percent of the Earth's total volume. The pressure, at the bottom of the mantle, is about 140 GPa (1.4 Matm). The mantle is composed of silicate rocks that are rich in iron and magnesium relative to the overlying crust. Although solid, the high temperatures within the mantle cause the silicate material to be sufficiently ductile that it can flow on very long timescales. Convection of the mantle is expressed at the surface through the motions of tectonic plates. The melting point and viscosity of a substance depends on the prevailing pressure. As there is intense and increasing pressure as one travels deeper into the mantle, the lower part of the mantle flows less easily than does the upper mantle (chemical changes within the mantle may also be important). The viscosity of the mantle ranges between 1021 and 1024 Pa·s, depending on depth. In comparison, the viscosity of water is approximately 10^{-3} Pa·s and that of pitch is 107 Pa·s (Jordan, 1979; Herndon, 1980; Thomson and Jonathan, 1991; Tarbuck and Lutgens, 1996).

2.1.3 The Core

The inner part of the earth is the core. This part of the earth is about 2,900 km below the earth's surface. The core is a dense ball of the elements iron and nickel. Seismic measurements show that the core is divided into two layers, the inner core and the outer core.

The inner core - the centre of earth - is solid and about 1,250 km thick. The solid inner core was discovered in 1936 by Inge Lehmann and is generally believed to be composed primarily of iron and some nickel.

The outer core is so hot that the metal is always molten, but the inner core pressures are so great that it cannot melt, even though temperatures there reach 6700ºF (3700ºC). The outer core is about 2,200 km thick. Because the earth rotates, the outer core spins around the inner core and that causes the earth's magnetism. The solid inner core is too hot to hold a permanent magnetic field but probably acts to stabilize the magnetic field generated by the liquid outer core (Jordan, 1978; Herndon, 1980; Thomson and Jonathan, 1991; Tarbuck and Lutgens, 1996).

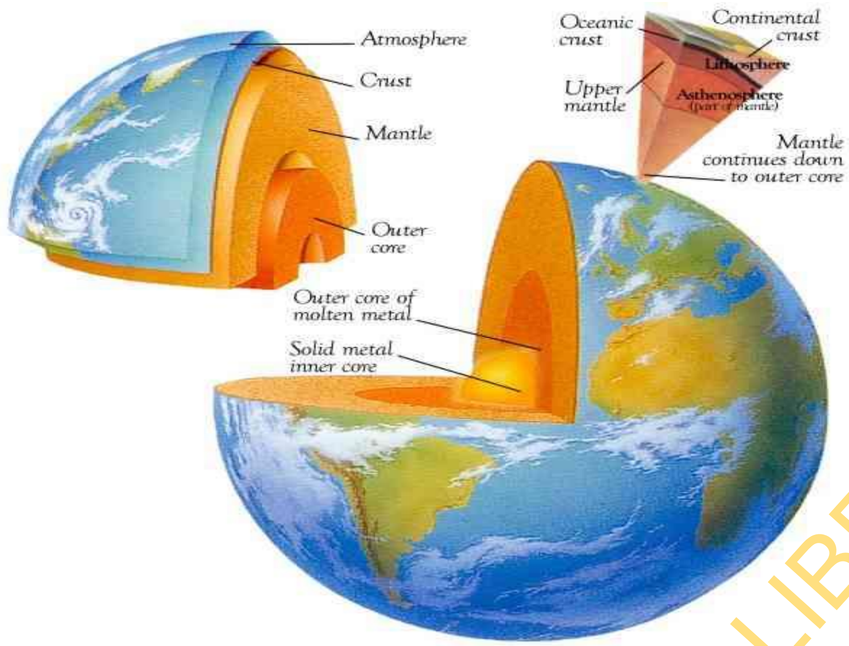

Fig 2.4a: The Structure of the Earth (After Kamland.Stanford.edu, 2014).

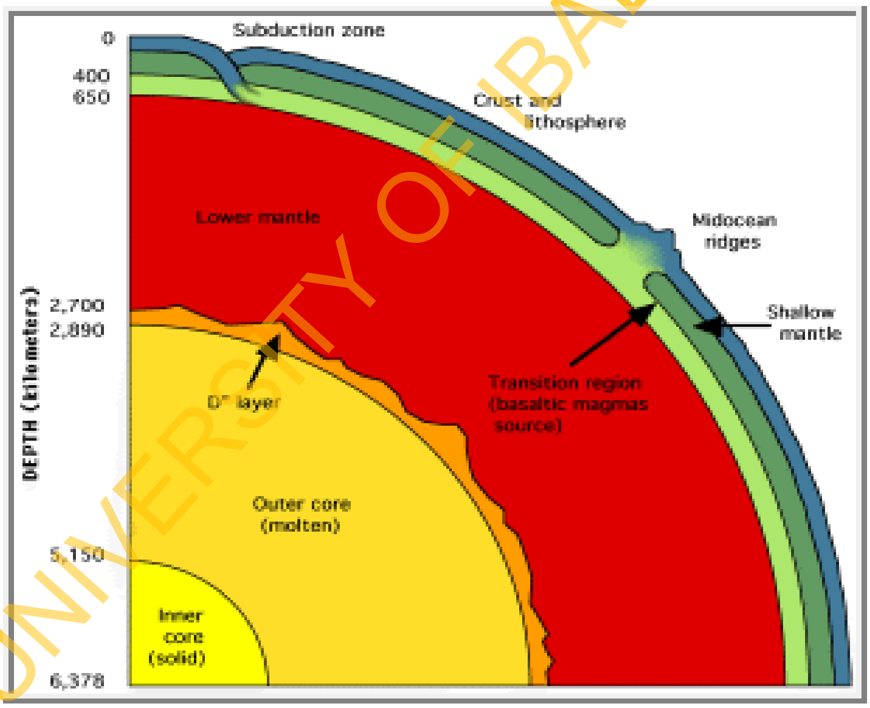

Fig 2.4b: The Structure of the Earth (After EZR, 2013).

2.1.4 Lithosphere

The lithosphere (cool and rigid), consist of the crust and the rigid uppermost part of the mantle, which constitute the hard and rigid outer layer of the planet. The lithosphere remains rigid for long periods of geologic time and deforms elastically and through brittle failure.

The lithosphere is underlain by the asthenosphere. The boundary between the lithosphere and the underlying asthenosphere is defined by a difference in response to stress. The lithosphere is broken up into what are called tectonic plates (Jordan, 1979; Herndon, 1980).

2.1.5 Types of lithosphere:

There are two types of lithosphere: Oceanic lithosphere, which is associated with Oceanic crust and Continental lithosphere, which is associated with Continental crust.

Oceanic lithosphere is typically about 50-100 km thick (but beneath the mid-ocean ridges is not thicker than the crust), while continental lithosphere has a range in thickness from about 40 km to 200 km; the upper 30 to 50 km of typical continental lithosphere is crust. The mantle part of the lithosphere consists largely of peridotite. The crust is distinguished from the upper mantle by the change in chemical composition that takes place at the Moho discontinuity. Oceanic lithosphere consists mainly of mafic crust and ultramafic mantle peridotite and is denser than continental lithosphere, for which the mantle is associated with crust made of felsic rocks. Oceanic lithosphere thickens as it ages and moves away from the mid-ocean ridge. This thickening occurs by conductive cooling, which converts hot asthenosphere into lithospheric mantle, and causes the oceanic lithosphere to become increasingly thick and dense with age.

Oceanic lithosphere is less dense than asthenosphere for a few tens of millions of years, but after this becomes increasingly denser than asthenosphere. This is because the chemically-differentiated oceanic crust is lighter than asthenosphere, but due to thermal contraction, the mantle lithosphere is denser than the asthenosphere. The gravitational instability of mature oceanic lithosphere has the effect that at subduction zones, oceanic lithosphere invariably sinks underneath the overriding lithosphere, which can be oceanic or continental. New oceanic lithosphere is constantly being produced at mid-ocean ridges and is recycled back to the mantle at subduction zones. As a result, oceanic lithosphere is much younger than continental lithosphere: the oldest oceanic lithosphere is about 170 million years old, while parts of the continental lithosphere are billions of years old.

The oldest parts of continental lithosphere underlie cratons, and the mantle lithosphere there is thicker and less dense than typical/usual. The relatively low density of such mantle roots of cratons helps to stabilize these regions (Jordan, 1979; O'Reilly, 2009; Daly, 1940; Barrell, 1914; Skinner and Porter, 1987).

2.1.6 Asthenosphere

The asthenosphere which means the weak sphere is the weak ductile-deforming region of the upper mantle of the Earth. It lies below the lithosphere, at depths between 100 and 200 km below the surface, but perhaps extending as deep as 400 km. It is the weaker, hotter, and deeper part of the upper mantle. Although solid, the asthenosphere has relatively low viscosity and shears strength and can flow like a liquid on geological time scales. The deeper mantle below the asthenosphere is more rigid again due to the higher pressure.

The asthenosphere is a portion of the upper mantle just below the lithosphere that is involved in plate movements and isostatic adjustments. In spite of its heat, pressures keep it plastic, and it has a relatively low density. Seismic waves pass relatively slowly through the asthenosphere, compared to the overlying lithospheric mantle, thus it has been called the low-velocity zone. This was the observation that originally alerted seismologists to its presence and gave some information about its physical properties, as the speed of seismic waves decreases with decreasing rigidity. Under the thin oceanic lithospheric plates the asthenosphere is usually much nearer the seafloor surface, and at mid-ocean ridges it rises to within a few kilometres of the ocean floor.

The upper part of the asthenosphere is believed to be the zone upon which the great rigid and brittle lithospheric plates of the Earth's crust move about. Due to the temperature and pressure conditions in the asthenosphere, rock becomes ductile, moving at rates of deformation measured in cm/yr over lineal distances eventually measuring thousands of kilometres. In this way, it flows like a convection current, radiating heat outward from the Earth's interior. While the asthenosphere deforms viscously and accommodates strain through plastic deformation, the lithosphere is broken into tectonic plates.

Above the asthenosphere, at the same rate of deformation, rock behaves elastically and, being brittle, can break, causing faults. The rigid lithosphere is thought to float or move about on the slowly flowing asthenosphere, creating the movement of crustal plates described by Plate tectonics theory (Turcotte and Schubert, 2002; McBride and Gilmour, 2004; Shearer, 2009).

2.2 Plate tectonics

Plate tectonics describes the large scale motions of the lithosphere. The theory of Plate tectonic arose out of the hypothesis of continental drift proposed by Alfred Wegener during the first decades of the 20th century (about 1912) and the concepts of seafloor spreading, which was understood during the 1960s.

2.3 Plate Tectonic Theory

The outer layer of the earth is divided into many sections known as plates, which are floating on the molten magma beneath the earth's crust. The movement of these plates is determined by the convection current in the molten magma. The heat makes these plates rise and vice versa. Therefore after intervals there are plates that get submerged in the molten magma and there are plates that rise upwards and at times even new crust is formed from the molten magma which in turn forms a new plate until it connects itself with the already existing ones. At times these plates can be pushed up to form mountains and hills and the movement is so slow that it is really hard to comprehend that there is any movement at all. The movement and the results come out to be visible suddenly. These plates are the bases on which the continents stand (Figure 2.2). When these plates move, the continents also move. Most of the earthquakes occur on the edges of the plates, where a plate is under another or across. This movement disrupts the balance and position of all plates, which leads to tremors or earthquakes (Holmes, 1978; Oreskes, 2003; Schubert et al, 2001; Toshiro and Thorne, 2000 and Stanley, 1999).

Tectonic plates are able to move because of the relative density of oceanic lithosphere and the relative weakness of the asthenosphere. Dissipation of heat from the mantle is acknowledged to be the original source of energy driving plate tectonics. The current view, although it is still a matter of some debate, is that excess density of the oceanic lithosphere sinking in subduction zones is the most powerful source of plate motion. When it forms at mid-ocean ridges, the oceanic lithosphere is initially less dense than the underlying asthenosphere, but it becomes denser with age, as it conductively cools and thickens. The greater density of old lithosphere relative to the underlying asthenosphere allows it to sink into the deep mantle at subduction zones, providing most of the driving force for plate motions. The weakness of the asthenosphere allows the tectonic plates to move easily towards a subduction zone. Although subduction is believed to be the strongest force driving plate motions, it cannot be the only force since there are plates such as the North American Plate which are moving, yet are not being subducted. The same is true for the enormous Eurasian Plate. The sources of plate motion are a matter of intensive research and discussion among earth scientists, there are eight major and many minor plates. The lithospheric plates ride on the asthenosphere and these plates move relative to one another at places called plate boundaries (Oreskes, 2003; Shearer, 2009).

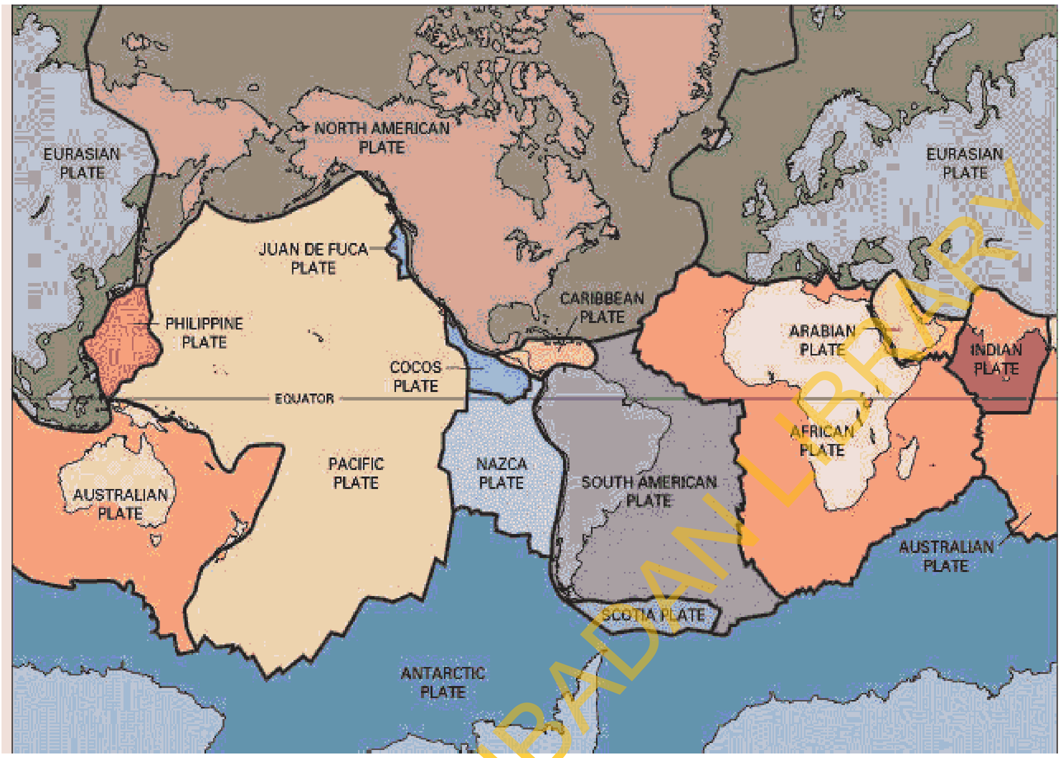

Figure 2.2: The tectonic plates of the world (after USGS, 2010).

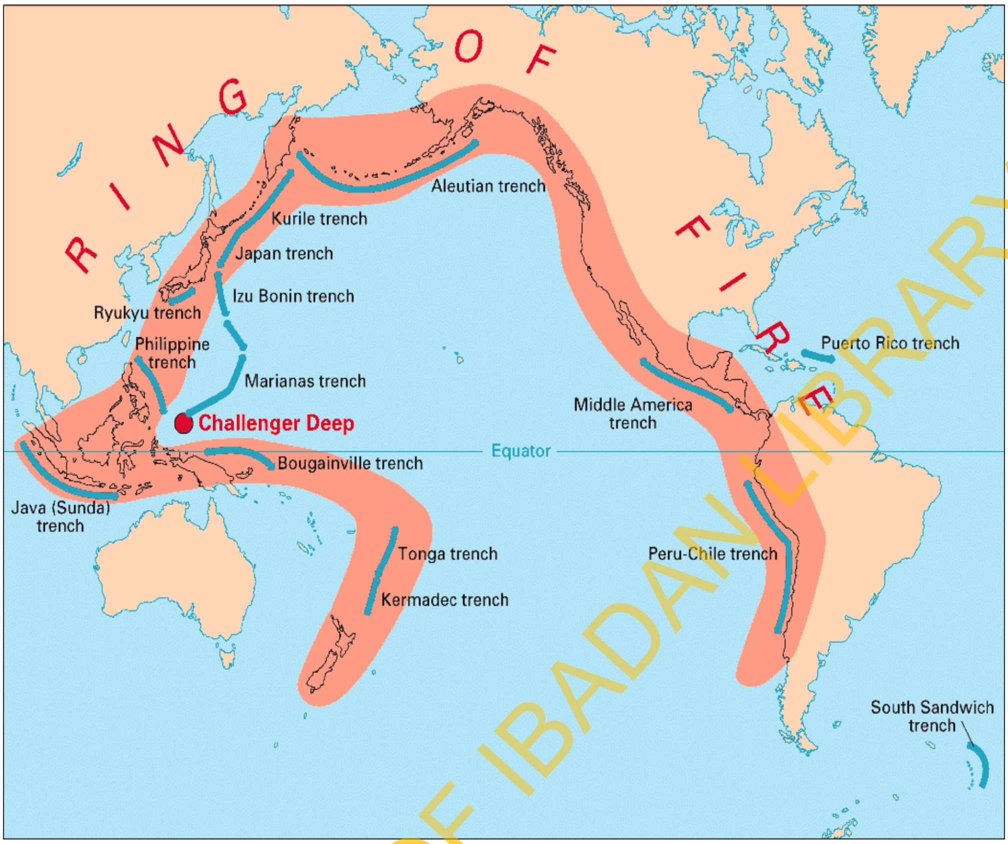

Figure 2.3: Ring of Fire (after USGS, 2010).

2.4 Plate boundaries

The location where two plates meet is called a plate boundary, and plate boundaries are commonly associated with geological events such as earthquakes and the creation of topographic features such as mountains, volcanoes, mid-ocean ridges, and oceanic trenches. The majority of the world's active volcanoes occur along plate boundaries, with the Pacific Ring of Fire (Figure 2.3) being the most active and most widely known.

2.5 Types of plate boundaries

Three types of plate boundaries exist, characterized by the way the plates move relative to each other. They are associated with different types of surface phenomena. The different types of plate boundaries are: convergent, or collision boundaries; divergent boundaries or spreading centres; and transform boundaries (Moores, 1995).

2.5.1 **Transform boundaries**

Transform boundaries occur where plates slide or grind past each other along transform faults. The relative motion of the two plates is either sinistral or dextral e.g. The San Andreas Fault in California. John Tuzo Wilson recognized that because of friction, the plates cannot simply glide past each other. Rather, stress builds up in both plates and when it reaches a level that exceeds the strain threshold of rocks on either side of the fault, the accumulated potential energy is released as strain. Strain may be accumulative or instantaneous depending on the rheology of the rock. The ductile lower crust and mantle accumulates deformation gradually via shearing, whereas the brittle upper crust reacts by fracture, or instantaneous stress release to cause motion along the fault. The ductile surface of the fault can also release energy instantaneously when the strain rate is too great. The energy released by instantaneous strain release is the cause of earthquakes, a common phenomenon along transform boundaries.

A good example of this type of plate boundary is the San Andreas Fault, which is found in the western coast of North America and is one part of a highly complex system of faults in this area. At this location, the Pacific and North American plates move relative to each other such that the Pacific plate is moving northwest with respect to North America. Other examples of transform faults include the Alpine Fault in New Zealand and the North Anatolian Fault in Turkey. Transform faults are also found offsetting the crests of mid-ocean ridges (for example, the Mendocino Fracture Zone offshore northern California) (Oreskes, 2003, Plate Tectonic.com).

2.5.2 Divergent boundaries

Divergent boundaries occur where two plates slide apart from each other. Mid-ocean ridges (e.g., Mid-Atlantic Ridge) and active zones of rifting (such as Africa's Great Rift Valley) are both examples of divergent boundaries.

At divergent boundaries, two plates move apart from each other and the space that this creates is filled with new crustal material sourced from molten magma that forms below. The origin of new divergent boundaries at triple junctions is sometimes thought to be associated with the phenomenon known as hotspots. Here, exceedingly large convective cells bring very large quantities of hot asthenospheric material near the surface and the kinetic energy is thought to be sufficient to break apart the lithosphere. The hot spot, which may have initiated the Mid-Atlantic Ridge system currently underlies Iceland which is widening at a rate of a few centimetres per year.

Divergent boundaries are typified in the oceanic lithosphere by the rifts of the oceanic ridge system, including the Mid-Atlantic Ridge and the East Pacific Rise, and in the continental lithosphere by rift valleys such as the famous East African Great Rift Valley. Divergent boundaries can create massive fault zones in the oceanic ridge system. Spreading is generally not uniform. Where spreading rates of adjacent ridge blocks are different, massive transform faults occur. These are the fracture zones that are major sources of submarine earthquakes. A sea floor map will show a rather strange pattern of blocky structures that are separated by linear features perpendicular to the ridge axis. If one views the sea floor between the fracture zones as conveyor belts carrying the ridge on each side of the rift away from the spreading centre the action becomes clear. Crest depths of the old ridges, parallel to the current spreading centre, will be older and deeper (Toshiro and Thorne, 2000; USGS, 2010).

2.5.3 Convergent boundary

Convergent boundaries occur where two plates move towards each other .The nature of a convergent boundary depends on the type of lithospheric plates that are colliding (Figures 2.4a, 2.4b and 2.4c).

2.5.3.1 Oceanic – Continental Convergent boundary

Where a dense oceanic plate collides with a less-dense continental plate (Figure 2.4a), the oceanic plate is typically thrust underneath because of the greater buoyancy of the continental lithosphere, forming a subduction zone. At the surface, the topographic expression is commonly an oceanic trench on the ocean side and a mountain range on the continental side. An example of a continental-oceanic subduction zone is the area along the western coast of South America where the oceanic Nazca Plate is being subducted beneath the continental South American Plate. Surface volcanism typically appears above the melts which form directly above downgoing or subducting plates. There is still debate in the geologic community as to why this is so. However, the general consensus from ongoing research suggests that the release of volatiles is the primary contributor. As the subducting plate descends, its temperature rises driving off volatiles (most importantly water) encased in the porous oceanic crust. As this water rises into the mantle of the overriding plate, it lowers the melting temperature of surrounding mantle, producing melts (magma) with large amounts of dissolved gases. These melts rise to the surface and are the source of some of the most explosive volcanism on Earth because of their high volumes of extremely pressurized gases. The melts rise to the surface and cool, forming long chains of volcanoes inland from the continental shelf and parallel to it. The continental spine of western South America is dense with this type of volcanic mountain building from the subduction of the Nazca plate. In North America the Cascade mountain range, extending north from California's Sierra Nevada, is also of this type. Such volcanoes are characterized by alternating periods of quiet and episodic eruptions that start with explosive gas expulsion with fine particles of glassy volcanic ash and spongy cinders, followed by a rebuilding phase with hot magma. The entire Pacific Ocean boundary is surrounded by long stretches of volcanoes and is known collectively as the Pacific ring of fire (Figure 2.3) (Moores 1995; USGS, 2009).

2.5.3.2 Continental - Continental Convergent boundary

Where two continental plates collide the plates may buckle and compress or one plate delves under or overrides the other (Figure 2.4b). Either action will create extensive mountain ranges. The most dramatic effect seen is where the northern margin of the Indian Plate is being thrust under a portion of the Eurasian plate, lifting it and creating the Himalayas and the Tibetan Plateau beyond. It may have also pushed nearby parts of the Asian continent aside to the east.

2.5.3.3 Oceanic – Oceanic Convergent boundary

When two plates with oceanic crust converge (Figure 2.4c) they typically create an island arc as one plate is subducted below the other. The arc is formed from volcanoes which erupt through the overriding plate as the descending plate melts below it. The arc shape occurs because of the spherical surface of the earth. A deep undersea trench is located in front of such arcs where the descending slab dips downward. Good examples of this type of plate convergence would be Japan and the Aleutian Islands in Alaska (NOAA, 2009; Geology.com, 2011).

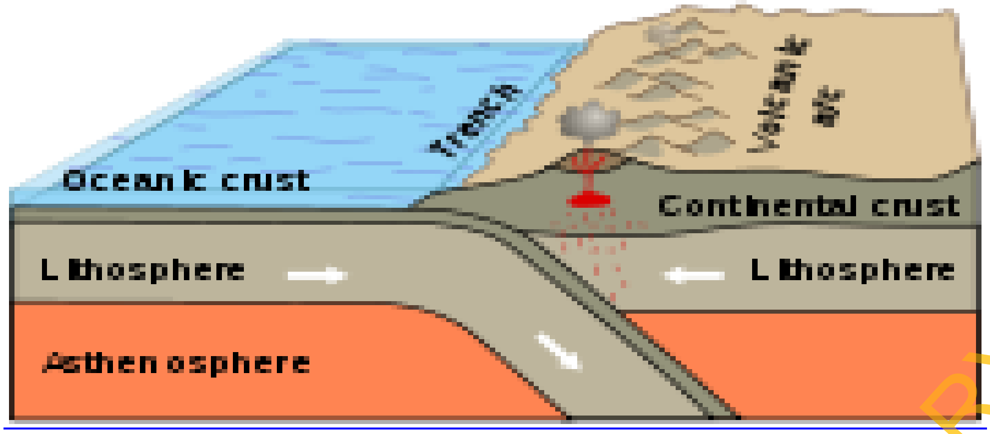

Fig. 2.4a: Oceanic – Continental boundary (after Geology.com, 2011).

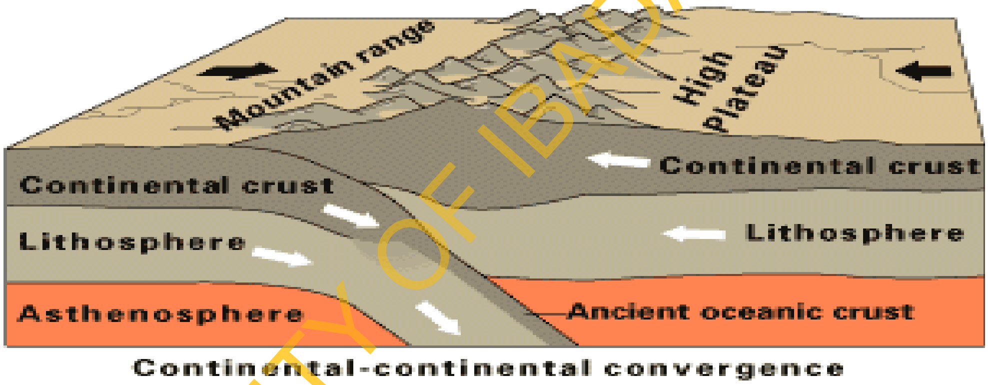

Fig. 2.4b: Continental – Continental boundary (after Geology.com, 2011).

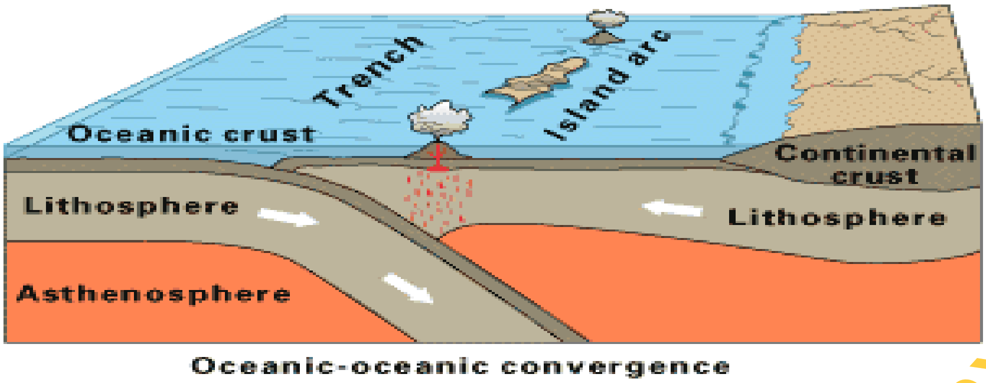

Fig. 2.4c: Oceanic – Oceanic boundary (after Geology.com, 2011).

One of the most significant correlations found is that lithospheric plates attached to downgoing or subducting plates move much faster than plates not attached to subducting plates.

The Pacific plate, for instance, is essentially surrounded by zones of subduction generally known as the Ring of Fire and moves much faster than the plates of the Atlantic basin, which are attached or somehow welded to adjacent continents instead of subducting plates. It is thus thought that forces associated with the subducting plate are the driving forces which determine the motion of plates, except for those plates which are not being subducted.

2.5.3.4 Subduction Zone

Subduction is the process that takes place at convergent boundaries by which one tectonic plate moves under another one, sinking into the Earth's mantle, as the plates converge.

A subduction zone is an area on Earth where two tectonic plates move towards one another and subduction occurs for example, the Pacific Plate is being subducted under the North American Plate forming the Aleutian Trench. Subduction zones are often noted for their high rates of volcanism, earthquakes, and mountain building. This is because subduction processes result in melting of the mantle that produces a volcanic arc as relatively lighter rock is forcibly submerged. Rates of subduction are typically measured in centimetres per year, with the average rate of convergence being approximately 2 to 8 centimetres per year about the rate a fingernail grows (Defant, 1998).

2.6 Causes of Earthquakes

There are two main causes of earthquakes; volcanic and tectonic activities.

Volcanic: Earthquakes can be linked to explosive volcanic eruptions, this is very common in areas of volcanic activity where they either precede or accompany eruptions.

When volcanoes erupt, it is because the molten magma under the crust of the earth is under enormous pressure and to release that pressure it looks for an opening and exerts pressure on the earth's crust and the plate in turn. A place, which is the seat of an active volcano, is often prone to earthquakes as well, because the pressure that is exerted by the magma exceeds the limit, these plates move and that causes earthquakes. Earthquakes are also caused after a volcanic eruption since the eruption also leads to a disturbance in the position of plates, which either move further or resettle and can result into severe or light tremors. The excessive exploitation of earth's resources for our own benefits like building dams to store large volumes of water and blasting rocks and mountains to build bridges and roads is also the reason behind such natural disruptions.

Tectonic activities: Earthquakes can be triggered by tectonic activity associated with plate margins and faults. The majority of earthquakes world wide are of this type. Tectonic earthquakes are triggered when the crust becomes subjected to strain, and eventually moves. The theory of plate tectonics explains how the crust of the Earth is made of several plates, which float on the Mantle. Since these plates are free to slowly move, they can either drift towards each other, away from each other or slide past each other. Many of the earthquakes, which we feel, are located in the areas where plates collide or try to slide past each other. The process that explains these earthquakes is known as Elastic Rebound theory.

2.7 Elastic Rebound theory

From an examination of the displacement of the ground surface which accompanied the 1906 earthquake, Reid (1910) concluded that the earthquake must have involved an elastic rebound of previously stored elastic stress.

Elastic rebound theory states that as tectonic plates move relative to each other, elastic strain energy builds up along their edges in the rocks along fault planes. Since fault planes are not usually very smooth, great amounts of energy can be stored (if the rock is strong enough) as movement is restricted due to interlock along the fault. When the shearing stresses induced in the rocks on the fault planes exceed the shear strength of the rock, rupture occurs.

If a stretched rubber band is broken or cut, elastic energy stored in the rubber band during the stretching will suddenly be released. Similarly, the crust of the earth can gradually store elastic stress that is released suddenly during an earthquake. This gradual accumulation and release of stress and strain is now referred to as the elastic rebound theory of earthquakes. Most earthquakes are the result of the sudden elastic rebound of previously stored energy (UCSB, 2012).

2.8 Mechanism of Plates Motion

Scientists generally agree with Harry Hess and Arthur Holmes that the force responsible for the motion of the lithospheric plates is from the convection flow of the soft and molten asthenosphere that lies below the rigid lithospheric plates.

Just as a solid metal like steel, when exposed to heat and pressure, can be softened and take different shapes, so too can solid rock in the mantle when subjected to heat and pressure in the Earth's interior over millions of years. The molten state and the convection flow of the asthenosphere come from heat within the interior.

Heat within the Earth comes from two main sources: radioactive decay and residual heat. The radioactive decay of naturally occurring chemical elements such as uranium, thorium, and potassium releases energy in the form of heat, which slowly migrates toward the Earth's surface. Residual heat is gravitational energy left over from the formation of the Earth billion of years ago. The motion of the tectonic plate is an undisputable fact among earth scientist but full details of the mechanism or forces responsible for the plate motion is a challenge (Schubert et al, 2001; ESZ, 2013; Plate Tectonic.com).

2.9 Impacts of earthquakes

Many highly or densely populated areas are located near active fault zones, such as the San Andreas. Millions of people have suffered personal and economic losses as a result of the destructive impacts of earthquakes. Impacts of earthquakes can be classified into various classes;

Ground rupture: It is the main result of an earthquake strike. Shaking of ground causes severe damage to the buildings or other structures on the ground including houses. Shaking of ground at a particular place depends upon the distance of that place from the epicentre. Severe shaking of ground causes destruction of all the buildings of a city and many people die by being buried under the building materials. This shaking of ground compels construction Engineers to develop buildings which are resistive to the strikes of earthquakes. The branch of engineering which deals with anti-earthquake construction is called Earthquake Engineering.

Landslides: Earthquakes causes instability of land resulting into landslides; which claims many lives at the effected zone.

Fire: Earthquake causes breaking of electrical power lines or gas supply lines which cause incidents of fires. Water lines also got ruptured and decreased pressure makes it impossible to control the spread of fire. In earthquake of San Francisco in 1906, more deaths occurred because of fire as compared to the earthquake itself (USGS, 2010).

Soil liquefaction: When severe shaking occur then soil or sand loses their strength for a temporary period and gets converted from solid to liquid. This liquefaction causes sinking of buildings and bridges for example, the 1964 Alaska earthquake (Jefferies and Been, 2006; USGS, 2010).

Tsunami and floods: When the epicentre of an earthquake is located near sea, then the travelling of seismic waves below the sea causes generation of Tsunami waves.

Tsunamis are long-wavelength, long-period sea waves produced by the sudden or abrupt movement of large volumes of water. In the open ocean the distance between wave crests can surpass 100 kilometres and the wave periods can vary from five minutes to one hour. Such tsunamis travel 600-800 kilometres per hour, depending on water depth. Tsunamis can also travel thousands of kilometres across Open Ocean and wreak destruction on far shores, hours after the earthquake that generated them. Sometimes, when earthquake - triggered landslides fall into sea, it leads to the creation of Tsunami waves. Subducting earthquakes under magnitude 7.5 on the Richter scale do not cause tsunamis, although some instances of this have been recorded. Most destructive tsunamis are caused by earthquakes of magnitude 7.5 or more (Doyle, 1995; Noson et al, 1988).

2.10 Seismicity

Seismicity or seismic activity is the distribution of earthquakes by frequency, type, size intensity, depth, magnitude (or energy) and geography (latitude and longitude), over a period of time.

2.11 Global Seismicity and plate boundaries

Earthquakes are not uniformly distributed on the earth surface but are concentrated along narrow regions in between lithospheric plate. One of the fundamental tenets of plate tectonics is that plates are rigid and undeformable. This idea arose largely from the observed distribution of earthquakes around the world.

Global seismicity maps show that the regions where seismicity is the highest correspond with the edges of the tectonic plates hence seismicity is one of the biggest factors in the development of plate tectonic theory.

Most events, especially in the oceans, are concentrated in relatively narrow bands or regions with broad aseismic areas between them. The narrow bands of seismicity are taken to indicate active plate boundaries, while the aseismic areas are the rigid interiors of the plates. However, no part of the world can be regarded as earthquake – free because intra-plate earthquakes do take place.

The major global seismic zones or belts are; the circum-Pacific belt which produce 75.4% of the global events, the Mediterranean and Tran's Asiatic/Alpine belt 22.9%, while the rest of the world produces about 2% (Geophysics.ou.edu, 2011).

All plate boundaries produce shallow earthquakes. However, earthquakes deeper than about 50 - 100 km occur only in a few places, nearly all in circum-Pacific belt and Indonesia. They are all associated with convergent plate boundaries (subduction zones). Historical documents indicate that seismicity may increase (in occurrence and magnitude) prior to and during an eruption (Gutenberg and Richter, 1965).

Though distribution of earthquakes virtually defines plate's boundaries there are exceptions, these include; incipient plate boundaries (e.g., east African rift), hot spots (e.g., Hawaii) and vestigial plate boundaries (e.g., seismicity associated with India/Asia collision) (Isacks et al, 1968; Kearey and Vine, 1996; Geophysics.ou.edu, 2011).

2.12 Seismicity of different types of plate boundary

2.12.1 Seismicity of Divergent boundaries

Earthquakes at divergent boundaries are virtually entirely confined to depths of 8 km or less, which may be taken to define the depth of the brittle–ductile transition or, effectively, the base of the zero-age lithosphere. Almost all earthquakes here are of moderate magnitude, usually less than magnitude 6, because the young, weak lithosphere and predominantly extensional faults do not support very large accumulations of stress before breaking or slipping (USGS, 2010).

2.12.2 Seismicity at Transform boundaries

Many of the continental transform fault systems are quite complex. These complexities are reflected in the distribution of seismic activity. Continental transform faults can generate larger earthquakes than those on mid-ocean ridges with magnitudes of about 7 or more (e.g. the 1994 North Ridge earthquake in California). These larger-magnitude events normally occur on faults with a component of thrusting, where larger stresses can build up. Seismicity on continental transform faults extends to depths of about 15 km, where much of the deformation appears to change from brittle to ductile (USGS, 2010).

2.12.3 Seismicity at Subduction zones

The largest-magnitude earthquakes found on Earth occur within subduction zones, mainly in the shallow region of thrusting, where very large stresses can build up. The great Alaska earthquake (Good Friday 1964 earthquake in Alaska with magnitude 9.2 on moment magnitude scale) occurred on the Aleutian subduction zone (Kanamori, 1977; Moores, 1995).

The plate created at divergent boundaries is destroyed at subduction zones. There, plates descend at an angle into the mantle. The traces of these dipping, subducted plates are marked by zones of earthquakes called Benioff or Wadati-Benioff zones after the Japanese (Kiyoo Wadati) and Californian (Hugo Benioff) seismologists who first recognized them (Stein and Wysession, 2003).

2.12.4 Seismicity at Continental collision zones

Here, the lithosphere, which is thicker but weaker than oceanic lithosphere, is broken into large numbers of tectonic blocks delimited by active faults in zones many hundreds or even thousands of kilometres wide. Most earthquakes in continental collision zones are relatively shallow, being confined to the thickness of the rigid lithosphere: 100 km or so. However, sinking lithospheric slabs may exist below this depth, either as the remnants of the subduction zones that led to the collision, or as recently delaminated blocks of lower lithosphere. These may be marked by deeper earthquakes extending hundreds of kilometres below the surface. As with subduction zones, continental collision zones can support large stresses, and so large-magnitude earthquakes are also found here (Isacks et al, 1968).

2.13 Induced seismicity

Induced seismicity is earthquake activity that is the result of human activity, which causes a rate of energy release, or seismicity, which would be expected beyond the normal level of historical seismic activity. Induced seismicity refers typically to minor earthquakes and tremors that are triggered by human activity that alters the stresses and strains on the Earth's crust. Most induced seismicity is of an extremely low magnitude (Kisslinger, 1976).

2.14 Causes of Induced seismicity

Research is still being carried out on the detailed causes of induced seismicity. There are many different applications, which have been associated with induced seismic activity. The following are number of ways in which induced seismicity has been seen to occur:

Extraction of fossil fuel and groundwater: Subsidence caused by extraction of groundwater, oil or natural gas can generate seismic waves and minor earthquakes (Eijsa et al, 2006).

Mining; Mining leaves voids that generally alter the balance of forces in the rock. These voids may collapse producing seismic waves and in some cases reactivate existing faults causing minor earthquakes (Redmayne, 1988).

Geothermal energy: An enhanced geothermal system (EGS) is a geothermal power technology that does not require natural convective hydrothermal resources. They are known to be associated with induced seismicity. EGS involves pumping fluids at pressure to enhance or create permeability through the use of hydraulic fracturing techniques. EGS actively creates geothermal resources through hydraulic stimulation. Depending on the rock properties, and on injection pressures and fluid volume, the reservoir rock may respond with tensile failure, as is common in the oil and gas industry, or with shear failure of the rock's existing joint set. This is thought to be the main mechanism of reservoir growth in EGS efforts (Tester, 2006).

Reservoirs: The mass of water in a reservoir alters the pressure in the rock below, which can trigger earthquakes. Reservoir-induced seismic events can be relatively large compared to other forms of induced seismicity. The extra water pressure created by vast reservoirs is the most accepted explanation for the seismic activity.

The first case of reservoir induced seismicity occurred in 1932 in Algeria's Quedd Fodda Dam. On August 1, 1975, a magnitude 6.1 earthquake at Oroville, California, was attributed to seismicity from a massive earth-fill dam and reservoir recently constructed and filled there. During the beginnings of the Vajont Dam in Italy, there were seismic shocks recorded during its initial fill. With scares of landslide emerging, the dam was drained and consequently seismic activity was almost non-existent. The filling of the Katse Dam in Lesotho and the Nurek Dam in Tajikistan is an example. In Zambia, Kariba Lake may have provoked similar effects. Some experts worry that the Three Gorges Dam in China may cause an increase in the frequency and intensity of earthquakes (Talwani, 1997; Chen and Talwani, 1998).

2.15 Theory of Seismic Wave

A seismic wave is a type of wave that vibrates through or under the surface of the Earth. Seismic waves are the waves of energy caused by the sudden breaking of rock within the earth or an explosion. They are the energy that travels through the earth and is recorded on seismographs. Seismologists can also evaluate the potential dangers from seismic waves and research ways to minimize their impact. Seismic waves propagate through the earth because the material within it, though solid, can undergo internal deformation (Stein and Wysession, 2003).

2.16 Types of Seismic Waves

There are several different kinds of seismic waves, and they all move in different ways. The two main types of waves are body waves and surface waves. Body waves can travel through the earth's inner layers, but surface waves can only move along the surface of the planet like ripples on water. Earthquakes radiate seismic energy as both body and surface waves (Yeats et al, 1997).

2.16.1 Body waves

Body waves are waves that travelled through the interior of the earth. Body waves flow through the inner parts of the Earth and can bend and retract depending on the substance through which they pass. They follow ray paths refracted by the varying density and modulus or stiffness of the Earth's interior. The density and modulus, in turn, vary according to temperature, composition, and phase. This effect is similar to the refraction of light waves, i.e. they obey the laws of geometrical optics. Body waves arrive before the surface waves emitted by an earthquake. These waves are of a higher frequency than surface waves.

2.16.1.1 Primary wave or P-wave

A primary wave, or P-wave, is a type of body seismic wave that travels at great velocity. It is the fastest kind of seismic wave, and, consequently, the first to arrive at a seismic station (Robinson, 1993).

Primary Waves (P-Waves) are identical in character to sound waves. They are high frequency, short-wavelength, longitudinal waves which can pass through both solids and liquids. Material moves back and forth in the direction in which the waves propagates as illustrated in Figure 2.5.

It can move through solids and liquids by compressing and decompressing (expanding) the material in its way, hence P waves are also known as compressional waves, The ground is forced to move forwards and backwards as it is compressed and decompressed. These pushing and pulling produces relatively small displacements of the ground.

P Waves can be reflected and refracted, and under certain circumstances can change into S-Waves. Typical speeds are 330 m/s in air, 1450 m/s in water and about 5000 m/s in granite.

2.16.1.2 Shear wave or secondary wave

Shear waves or secondary waves just like P-Waves are high frequency, short-wavelength waves, but instead of being longitudinal they are transverse, which means that the ground is displaced perpendicularly to the direction of propagation (Figure 2.6).

They move in all directions away from their source, at speeds, which depend upon the density of the rocks through which they are moving. A secondary wave is slower than the primary wave and so arrives second in a seismic station because of their slower speed. Since they have greater wave amplitude, they cause greater damage than P waves (Tobin and Burrell, 1997).

Shear waves can only move through solid rock, not through any liquid medium as fluids (liquids and gases), which do not support shear stresses. Since the outer layer of the Earth's core is made out of liquid molten lava, the waves need to bend and go around it to get to the site of the earthquake. Seismologists timed and used this property of secondary waves to prove the existence of the core itself and their conclusion that the Earth's outer core is a liquid. On the surface of the Earth, S-Waves are responsible for the sideways displacement of walls and fences, leaving them S shaped (Robinson, 1993).

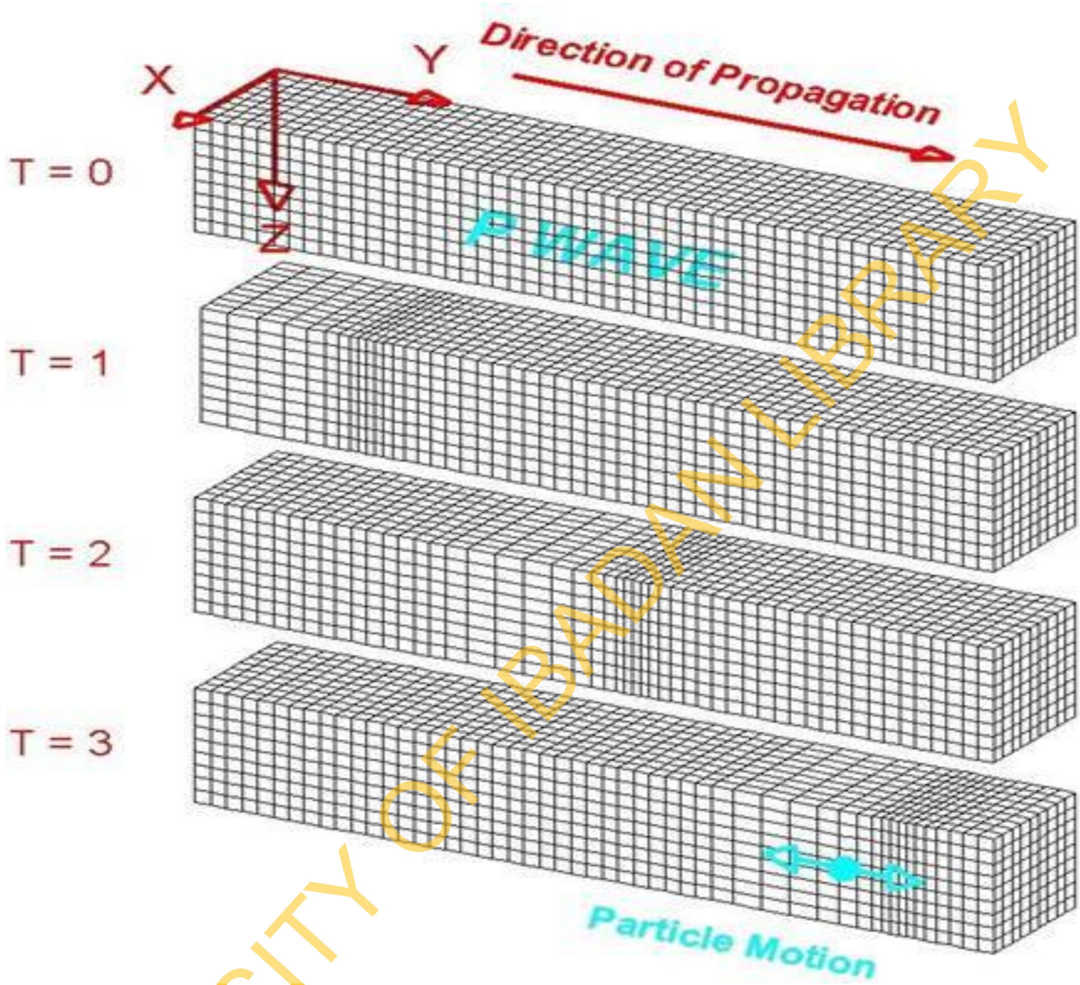

Figure 2.5: The propagation effect of Primary wave (After Geo.mtu.edu, 2014)

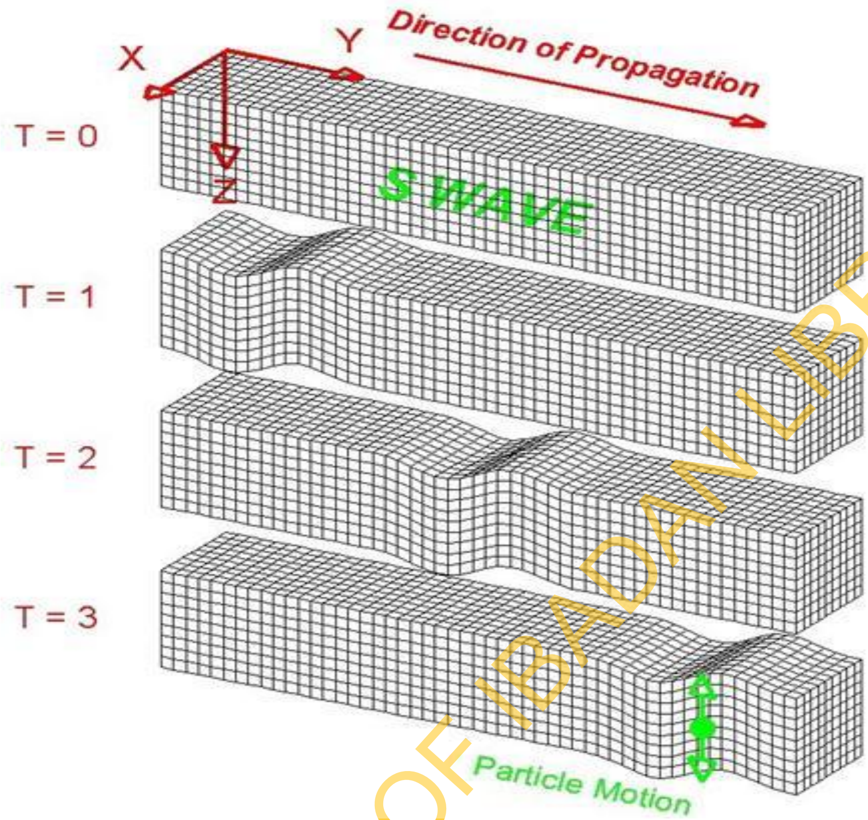

Figure 2.6: The propagation effect of secondary or shear wave (After Geo.mtu.edu, 2014)

2.16.2 Surface Waves

Surface Waves or L waves are low frequency transverse waves with a long wavelength, they are generated when the source of the earthquake is close to the surface, surface waves are of a lower frequency than body waves, and are easily distinguished on a seismogram as a result. Though they arrive after body waves, Surface waves are generally responsible for the largest amount of destruction associated with earthquake.

This type of seismic wave moves only through the Earth's crust and is similar to a water wave. This is because L Waves have a motion similar to that of waves in the sea. The ground is made to move in a circular motion, causing it to rise and fall as visible waves move across the ground (Figures 2.7 and 2.8).

Because of their low frequency, long duration, and large amplitude, they can be the most destructive type of seismic wave. They are responsible for the majority of the building damage caused by earthquakes though this damage and the strength of the surface waves are reduced in deeper earthquakes. They are created close to the epicentre and can only travel through the outer part of the crust.

Surface waves are also divided into two subtypes: Rayleigh waves, which travel as ripples and can be spotted by the human eye, and Love waves, which split the ground horizontally.

2.16.2.1 Rayleigh wave

Rayleigh waves are surface waves that travel as ripples with motions that are similar to those of waves on the surface of water.

Rayleigh wave rolls along the ground just like a wave rolls across a lake or an ocean. Because it rolls, it moves the ground up and down and side-to-side in the same direction that the wave is moving (Fig. 2.7). Most of the shaking felt from an earthquake is due to the Rayleigh wave, which can be much larger than the other waves. The existence of these waves was predicted by John William Strutt, Lord Rayleigh in 1885. They are slower than body waves.

2.16.2.2 Love wave

Love waves are surface waves that move the ground from side-to-side and produce entirely horizontal motion that is confined to the surface of the crust (Fig.2.8). They are named after Augustus Edward Hough Love**,** a British mathematician who created a mathematical model of the waves in 1911. They usually travel slightly faster than Rayleigh waves (Tobin and Burrell, 1997; Geo. mtu.edu, 2009).

Earthquakes generate an array of primary, secondary and surface waves due to the complexity in the strain-release pattern at the source and complexity in the earth materials through which the waves pass to reach a seismograph (Yeats et al, 1997). A combination of these waves cause ground shaking damage (Tobin and Burrell, 1997).

Seismographs record the ground shaking that result from the release of energy from earthquakes and help locate the epicentre and focus of an earthquake (Yeats et al, 1997). They have a mass freely suspended from a support that is attached to the ground. When the vibration from a distant earthquake reaches the instrument, the movement of Earth in relation to the stationary mass is recorded. The greater the interval between the arrival of the first primary wave and first secondary wave, the greater distance to the earthquake (Tarbuck et al, 1996).

Modern seismology uses P wave's first motions and the amplitudes of direct P and S waves, surface waves and waves reflected many times from the surface of the earth to understand the earthquake source (Yeats et al, 1997). An earthquake may be initially located by comparing the differences in arrival times of various phases with standard time-tables and curves (Doyle, 1995). From there, earthquake depths are estimated by the arrival time of reflected waves from the surface above the focus. Earthquake depths vary and are generally categorized as shallow; with a focus within 70 km of the surface, intermediate; with a focus between 70 and 300 km of the surface, and deep; with a focus greater than 300 km below the surface. The majority of earthquakes are shallow, within the upper cooler crust and in the most brittle part of the lithosphere. Ninety percent of all earthquakes occur at depths less than 100 km and almost all of the very damaging earthquakes appear to originate at shallow depths (Tarbuck et al, 1996).

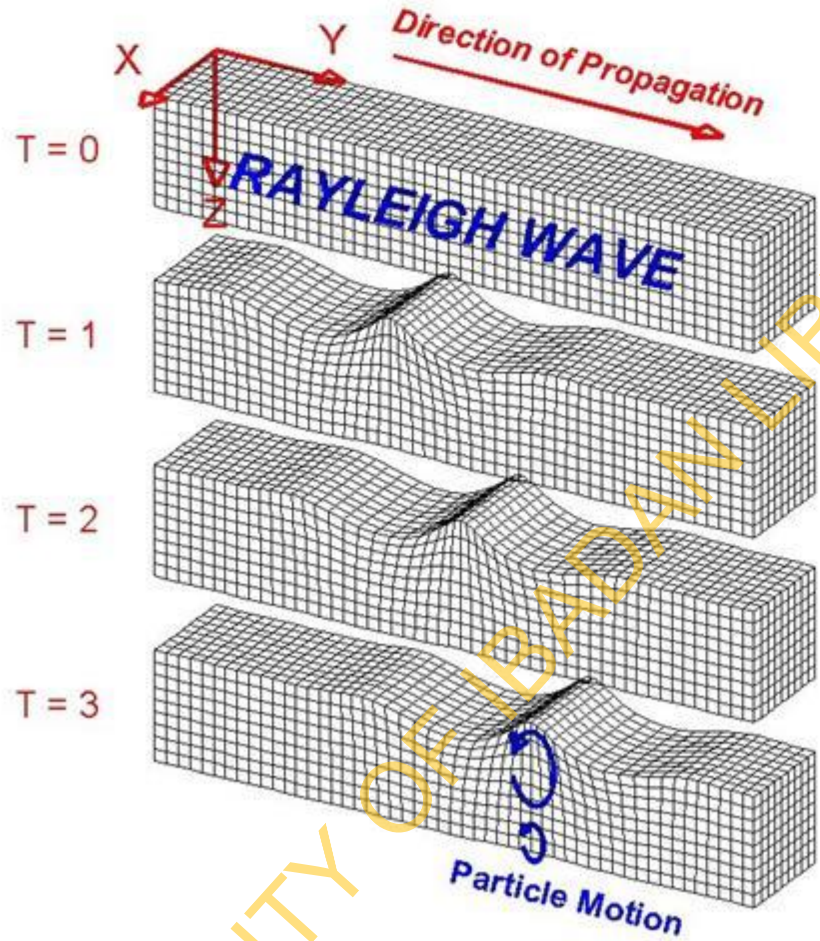

Figure 2.7: The propagation effect of Rayleigh Waves (After Geo.mtu.edu, 2014)

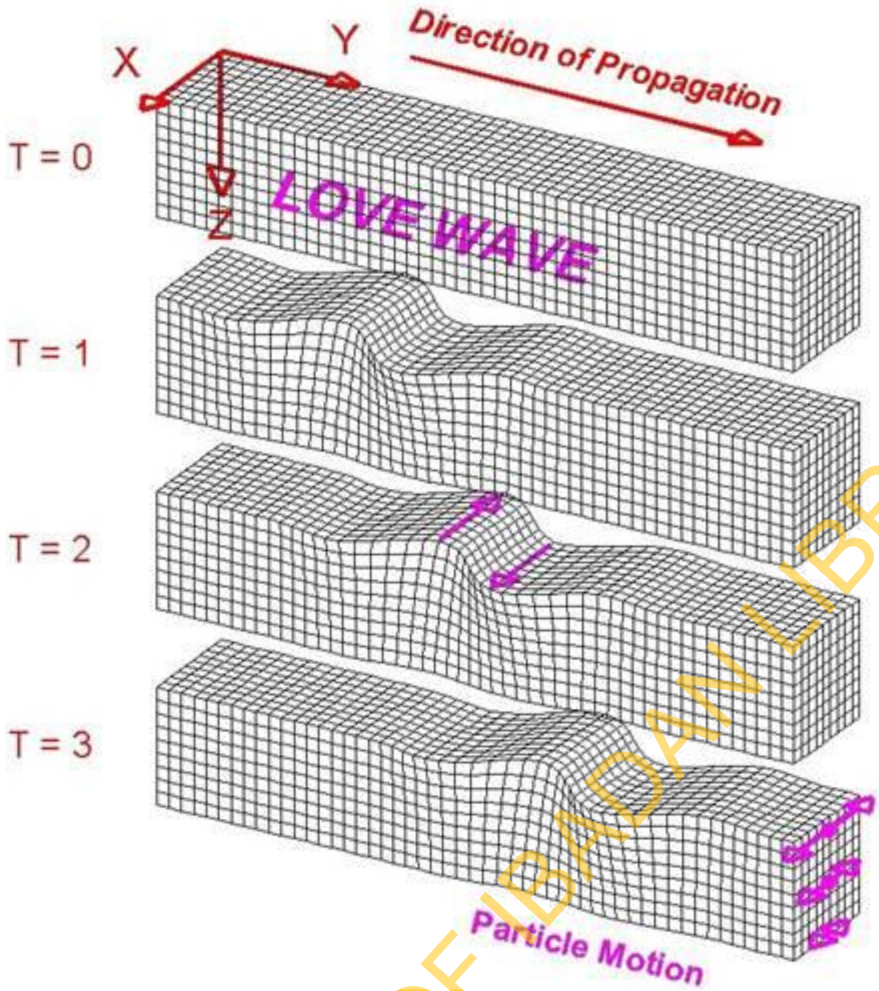

Figure 2.8: The propagation effect of Love Waves (After Geo.mtu.edu, 2014)

2.17 Magnitude and Intensity of Earthquake

Magnitude of earthquake is a measure of the amount of energy released during an earthquake. It is a number that characterizes the relative size of an earthquake. Magnitude is based on measurement of the maximum motion recorded by a seismograph (Doyle, 1995). Since magnitude is representative of the earthquake itself, there is only one magnitude per earthquake. Intensity is a measure of the shaking and damage caused by the earthquake, and this value changes from location to location. The Intensity scale is designed to describe the effects of an earthquake, at a given place, on natural features, on industrial installations and on human beings (Coffman and Carl, 1982). The intensity differs from the magnitude which is related to the energy released by an earthquake. The damage pattern of two earthquake of the same magnitude may be very different. The effects or intensities experienced at different places were different, but the magnitude of the earthquake is unique; in this example, it was 6 on the Richter scale. Magnitude thus has more to do with the effects of the earthquake overall.

The magnitude scale is logarithmic. This means that, at the same distance, an earthquake of magnitude 6 produces vibrations with amplitudes 10 times greater than those from a magnitude 5 earthquake and 100 times greater than those from a magnitude 4 earthquake. In terms of energy, an earthquake of magnitude 6 releases about 30 times more energy than an earthquake of magnitude 5 and about 1000 times more energy than an earthquake of magnitude 4 (Moores, 1995; Doyle, 1995; Yeats et al, 1997).

2.18 Ground shaking and earthquakes

Most earthquake damage is caused by ground shaking. The magnitude or size of an earthquake, distance to the earthquake focus or source, type of faulting, depth, and type of material are important factors in determining the amount of ground shaking that might be produced at a particular site. Where there is an extensive history of earthquake activity, these parameters can often be estimated.

The magnitude of an earthquake, for instance, influences ground shaking in several ways. Large earthquakes usually produce ground motions with large amplitudes and long durations. Large earthquakes also produce strong shaking over much larger areas than do smaller earthquakes. In addition, the amplitude of ground motion decreases with increasing distance from the focus of an earthquake. The frequency content of the shaking also changes with distance. Close to the epicenter, both high (rapid) and low (slow)-frequency motions are present. Farther away, low-frequency motions are dominant, a natural consequence of wave attenuation in rock. The frequency of ground motion is an important factor in determining the severity of damage to structures and which structures are affected.

2.19 Radiant Energy

The total energy from an earthquake includes energy required to create new cracks in rock, energy dissipated as heat through friction, and energy elastically radiated through the earth. Of these, the only quantity that can be measured is that which is radiated through the earth. It is the radiated energy that shakes buildings and is recorded by seismographs.

The radiated energy can be obtained in various ways. Historically, the radiated energy was estimated empirically (from observations) from magnitude Ms through the Richter formula equation 2.1a.

$$\text{Log Es} = 4.8 + 1.5\text{Ms} \qquad (2.1a)$$

$$\text{Me} = (2/3)\ \text{Log Es} - 2.9 \qquad (2.1b)$$

$$\text{Mw} = (2/3)\ \text{Log Mo}\ 6.0 \qquad (2.1c)$$

where Es is seismic energy in Joules, Ms is the surface wave magnitude, Me is the energy magnitude, Mw is the moment magnitude and Mo is the seismic moment.

The magnitude is measured first, after which equation 2.1a is used to obtain Es. With modern instrumentation, energy can be measured directly from velocity seismograms and converted to a magnitude. If Es is energy in joules, the energy magnitude (Me) is obtained from equation 2.1b. If Me is not available, the seismic moment (Mo) of an earthquake can provide an empirical estimate of radiated energy. After Mo is measured, it is converted to a moment magnitude Mw using equation 2.1c. Mw is then used as the magnitude in the Richter formula to obtain an estimate of radiated energy. Me and Mw do not necessarily have the same numerical value because they measure different physical quantities. Mw is a magnitude that is derived from low-frequency displacement spectra whereas Me is measured from higher frequency velocity spectra. Mw is a measure of the area of rupture and the average slip across the fault, whereas is Me is a measure of the shaking from an earthquake (Kanamori 1977, 1983). Once the energy is known in Joules, it can be compared to the explosive energy of TNT. One ton of TNT has energy of 4.2 $\times 10^9$ Joules.

2.20: Classes of Earthquake Magnitude

Magnitude of earthquakes ranges from 1 to 10, earthquakes are classified in categories from micro to large based on this magnitude. Earthquakes are classified as great or large if the magnitude is greater than or equal to 8; major earthquake if the magnitude is between 7.0 and 7.9; strong earthquake if the magnitude is between 6.0 and 6.9; moderate earthquake if the magnitude is between 5.0 and 5.9; light earthquake if the magnitude is between 4.0 and 4.9; minor earthquake if the magnitude is between 3.0 and 3.9 and micro if the magnitude is less 3.0. Micro earthquakes are usually not felt but can be recorded by seismograph while large earthquakes are capable of tremendous damage. Bigger earthquakes last longer and release their energy over a much larger area (Natural Resources Canada, USGS, 2010; Geo.mtu.edu, 2011).

2.21 Types of Earthquakes Magnitudes Scales

Several scales have been defined, but the most commonly used are local magnitude ML commonly referred to as Richter magnitude, surface-wave magnitude Ms, body-wave magnitude Mb, and moment magnitude Mw. All these scales measure the amplitude of some aspect of ground motion (velocity or acceleration) at different distances and in different frequency bands.

The first three scales have limited range and applicability and do not satisfactorily measure the size of the largest earthquakes.

Despite various shortcomings, the earthquake magnitude scale is one of the most fundamental earthquake source parameters to be used for catalogs. Although use of a uniform scale is desirable, it is not always possible because of changes in instrumentation, the data reduction method and the magnitude formula, the station distribution, etc.

As a result, various magnitude scales have been developed and are currently in use. Recent developments in seismometry and earthquake source theories provide more quantitative source parameters than the magnitude. In order to maintain continuity and uniformity of the data, it is important to relate these magnitude scales and the new parameters. In view of this importance, relations between different magnitude scales are examined with an emphasis on the difference in the period of the waves used for the magnitude determination. Use of several magnitude scales determined at different periods provides a convenient method for characterizing earthquakes **(**Kanamori 1983).

2.22 Homogenous Magnitude Scale

An earthquake catalog containing homogeneous size estimations for all events is highly desirable for many earthquake related studies such as seismic hazard assessment, derivation of ground-motion prediction equations, determination of long-term seismic strain rates and nuclear activity verification (Yenier1 et al, 1997).

The existence of several magnitude scales used by seismological centres all over the world and the compilation of earthquake catalogs by many authors has rendered globally valid relations connecting magnitude scales a necessity. This would allow the creation of a homogeneous global earthquake catalog, a useful tool for earthquake research. Of special interest is the definition of global relations converting different magnitude scales to the most reliable and useful scale of magnitude, the moment magnitude, Mw (Scordilis, 2006).

2.23 The moment magnitude Scale

Seismologists have developed a new scale, called moment magnitude to describe the size of an earthquake. The moment magnitude (Mw) scale, based on the concept of seismic moment, is uniformly applicable to all sizes of earthquakes but is more difficult to compute than the other types.

Moment is a physical quantity proportional to the slip on the fault times the area of the fault surface that slips. The moment can be estimated from seismograms and also from geodetic measurements. The moment is then converted into a number similar to other earthquake magnitudes by a standard formula. The result is called the moment magnitude. The moment magnitude provides an estimate of earthquake size that is valid over the complete range of magnitudes, a characteristic that was lacking in other magnitude scales (USSG, 2010).

Unlike other magnitude scales that measure only one part of the ground motion, moment magnitude is based on a physical quantity, called moment that can be determined either from the geometry of the fault plane or from the total energy recorded on a seismogram. It is equal to the area of the fault times the amount of slip across the fault times the rigidity of the rock. Several recent earthquakes have confirmed that moment determined by geologists measuring the fault in the field matches the moment determined by seismologists from a seismogram. (Kanamori, 1983)

Moment magnitude has many advantages over other magnitude scales because it uses the complete seismogram and it does not saturate hence large earthquakes can be measured. It can be determined either instrumentally or geologically. It can be use to measure the size of old earthquakes and compare them to instrumentally recorded events.

Unlike the other scales, the Mw scale takes into account the geometrical relationships between the fault's orientation and the observers. Magnitudes based on seismic moment give a truer picture of large earthquakes than the other scales do

In particular, for very large earthquakes moment magnitude gives the most reliable estimate of earthquake size.

2.24 Frequency – Magnitude Distribution

An empirical formula $\mathrm{Log}_{10}N = a - bM$ (2.2a)

$$N = 10^{a-bM} \quad (2.2b)$$

known in the east as Ishimoto and Iida (1939) relation and in the west as the Gutenberg and Richter (1942) relation defines the distribution of earthquakes with respect to the magnitude. For a certain region and time interval, equations 2.2a and 2.2b provides the number of earthquakes, N, with magnitude, M, where a and b are positive, real constants.

Generally constant a is the logarithm number of events with M=0, it describes the rate of seismic activity. It is determined by the event rate and for certain region depends upon the volume and time window considered. b, which is typically close to 1, is a tectonic parameter describing the relative abundance of large to smaller shocks. It seems to represent properties of the seismic medium in some respect, like stress and/or material conditions in the focal region. The relation is usually referred to as the Gutenberg-Richter magnitude-frequency relationship or the Gutenberg–Richter Law, it is a major tool in probabilistic hazard assessment. It allows extrapolation from the rates of small earthquakes, which we observe easily, to the likelihood of large events (Kanamori and Brodsky, 2004).

2.24.1 Cumulative and Incremental Distributions

G-R relation applies to cumulative number N as well as to incremental numbers n. In other words, N is the cumulative number of earthquakes with magnitude larger than M, while n is the number of events with magnitudes in the range M±ΔM (incremental or interval distribution). A choice of proper ΔM is a crucial task in any incremental b evaluation. Reported magnitudes are not continuous quantities, as assumed in equation 2.2a but discrete quantities determined with accuracy of 0.1 magnitude unit in most of global catalogs. Thus, a proper choice of ΔM will be a compromise between the magnitude sampling as close to 0.1 as possible and statistically large numbers of events in each magnitude group. The cumulative distribution is preferred because it provides better linear fit since numbers are larger and less degraded by statistics of small numbers. It also circumvents the problem of designing a proper ΔM (Kulhanek, 2005**).**

2.25 Pattern Recognition

Pattern Recognition theory is a relatively new theory in the field of seismicity and tectonophysics that attempts to understand symptoms that are associated with failure events in a complex system especially in the absence of fundamental equation describing them (Keilis-Borok and Soloviev, 2009). It is based on the use of earthquakes' catalogs to describe the dynamics of seismic regions and derive precursory seismic pattern associated with earthquakes (Kossobokov and Shebalin 2003). This pattern may reflect the geodynamic characteristics of a region (Baskoutas et al 2004).

Several types of seismic patterns have been proposed (Kossobokov and Carison, 1995; Shebalin et al, 2000; Keilis et al, 2002), however no regularity has been established (Baskoutas et al 2004). It has been suggested that though the result of seismic pattern may not be an outright solution but it may help in stimulating hypothesis and extraction of physical meaning from data (Papadopoulos and Baskoutas 2009).

Tectonics is the study of the relative movements of lithospheric plates which are responsible for earthquakes occurrences while seismotectonic is the relationship between earthquake occurrence and tectonic processes. Earthquakes have been described as a symptom or an agent of active tectonics (Saskia, 2003).

2.26 Seismic Parameters.

Basic seismotectonic or seismic parameters are the number of earthquakes N or Log N, the seismic energy and the b value (Baskoutas et al 2004). They are seismological indicators, because they contain information that can be useful for seismotectonic interpretation (Papazachos, 1999; Wiemer and Wyss, 2002; Papadopoulos and Baskoutas, 2009).

Once a and b in GR relation are determined for a given region and time window, then one already has the information necessary to assess parameters of seismic hazard such as maximum expected magnitude of an earthquake and the return period (Scholz et al, 1973 and Comninakins, 1975).

2.26.1 Seismic b – value

The b – value is defined as the slope of frequency – magnitude distribution of earthquakes. It is an important seismic parameter for characterizing the seismicity and it is critical for both hazard analysis and physical understanding of earthquakes.

It can be used to study earthquake evolution process and its temporal variation as earthquake precursor (Papazachos, 1999; Wang and Jackson, 2008; Papadopoulos and Baskoutas, 2009). It can be used to compute the probable occurrence of earthquake of magnitude M (Scholz et al, 1973; Yegulalp and Kuo, 1974; Rikitake 1975; Mogi, 1980, 1981, 1985) and the mean return period Tm of an earthquake (Comninakins, 1975; Tsapanos, 1988; and Bayrak et al 2009). It can be used to identify volumes of active magma bodies (Wiemer and Benoit, 1996; Wiemer et al., 1998), and roots of regional volcanism (Monterroso and Kulhanek, 2003). It can be used to forecast major tectonic earthquakes (Monterroso, 2003 and Nuannin et al., 2005) and for studies related to induced seismicity (Gibowicz and Lasocki, 2001 and Nuannin et al., 2002).

Some seismologists have shown the variability of b-value. (Wiemer and Wyss, 1997; Mogi, 1962; Mogi, 1967; Mori and Abercronbie 1997;Wiemer et al.,1998; Gerstenbergeret et al. 2001 Monterroso and Kulhanek, 2003 and Schorlemmer et al, 2007). While some seismologists opposed the variability of b value, they argued that case studies showing variability of b suffer from artefacts caused by error in data and a lack of statistical rigour (Frohlich and Davi, 1993; Kagan, 1999).

Space and temporal variations of the b-value have earlier been employed in numerous seismicity studies. After the pioneering works of Mogi (1962), Scholz (1968) and Wyss (1973), they have been extensively used by other researchers for example b-value studies related to induced seismicity have been carried out with results published in numerous scientific papers (Gibowicz and Lasocki, 2001).

In spite of some opposition from e.g. Kagan, (1999) who advocates that b is essentially constant, others such as (Okal and Romanowicz, 1994; Wiemer and Benoit, 1996; Ayele and Kulhanek, 1997; Wiemer et al., 1998; Gerstenbergeret et al. 2001; Enescu and Ito, 2002, 2004; Bayrak and Ozturk, 2004) supported by numerous observations argue that significant spatial and temporal variations in b exist. Near or local events are often associated with b-variations of duration of days or even hours (Grunthal et al., 1982; Hurtig and Stiller, 1984; Udias and Mezcua, 1997; McNally, 1989; McGarr, 1984; Monterroso and Kulhanek, 2003; Nuannin et al, 2002; Katsumata, 2006)

There are several plausible explanations for observed variations in b-values such as high and low stresses being responsible for earthquake series with low and high b-values (Scholz, 1968; Wyss, 1973). This observation is employed to study stress levels and structural anomalies in the crust and/or upper mantle (subduction) for example in earthquake prediction and in identifying volumes of active magma bodies (Wiemer and Benoit 1996; Mori and Abercrombie, 1997; Wiemer at al., 1998) or roots of regional volcanism (Monterroso and Kulhanek, 2003) and material heterogeneity (Mogi, 1962). Large heterogeneities correspond to higher b-values. Laboratory tests showed (Warren and Latham, 1970) that an increase of thermal gradients caused an increase of b from 1.2 to 2.7.

2.26.2 Techniques for estimating seismic b-values

There are at least three techniques currently utilized in b-value determinations

Linear curve fitting method (Kulhanek 2005),

Linear least-squares method (Bender 1983, Lin et al 2008) and

Maximum-likelihood method (Utsu, 1965; Aki 1965; Gertenberger et al 2001).

There are two options for window size; constant-size windows and constant-number of events in the window. Both spatial and temporal variations in b are examined by making use of sliding space- and time-windows, respectively. In both cases we have the option to employ constant-size windows or constant-number of events in the window.

The constant-size windows approach implies a varying number of events in each window; for each b calculation and consequently each b is determined with different statistical significance. Selection of a proper window length will depend on data available and may complicate the analysis.

The constant-number of events in the window technique implies different window size as the window moves over the grid in which b-values are to be determined. This in its turn has a negative impact on the time scale (for temporal variation examinations) which now becomes non-linear. Constant-number of events technique may suffer from a drawback generated by time intervals with low level seismicity (e.g. due to a pause in mining operations). If this is the case, long time windows will be applied resulting in window lengths much larger than grid-elements and an undesired strong smoothing effect will take place. The final window size (usually determined empirically) will be a reasonable compromise between required resolution and smoothing between grid nodes.

Generally speaking, ΔM should be small to approximate well continuous magnitudes but at the same time each magnitude group should comprise large numbers of data. These are obviously two opposing requirements and a proper compromise must be found. When studying spatial or temporal variations in b-values, results must be stable or robust and not dependent on personal choice of input parameters. It is advisable to carry out tests with different catalogs, catalog time spans, window lengths, threshold magnitudes and magnitude sampling (Kulhanek, 2005).

2.27 Chaos Theory

In non –technical terms chaos means a state of complete disorder. In science it is a non-linear dynamical system that lies between regular deterministic system and stochastic system. A chaotic system is deterministic but difficult to predict because it is sensitive to initial condition (the butterfly effect). For a dynamical system to be classified as chaotic, it must have the following properties: It must be sensitive to initial conditions (i.e. nearby trajectories separate exponentially), must be topologically mixing and its periodic orbits must be dense.

2.28 Deterministic system

A deterministic system is a system in which the later states of the system are determined by the earlier or initial states or the present state determine what the future will be, such that similar initial states will always produce the same result or output. The future dynamics of a deterministic system are fully defined by their initial conditions with no elements of randomness involved in the development of future states of the system. Such a system contrasts with a stochastic or random system in which future states are not determined from previous ones.

2.29 Predictability

Predictability is the degree to which a correct prediction or forecast of a system's state can be made either qualitatively or quantitatively.

Perfect predictability implies strict determinism, but lack of predictability does not necessarily imply lack of determinism. Limitations on predictability could be caused by factors such as a lack of information or excessive complexity (Kiekeben 1999). Perfect prediction is practically impossible because there may be observational errors in determining variables and physical observables in experimental science. Experiments which have only one possible result or outcome i.e. experiment whose result is certain or unique are called deterministic or predictable experiments. The result of these experiments is predictable with certainty and is known prior to its conduct. This approach stipulates that the conditions under which the experiment is conducted would determine its result.

2.30 Stochastic or Random system

A stochastic or random process is a probabilistic process as opposed to a deterministic process because there is some indeterminacy such that even if the initial condition or starting point is known, there are several many directions in which the process may evolve. A similar initial condition may give entirely different result or output.

Randomness has to do with whether something is deterministic or not. In general, something is considered random if the output can't be determined from the input. Dynamical systems are deterministic if there is a unique consequent to every state, or random if there is a probability distribution of possible consequents e.g. the coin tossing has two consequents with equal probability for each initial state.

Markov chains and other random walks are not deterministic systems, because their development depends on random choices. An example of a stochastic system would be the sequence of heads or tails of an unbiased coin, or radioactive decay.

2.31 Chaotic system

Chaos is a type of motion that lies between regular deterministic trajectory that are predictable and the unpredictable stochastic behaviour that is characterized by complete randomness, in other words the system follows deterministic rule but its evolution appear random (Goldstein et al, 2002). Non-linear dynamical systems that appear to have random, unpredictable behaviour. Chaotic system is dynamic system that is deterministic, non-linear, sensitive to initial condition hence difficult to predict. Stochastic behaviour occurring in a deterministic system. Chaos is the study of deterministic systems that are so sensitive to measurement that their output appears random (Turcotte, 1991; Goldstein et al, 2002).

One characteristic of a chaotic system is that although the motion is deterministic i.e. given an exact initial condition, we can exactly describe its future motion mathematically, it is nonperiodic; i.e., it never quite repeats itself exactly. Chaotic system been a deterministic system, is predictable on a short time scale, but on a long time scale, chaotic systems become unpredictable. They behave seemingly irregular, that is why such systems are called chaotic. Predictability is lost at a time, called prediction horizon, which depends only logarithmically on the uncertainty of the initial conditions. Thus, the prediction horizon increases fairly slowly with increasing knowledge of the initial condition. There is an ultimate prediction horizon because the error of the initial condition can not be smaller than the unavoidable thermal noise. We can not foresee the future beyond this horizon. It depends on the system how far away this horizon actually is.

Chaos presents itself in an incredibly diverse range of areas of science, e.g. Medicine; Irregular heart rhythms studied by cardiologists. Astronomy; the erratic motion of some planetary satellites, such as Saturn's moon. Electronic engineering; the observed quirky behaviour in electronic circuits. Biology, mathematics, chemistry, economics, ecology, the stock market and, perhaps, even the quantum world all cross paths with chaos. Even, many experimental data in chemical kinetics or electronics have shown that chaos can be found in such systems. So more than a mathematical artefact chaos seems to be the essence of nonlinear and long-range unpredictable systems. Detecting the presence of chaos in a dynamical system is an important problem that is solved by measuring the largest Lyapunov exponent. Lyapunov exponents quantify the exponential divergence of initially close state-space trajectories and estimate the amount of chaos in a system (Rosenstein et al 1993).

Long term behaviour is difficult or impossible to predict: Even very accurate measurements of the current state of a chaotic system become useless indicators of where the system will be. One has to measure the system again to find out where it is. A key element of deterministic chaos is the sensitive dependence of the trajectory on the initial conditions.

2.32 Chaotic Trajectory

Chaotic trajectory is a trajectory in which the motion wanders around an extensive and an irregular shaped region of phase space in a manner that appears to be random, but that in fact is tempered by constraints. Chaotic trajectory is also known as Chaos Sea.

2.33 Lyapunov Exponents

A defining feature of a chaotic system is sensitivity to initial conditions. If two trajectories which start off close to each other deviate more and more with increasing time, the system is said to be chaotic. The rate at which nearby trajectories deviate from each other with time is characterized by a quantity called the Lyapunov exponent. The exponential divergence or convergence of nearby trajectories (Lyapunov exponents) is conceptually the most basic indicator of deterministic chaos, (Sano and Sawada, 1985). Lyapunov exponents quantify the exponential divergence of initially close state-space trajectories and estimate the amount of chaos in a system (Rosenstein et al, 1993). It is the most useful diagnostic for dynamical system (Wolf et al, 1985).

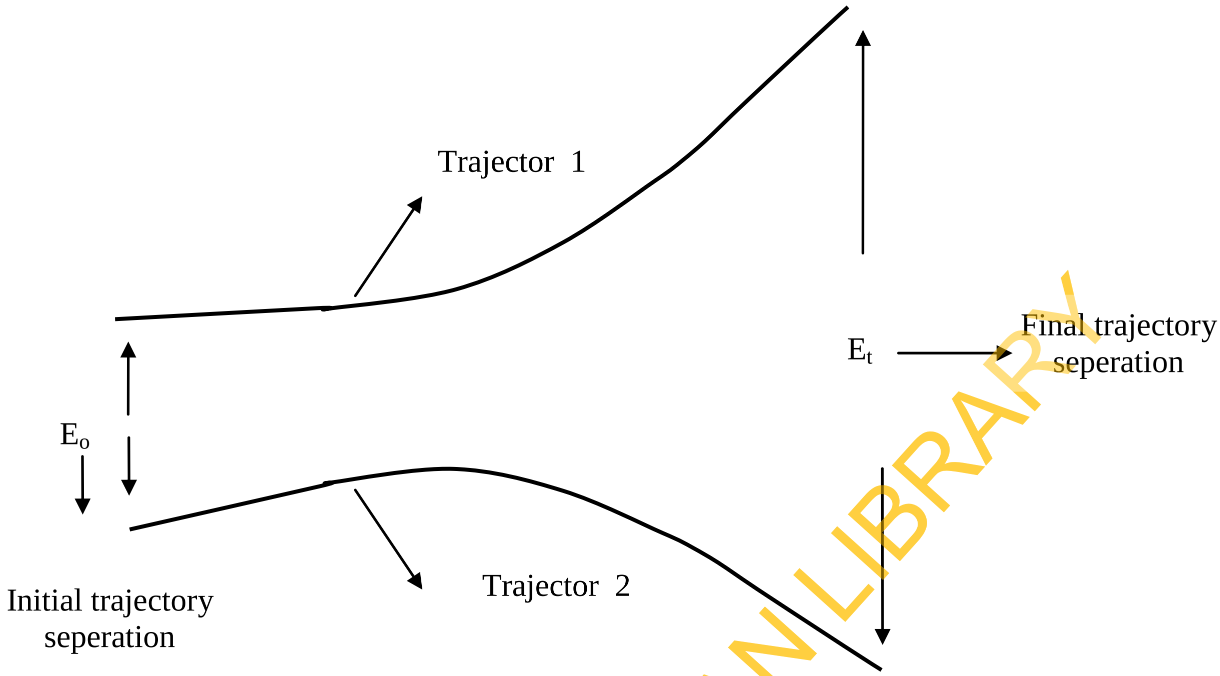

Fig 2.9: Diagram showing the separation of two trajectories (After Wolf et al, 1985).

This exponential divergence can be measure and characterize using Lyapunov exponents. In figure 2.9 ε_0 is the observed separation of two very close points on separate trajectories on the attractor. After an elapsed time, t, the trajectories have diverged and their separation is now ε_t. As this separation is exponential, we may write as

$$\varepsilon_t = \varepsilon_o e^{\lambda t} \tag{2.3}$$

$$\lambda = \frac{1}{t} \ln \left| \frac{\varepsilon_t}{\varepsilon_o} \right| \tag{2.4}$$

The above expression for the Lyapunov exponent is used to measure the average divergence properties of experimental strange attractors. This is done by following a reference trajectory through time and comparing the divergence of close by trajectories over a portion of the attractor period. The method is illustrated in figure 2.9, where the reference, or fiducially, trajectory is followed and its divergence from a nearby trajectory is monitored. Once the separation becomes too large, another nearby trajectory is selected and so on. The Lyapunov exponent is calculated many times at various locations on the attractor, and an average taken. If we monitor N nearby trajectory segments, the averaged Lyapunov exponent for the attractor is then,

$$\lambda = \frac{1}{N} \sum_{i=1}^{N} \frac{1}{t} \ln \left[\frac{\varepsilon_{ti}}{\varepsilon_{oi}} \right] \tag{2.5}$$

Nearby trajectories on strange attractors diverge, while still remaining in a bounded region of phase space due to the folding process. To fully characterize the divergence and convergence properties of an attractor we require a set of Lyapunov exponents, one for each orthogonal direction of divergence or convergence in phase space. The number of Lyapunov exponents required to define the attractor is equal to the dimension of its phase space. Thus, the Lyapunov exponent is a valuable measure which may be used to categorize chaotic attractors. If we calculate the Lyapunov exponent for orthogonal directions of maximum divergence in phase space, we obtain a set of Lyapunov exponents ($\lambda 1$, $\lambda 2$, $\lambda 3$, . . ., λn), where n is the dimension of the phase space. This set of Lyapunov exponents is known as the Lyapunov spectrum and is usually ordered from the largest positive Lyapunov exponent, λ1, down to the largest negative exponent, λn,, i.e. maximum divergence to maximum convergence. The sum of Lyapunov exponents is the average contraction rate of volumes in phase space, this sum is less than zero in dissipative dynamical system.

$$\sum_{t=1}^{n} \lambda_i < 0 \qquad 2.6$$

where n is the number of Lyapunov exponents in the spectrum.

The positive Lyapunov exponents are directly related to the directions of trajectory divergence in phase space. Knowledge of these positive exponents enables us to quantify the limitations of predictions of the future state of the dynamical system based on the knowledge of the current state of the system to a finite resolution. The error inherent within a finite precision measurement blows up exponentially and soon becomes of the order of the attractor itself.

$$t_p = \frac{1}{\lambda_t} \ln \frac{\varepsilon_a}{\varepsilon_e} \qquad 2.7$$

If we denote the attractor size by ε_a, and the measurement error by ε_e, then the time required for the error to blow up to the size of the attractor is where t_p is the prediction horizon, i.e. the time above which predictions are useless.

2.34 Measurement of Lyapunov Exponents

A search for information on the practical measurement of Lyapunov exponents should begin with the paper by Wolf et al (1985) in which program listings are given for the determination of the principal Lyapunov exponent, λ1, and also λ1 + λ2. In addition, Lyapunov spectra are given for various systems including the Lorenz and Rössler systems together with their calculated Lyapunov dimensions (Kaplan and Yorke 1979). Methods for determining the Lyapunov spectra of a chaotic time series are given by Froyland and Alfsen (1984), Sano and Sawada (1985), Eckmann et al (1986) and Darbyshire and Broomhead (1996). In addition, Froyland and Alfsen (1984) present the Lyapunov exponents for the Lorenz model over a wide range of the r control parameter. Similarly, Zeni and Gallas (1995) have used the Lyapunov exponent to investigate the occurrence of chaos in the Duffing oscillator over a wide range of control parameters. The problem of noisy and spurious Lyapunov exponents is dealt with by Bryant et al (1990) and Parlitz (1992). Velocity dependent Lyapunov exponents have been developed by Deissler and Kaneko (1987) for characterizing chaotic systems where the dynamical processes of interest are in a moving frame of reference (Yang et al 1996; Mehra and Ramaswamy, 1996).

Lyapunov exponents have been used to characterize dynamical systems, both real and modelled. A good example is by Brandstäter et al (1983), who use both characterization techniques to investigate chaos in Taylor–Couette flow. Brandstäter and Swinney (1987) investigate the same system and provide examples of the use the minimum mutual information criterion, power spectra, phase portraits and dimension estimates, together with a discussion of the potential problems associated with dimension estimates.

2.35 Sign of Lyapunov exponents

The signs of the Lyapunov exponents provide a qualitative picture of a system's dynamics, its sign indicates whether the system is chaotic or not chaotic.

Lyapunov exponents provide a way to identify the qualitative dynamics of a system, because they describe the rate at which neighbouring trajectories converge or diverge from one another in orthogonal directions. If the dynamics occur in an n- dimensional system, there are n exponents. Since the maximum exponent will dominate, this limit is practically useful only for finding the largest exponent. Chaos can be defined as the divergence between neighbouring trajectories and the presence of a positive exponent could be considered as the diagnostic of chaos (Liu et al 2007).

$\lambda<0$ – a periodic orbit or a fixed point; The system attracts to a fixed point or stable periodic orbit. These systems are non conservative (dissipative) and exhibit asymptotic stability.

$\lambda=0$ – a marginally stable orbit; The system is neutrally stable. Such systems are conservative and in a steady state mode. They exhibit Lyapunov stability.

$\lambda>0$ – chaos.; The system is chaotic and unstable. Nearby points will diverge irrespective of how close they are.

The Lyapunov exponent is positive when neighbouring trajectories diverge from each other at large n, which corresponds to chaos. However if the trajectories converge to a fixed point or limit cycle they will get closer together, which corresponds to negative Lyapunov exponents.

Hence it can be determine whether or not the system is chaotic by the sign of the Lyapunov exponent. It is a way of distinguishing between a stochastic process and a deterministic system. Lacasa and Toral (2010) or a quantitative measure of the sensitive dependence on the initial conditions is the Lyapunov exponent. It is the averaged rate of divergence (or convergence) of two neighbouring trajectories in the phase space. There is a whole spectrum of Lyapunov exponents, their number is equal to the dimension of the phase space. If one speaks about the Lyapunov exponent, this refers to the largest one. The maximum Lyapunov exponent can be found using equation 2 .8 by Wolf et al, 1985.

$$\lambda_n = \frac{1}{n}\sum_{j=1}^{n} \ln\left|\frac{d_j}{d_0}\right| \qquad (2.8)$$

where d_j is the distance between the jth point-pair.

2.36 Computation of Lyapunov Exponents from experimental data

Obtaining the Lyapunov exponents from a system with known differential equations is no real problem and was dealt with by Wolf et al (1985). In most real world situations we do not know the differential equations and so we must calculate the exponents from a time series of experimental data. Extracting exponents from experimental data is a complex problem and requires care in its application and the interpretation of its results (Lacasa and Toral, 2010).

2.37 Phase Space

An understanding of the way in which dynamical systems evolve in time is facilitated by considering the concept of phase space, which has coordinates corresponding to the independent dynamical variables of the system.

Phase space is the collection of possible states of a dynamical system. A phase space can be finite (e.g. for the ideal coin toss, we have two states heads and tails), countably infinite (e.g. state variables are integers), or uncountably infinite (e.g. state variables are real numbers). A point in phase space may be a fixed (or equilibrium) point if at that point all the momentum coordinates are zero and the position coordinates are such that no net forces exist in the system. The trajectory then ends at the fixed point. If a phase-space point is not an equilibrium point, the time-reversal symmetry of classical mechanics dictates that the trajectory leading to it must also be unique. A main conclusion that can be draw from these observations is that phase-space trajectories cannot cross and can only terminate at equilibrium points.

If the possible forms that trajectories can take in a two-dimensional phase space is considered (corresponding to a particle moving in one spatial dimension), the possibilities are very limited: there can be fixed points, curves that end at or spiral toward or away from points (without crossing each other), perhaps closed loops (which describe periodic orbits), or simply families of curves that neither terminate nor cross. But when the phase space has more than two dimensions, more complicated nonintersecting trajectories can, and do occur. Under suitable conditions these lead to an extremely strong dependence on initial conditions and the resulting chaotic motion is called deterministic chaos.

The fundamental starting point of many approaches in nonlinear data analysis is the construction of a phase space portrait of the considered system. The state of a system can be described by its state variables. The state variables at time t form a vector in a d-dimensional space which is called phase space. The state of a system typically changes in time, and, hence, the vector in the phase space describes a trajectory representing the time evolution, the dynamics, of the system. The shape of the trajectory gives hints about the system; periodic or chaotic systems have characteristic phase space portraits.

2.38 Analysis of Phase Space

The phase-space trajectories of a dynamical system can be used as an indicator to determine whether the motion of that system is chaotic. However, for any system of real interest the phase space is of too great a dimension to make its trajectories easy to visualize, and there are two techniques that have been found helpful for that purpose. First, the trajectories can be projected onto a plane; if the trajectory is periodic, so also will be its projection. The projected curves may have intersections, but these do not signify intersections of the actual trajectories, as the curves that intersect have different values of at least one coordinate not in the plane of projection. Projected curves that are not periodic but neighbouring at one point may remain neighbouring as they travel on the plane of projection, but it is also possible that they deviate wildly from each other upon extension in time, and may even more or less densely fill the entire regions of the projected space in a chaotic or seemingly random manner. This is an indication of chaos.

2.39 Phase Space Reconstruction

In dissipative dynamical systems, variables evolve asymptotically toward low‐dimensional attractors that define their dynamical properties. Unfortunately, real world dynamical systems are generally too complex for us to directly observe these attractors. Fortunately, there is a method called phase space reconstruction that can be used to indirectly detect attractors in real world dynamical systems using time series data on a single variable (Broomhead and King, 1985; Schaffer and Kot, 1985; Kot et al, 1988; Williams, 1997). Armed with this knowledge, we can formulate more accurate and informative models of real‐world dynamical systems. (Huffaker, 2010). Phase space reconstruction is a potentially useful method for detecting the dynamical structure of real world systems that generate the historical data we observe. As a part of diagnostic modelling, it can improve the formulation and performance of dynamical models.

The method uncovers surprising structure in apparently random data. This justifies more extensive use of deterministic modelling based on principles of theory as opposed to application of stochastic methods, when faced with apparently random data. The phase space reconstruction is not exactly the same to the original phase space, but its topological properties are preserved. Using the time delay embedding, we can reconstruct this phase space portrait using only one observation, the reconstructed phase space is almost the same as the original phase space. The characteristic properties of chaotic systems can be revealed from this reconstruction as well.

CHAPTER THREE

DATA AND METHOD

3.1 Study Area

The Circum-Pacific seismic zone or Pacific Ring of Fire is a zone of frequent earthquakes and volcanic eruptions. The horseshoe –shaped zone encircles the basin of the Pacific Ocean and it is about 40,000 km in length. It is the source of 90% of the world‘s major earthquakes. The earthquakes in the zone are the most recorded according to the United States Geological Survey Department.

The Pacific Ring of Fire (sometimes called the Ring of Fire) is an area where large numbers of earthquakes and volcanic eruptions occur in the basin of the Pacific Ocean. The area is associated with a nearly continuous series of oceanic trenches, volcanic arcs, volcanic belts and plate movements. The Ring of Fire has 452 volcanoes and is home to over 75% of the world's active and dormant volcanoes

The eastern section of the ring is the result of the Nazca Plate and the Cocos Plate being subducted beneath the westward moving South American Plate (Figures 3.1 and 3.2). The Cocos Plate is being subducted beneath the Caribbean Plate, in Central America. Portions of the Pacific Plate along with the small Juan de Fuca Plate are being subducted beneath the North American Plate. Along the northern portion the northwestward moving Pacific plate is being subducted beneath the Aleutian Islands arc. Further west, the Pacific plate is being subducted along the Kamchatka Peninsula arcs on south past Japan (Figures 3.1 and 3.2).

The southern portion is more complex with a number of smaller tectonic plates in collision with the Pacific plate from the Mariana Islands, the Philippines, Bougainville, Tonga, and New Zealand; this portion excludes Australia, since it lies in the centre of its tectonic plate. Indonesia lies between the Ring of Fire along the northeastern islands adjacent to and including New Guinea and the Alpide belt along the south and west from Sumatra, Java, Bali, Flores, and Timor (Fig 3.2). The famous and very active San Andreas Fault zone of California is a transform fault which offsets a portion of the East Pacific Rise under southwestern United States and Mexico. The motion of the fault generates numerous small earthquakes, at multiple times a day, most of which are too small to be felt (Gibson and Byrd, 2007; USGS, 2010; Geography.about.com, 2010).

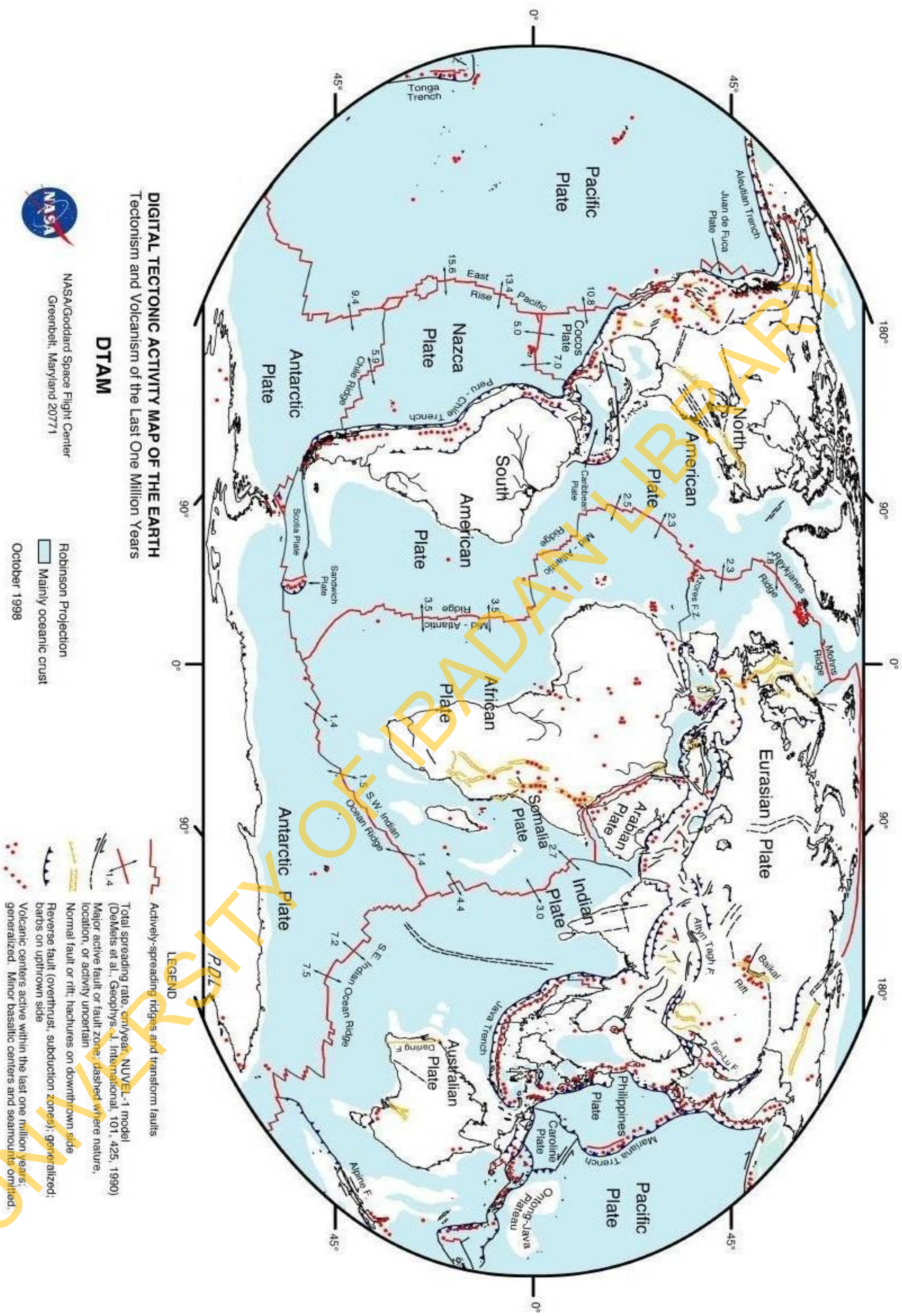

Fig 3.1; Tectonic Map of the Earth (After NASA, 1998).

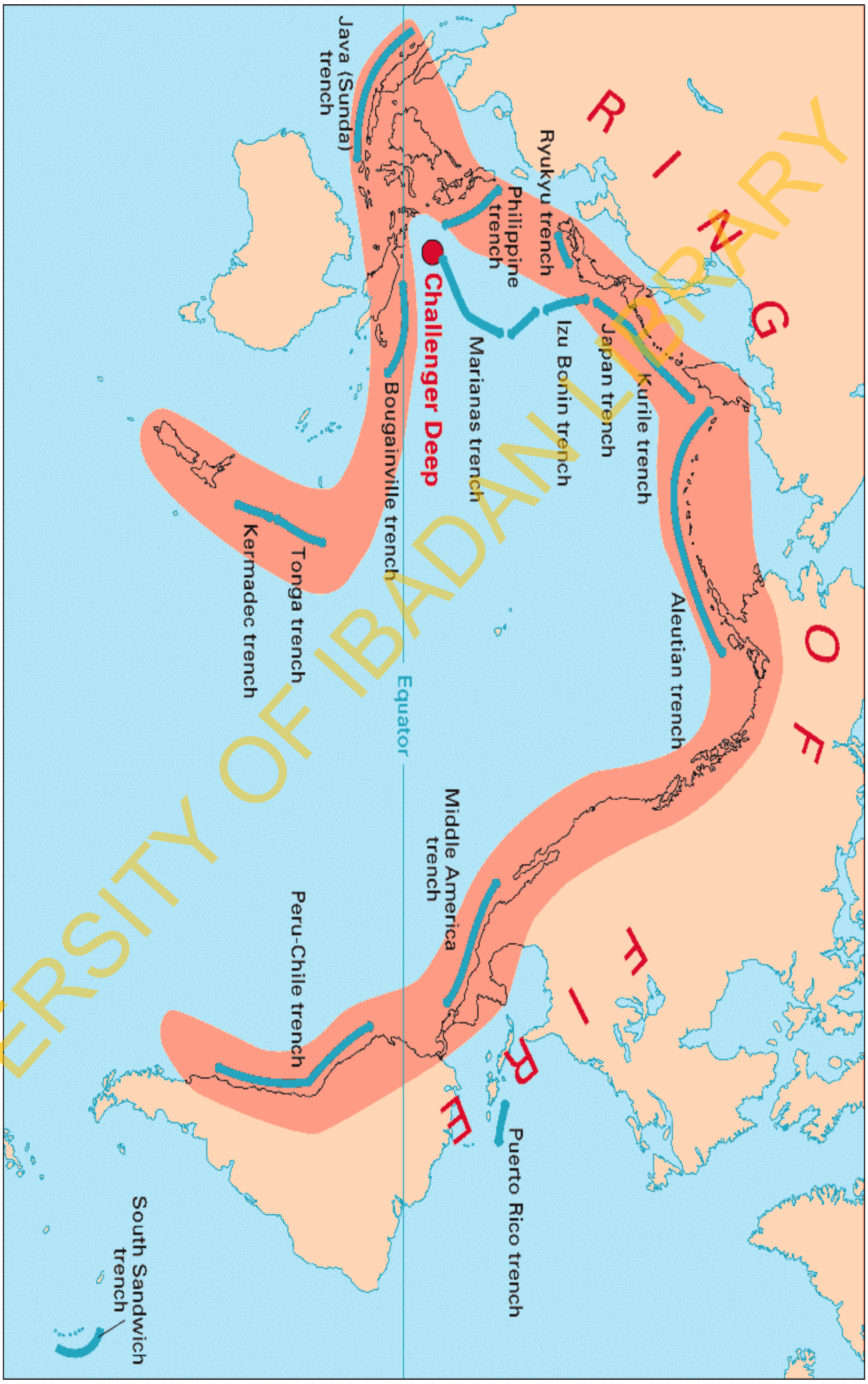

Fig 3.2; The Circum Pacific Zone’s Ring of fire (After USGS, 1999).

3.2 Data Acquisition

The data used in this study were obtained from Earthquake catalog of Advanced National Seismic System (ANSS), Northern California Earthquake Data Centre, and USA, Period of catalogue 1899-2009. The catalog contain the origin time, date, epicentre, depth in kilometre, latitude , longitude, magnitude , magnitude type (ML –local magnitude, Mb- body wave magnitude, Ms- surface wave magnitude, Me – energy magnitude and Mw - moment magnitude), and Event Identification number. Total number of events were 805, 740.

Table 3.1 showed the locations and magnitudes of large earthquakes globally from 1899 to 2009. A total of 38 events were identified. Large earthquake in the circum-pacific zone were mapped and divided into five regions as shown in Fig. 3.3.

Table 3.1; Large earthquakes (M≥ 8) global, from 1899-2009

S/N	YEAR	MONTH	DAY	LAT	LONG	DEPTH	MAG	ZONE
1	1899	9	4	60	-142	25	8.3	Subduction
2	1899	9	10	60	-140	25	8.6	Subduction
3	1900	10	10	57.09	-153.48	0	8.3	Subduction
4	1903	6	2	61.56	-158.54	0	8.3	Subduction
5	1906	8	17	50.77	179.73	0	8	Subduction
6	1929	3	7	51	-170	50	8.6	Subduction
7	1938	11	10	55.5	-158	25	8.7	Subduction
8	1949	8	22	53.62	-133.27	0	8.1	Subduction
9	1957	3	9	51.47	-175.72	33	8.6	Subduction
10	1963	10	13	44.8	149.5	60	8.25	Subduction
11	1964	3	28	61.05	-147.48	23	8.5	Subduction
12	1969	2	28	36.008	-10.573	22	8	Subduction
13	1971	1	10	-3.132	139.697	33	8.1	Subduction
14	1976	1	14	-28.427	-177.657	33	8	Subduction
15	1978	12	6	44.592	146.581	91	8.1	Subduction
16	1985	9	19	18.19	-102.533	27.9	8.1	Subduction
17	1986	10	20	-28.117	-176.367	29.1	8.1	Subduction
18	1989	5	23	-52.341	160.568	10	8.2	Ridge
19	1993	8	8	12.982	144.801	59.3	8	Subduction
20	1994	6	9	-13.841	-67.553	31.3	8.2	Subduction
21	1994	10	4	43.773	147.321	14	8.1	Subduction
22	1995	4	7	-15.199	-173.529	21.2	8	Subduction
23	1995	10	9	19.055	-104.205	33	8	Subduction
24	1996	2	17	-0.891	136.952	33	8.2	Subduction
25	1998	3	25	-62.877	149.527	10	8.1	Subduction
26	2000	11	16	-3.98	152.169	33	8	Subduction
27	2001	6	23	-16.265	-73.641	33	8.4	Subduction
28	2003	9	25	41.815	143.91	27	8.3	Subduction
29	2004	12	23	-49.312	161.345	10	8.1	Ridge
30	2004	12	26	3.295	95.982	30	9	Subduction
31	2005	3	28	2.085	97.108	30	8.6	Subduction
32	2006	5	3	-20.187	-174.123	55	8	Subduction
33	2006	11	15	46.592	153.266	10	8.3	Subduction
34	2007	1	13	46.243	154.524	10	8.1	Subduction
35	2007	4	1	-8.466	157.043	24	8.1	Subduction
36	2007	8	15	-13.386	-76.603	39	8	Subduction
37	2007	9	12	-4.438	101.367	34	8.5	Subduction
38	2009	9	29	-15.489	-172.095	18	8.1	Subduction

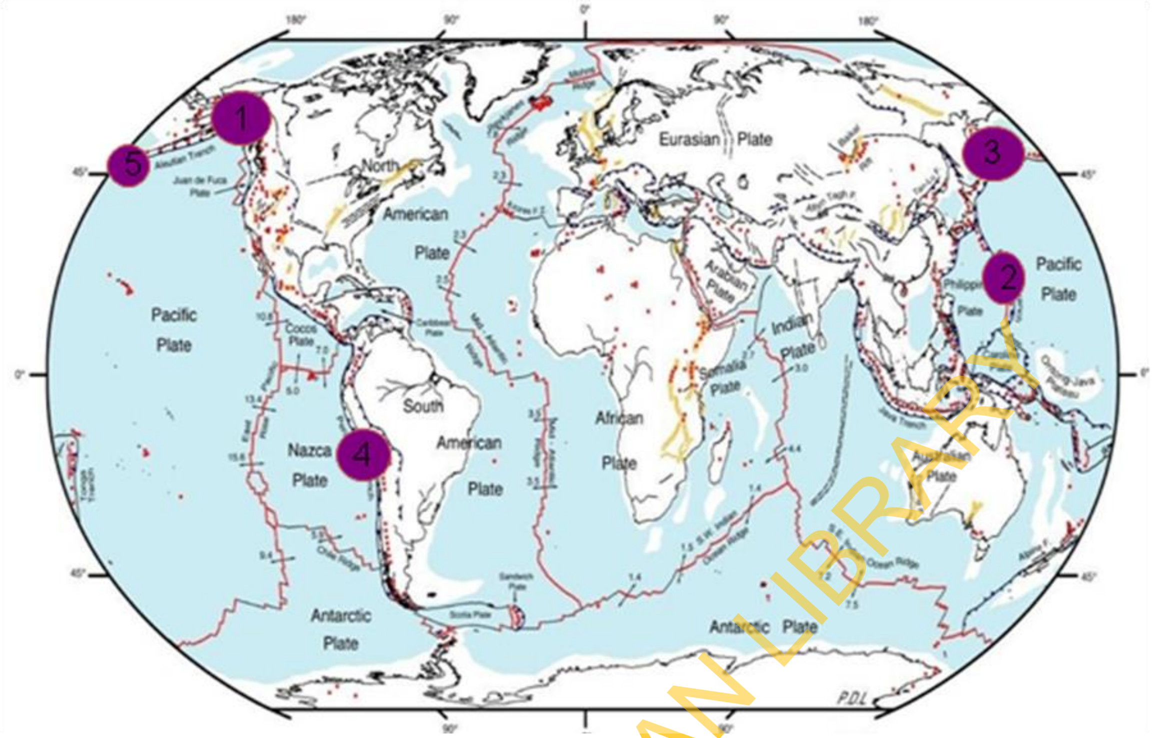

Fig 3.3: Tectonic Map of the study area (Modified After NASA, 1998).

Legend: 1: Region 1

2: Region 2

3: Region 3

4: Region 4

5: Region 5

3.3 Data Treatment

An essential requirement for a reliable determination of seismic b value is the availability of uniform or homogeneous magnitudes, completeness of data and a robust catalogue that have time span which must be at least comparable and possibly larger than the return period of the large earthquake or the largest expected event.

3.3.1 Homogeneity of magnitudes

The moment magnitude Mw was employed in this study and other magnitude types were converted to Mw using the following empirical relations and models (Geller, 1976; Kanamori, 1977; Hanks and Kanamori, 1979; Ambraseys and Boomer, 1990).

Mw does not saturate so it gives a reliable representation of the total energy released in an earthquake.

Mb = Ms +1.33	Ms < 2.86
Mb= 0.67Ms + 2.88	2.86 < Ms < 4.90
Mb = 0.33Ms + 3.91	4.90< Ms < 6.27
Mb = 6.0 Ms > 6.27	
Log Mo = Ms + 18.89	Ms < 6 .76
Log Mo = 1.5 Ms + 15.51	6.76 < Ms < 8.12
Log Mo = 3Ms + 3.33	8.12 < Ms < 8.22
Log Mo = 8.2	Log Mo > 28

Mw = 2/3 Log Mo -10.73

3.3.2 Magnitude of completeness (Mc)

Mc indicates the threshold magnitude below which a catalogue shows incompleteness in reporting for smaller magnitudes. Events in a catalogue can be interpreted to have been completely detected and recorded above Mc. Frequency – Magnitude distribution can be scale invariant down to magnitude M = 0 earthquakes if catalogue can be compiled completely for small magnitudes.

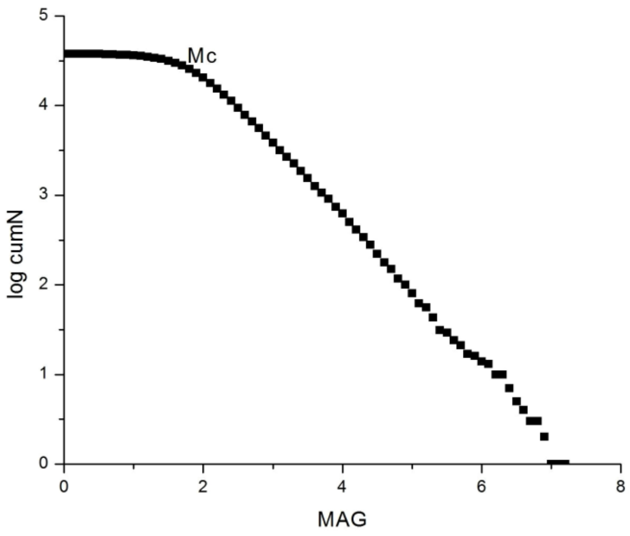

Fig. 3.4a; Graph showing the magnitude of completeness Mc for cumulative magnitude distribution.

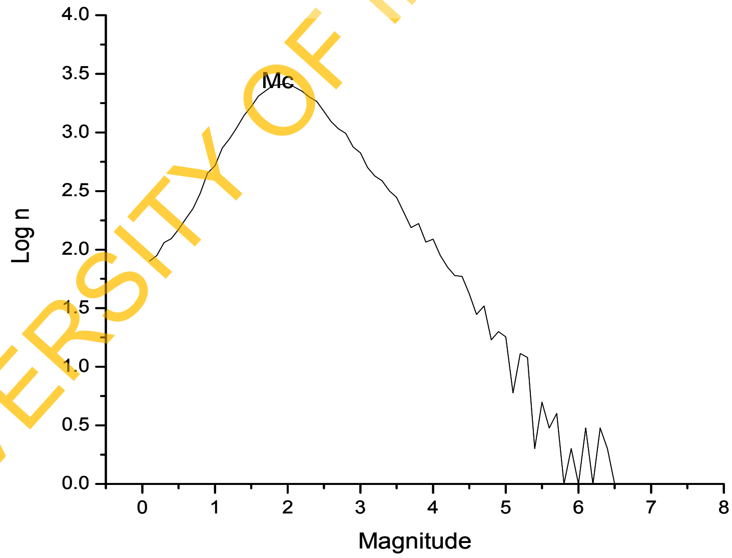

Fig. 3.4b: Graph showing the magnitude of completeness Mc for incremental distribution.

3.4 Methodology

The study area was divided into five regions.

Region 1; Latitude (67.545 to 53.197), Longitude (-163.76 to -134.498)

Region 2; Latitude (44.565 to 32.009), Longitude (148.669 to 134.406)

Region 3; Latitude (50.594 to 39.356), Longitude (157.3 to 140.72)

Region 4; Latitude (-43.3 to -29.814), Longitude (-80.2 to -66.019)

Region 5; Latitude (56.724 to 49.612), Longitude (-177.484 to -167.096)

Events in each region were divided into constant time intervals (e.g. 2, 2.5, 5, 10 years) for the investigation of the temporal distribution of earthquakes. The study area was gridded at annular width of 100km from a chosen reference centre to 700km radius for the spatial distribution.

3.4.1 Method 1; Variation of seismic b-value

The b values were obtained for each volume of spatial and temporal distribution by the linear curve fitting method, using the Gutenberg – Richter law

$$\text{Log}_{10} N = a - bM \tag{3.1}$$

where N is the cumulative number of earthquakes, Mw is the magnitude, and a and b are constants. The intercept of equation 3.1 is the constant a, it describes the rate of seismic activities while b is the slope of equation 3.1 known as seismic b value. It is a tectonic parameter for characterizing seismicity, hazard analysis and understanding earthquakes processes and evolution.

$$Mc \leq Mw < 8 \tag{3.2}$$

$$M_w = M_{c+n\Delta m} \tag{3.3}$$

where n=0,1,2----------59, the limit is determine by Mc

Δm is the magnitude increment (0.1). e.g. 0.1, 0.2 etc

In this study, Δm is equal to 0.1, this small value was chosen in other to obtain an approximately continuous magnitude. Mc value was determined separately for each region, this ensured that each magnitude group comprise large enough numbers of data.

3.4.2 Method 2; Propagation of Maximum Seismic Energy

Each selected grid volume was analyzed with CompiCat software to determine the location of the maximum seismic energy released and the highest rate of activity i.e. frequency.

CompiCat is a software program designed for studies of seismic activity based on catalogs of earthquakes. It is an application for editing and compiling catalogs of earthquakes, which is an essential part of any study of seismic activity. The application combines the features of EdCat and Catal console applications.

CompiCat program is a C++ code using Qt C++ tool kit for multiplatform Graphic User Interface and application development. It has single-source portability across Linux, UNIX, and Windows. CompiCat program was designed for reproducible studies of seismic activity based on catalogs of earthquakes. Figures 4.12 a and b shows a snapshot of the typical visualization output window of the program/software.

Equation 3.4 was formulated to study the pattern of propagation of the seismic energy and frequency with respect to a major earthquake in each sub-zone.

$$R^2 = (X - X_0)^2 + (Y - Y_0)^2 \qquad (3.4)$$

X and Y are the latitude and longitude of the reference large earthquake in the region while Xo and Yo are the latitude and longitude of the location of the maximum seismic energy released in each volume in the region respectively.

3.4.3 Method 3: Phase Space plot

Phase portraits of the seismic activities were constructed in order to study the space clustering of the seismic events associated with large earthquake.

If the position vector of an object in 2 dimension is given as r = xi + yj, the phase space plot is r’ vs r, where r’ and r are given below

$$|r| = \sqrt{(x^2 + y^2)} \qquad (3.5)$$

$$r'_n = \frac{r_n - r_{n+1}}{2} \qquad (3.6)$$

3.4.4 Method 4; Lyapunov exponent and Spectrum

The Lyapunov exponent is a quantitative measurement of the rate of exponential divergent or convergent of a dynamic system. The sign of the Lyapunov exponents provide a qualitative picture of a system’s dynamics. Its sign indicates whether the system is chaotic or not. The magnitude of the Lyapunov exponent reflect the time scale in which the system dynamic become unpredictable while its sign indicates sensitivity to initial condition (Shaw 1984; Wolf et al 1985).

If two orbits are separated by a small distance d_o at time t = 0, then at a later time t, their separation is given by d (t) = $d_o e^{\lambda t}$

$$E_n = E_0 e^{\lambda t} \tag{3.7}$$

If the system evolves through an iteration process then d (n) = $d_o e^{\lambda n}$

Where n is the number of iteration hence λ is dimensionless.

$$\lambda_n = \frac{1}{n}\sum_{j=1}^{n} \ln\left|\frac{d_j}{d_o}\right| \tag{3.8}$$

$$d_j = \sqrt{\left((x_a - x_b)^2 + (y_a - y_b)^2\right)} \quad (3.9$$

$$d_0 = \sqrt{\left((x_{ao} - x_{bo})^2 + (y_{ao} - y_{bo})^2\right)} \tag{3.10}$$

For a two dimensional system with variables x and y, the separation is defined by equation 3.9 where a and b denote the two orbits (Sprott 2003). If a and b denote two orbits, the separation between the jth pair of nearest neighbours is defined by dj while d_o is the initial separation.

Obtaining the Lyapunov exponents from a system with known differential equations is no real problem but difficult or nearly impossible for experimental data without known differential equations (Wolf et al, 1985). Experimental data typically consist of measurements of a single observable. There is a need to employ reconstruction and locating the nearest neighbour on the trajectory. The nearest neighbour is at a minimal point or distance form the reference point.

In this study, since earthquake is a single observable, x and y are defined as latitude and longitude respectively. x_a is the latitude and y_a is the longitude of the reference large earthquake while x_b and y_b are the latitude and longitude of the subsequent earthquakes respectively. The initial pair of nearest neighbours are the referenced large earthquake and the first subsequent earthquake (in time and space) within the region hence d_o is defined as the initial separation between the first subsequent earthquake and the reference large earthquake while dj is the separation between the jth subsequent earthquake and the reference large earthquake, this is necessary because earthquake is a single observable.

CHAPTER FOUR

RESULTS AND DISCUSSION

4.1 Pattern of variation of seismic b-value

The result for temporal variation of b values Table 4.1 showed an increase from 0.64228 in 1965 - 1969 period to 1.03181 in 1980 to 1984 period for Region 1 while the spatial variation Table 4.2 has the least value of 0.67034 for the volume within 500 - 600km annular width and the highest value of 0.88382 within 200 to 300km annular width. Figure 4.1 is the graphical presentation of the temporal variation of Table 4.1 while Figure 4.2 is the graphical presentation of Table 4.2 for the spatial variation. These revealed an undulating pattern for the temporal and spatial variation of b value, it also showed that the b value varies temporally and spatially.

Table 4.3 and Table 4.4 showed the results for temporal and spatial variation of b values for Region 2 respectively. There was an increase from 0.7700 in 1960 - 1964 period to 0.9290 in 1990 to 1994 period for the temporal distribution while the spatial distribution has the least value of 0.72213 for the volume within 0 - 100km annular width and the highest value of 0.84293 within annular width 300 to 400km annular width. Figure 4.3 is the graphical presentation of the temporal variation in Table 4.3 while Figure 4.4 is the graphical presentation of Table 4.3 for the spatial variation, the results shows that the b value varies temporally and spatially.

Table 4.5 shows the temporal variation of b-value on a 5 year interval from 1960 to 2009 for Region 3. The lowest value of 0.7900 was obtained within the period 1960 to 1964 while the highest value 0.9700 was obtained in 2005 to 2009. Two temporal volumes 1975 to 1979 and 1995 and 1999 have the same b value of 0.9630. The graphical presentation in Figure 4.5 shows a non linear variation of b value.

Table 4.1; Temporal variation of b-values for Region 1

T(yr)	b
1960-1964	0.66572
1965-1969	0.64228
1970-1974	0.75570
1975-1979	0.81079
1980-1984	1.03181
1985-1989	0.75138
1990-1994	0.88528
1995-1999	0.88699
2000-2004	0.70502
2005-2009	0.94625

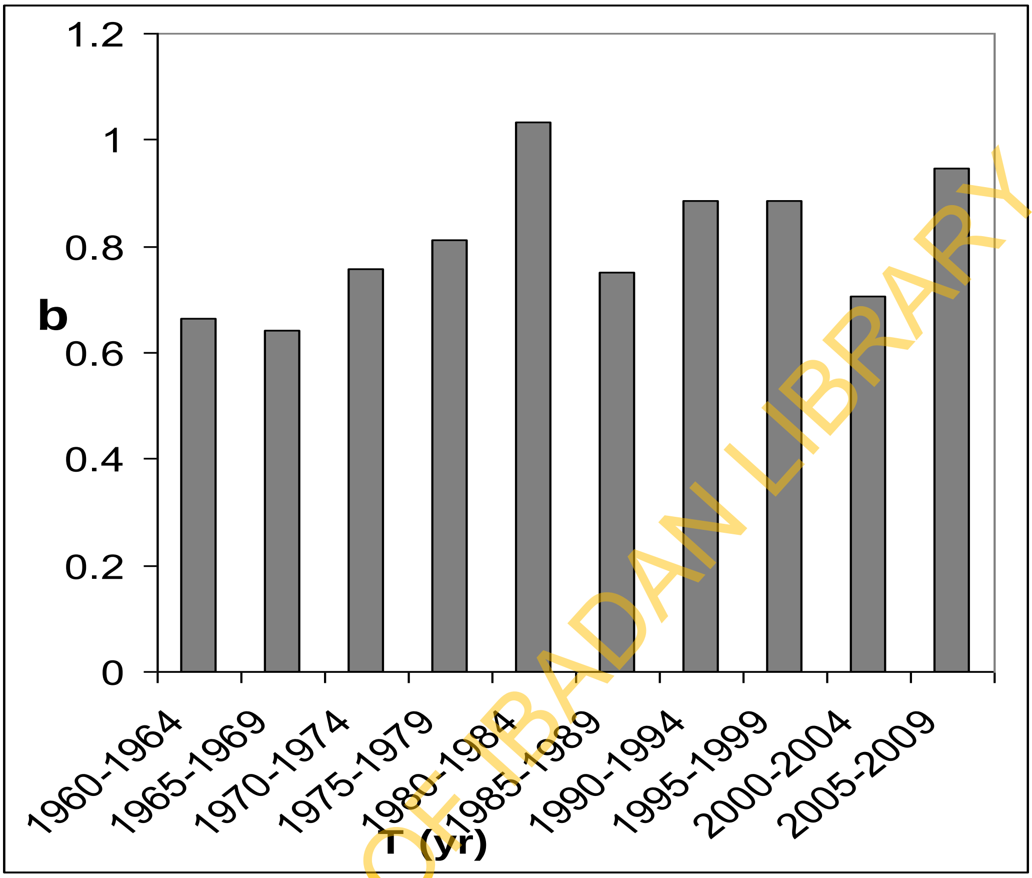

Fig. 4.1; Graphical representation of temporal variation of b-values for Region 1

Table 4.2; Spatial variation of b-values for Region 1

W(km)	**b**
0-100	0.73879
100-200	0.79196
200-300	0.88382
300-400	0.80568
400-500	0.74510
500-600	0.67034
600-700	0.70835

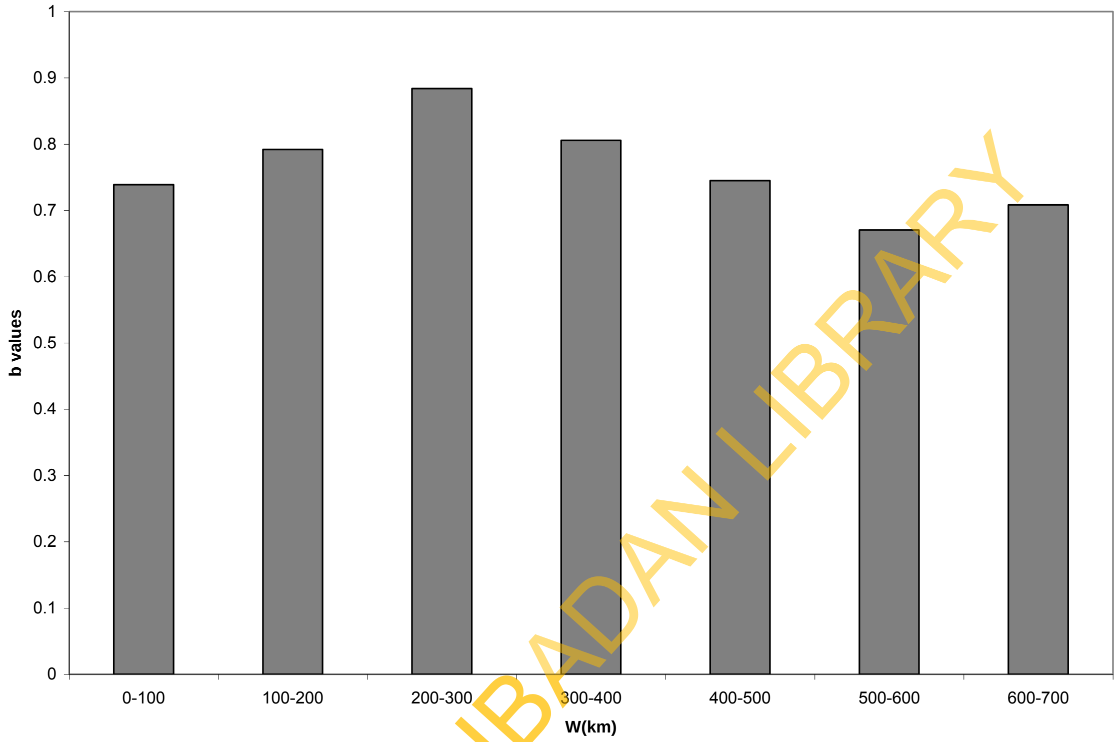

Fig. 4.2; Graphical representation of the spatial variation of b-values for Region 1

Table 4.3: Temporal variation of b-values for Region 2

T(yr)	b
1960-1964	0.7700
1965-1969	0.8400
1970-1974	0.8200
1975-1979	0.8980
1980-1984	0.8133
1985-1989	0.8796
1990-1994	0.9290
1995-1999	0.8710
2000-2004	0.7980
2005-2009	0.8780

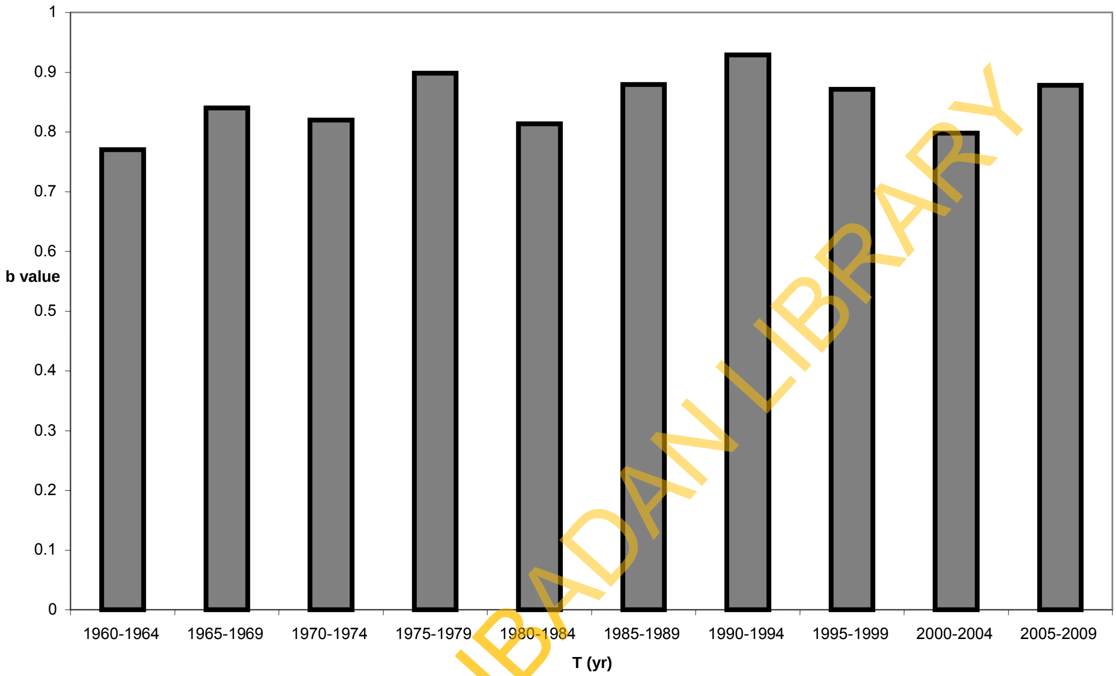

Fig. 4.3; Graphical representation of temporal variation of b-values for Region 2

Table 4.4: Spatial variation of b-values for Region 2

W(km)	**b**
0-100	0.72213
100-200	0.78178
200-300	0.84293
300-400	0.81273
400-500	0.75243
500-600	0.73390
600-700	0.73790

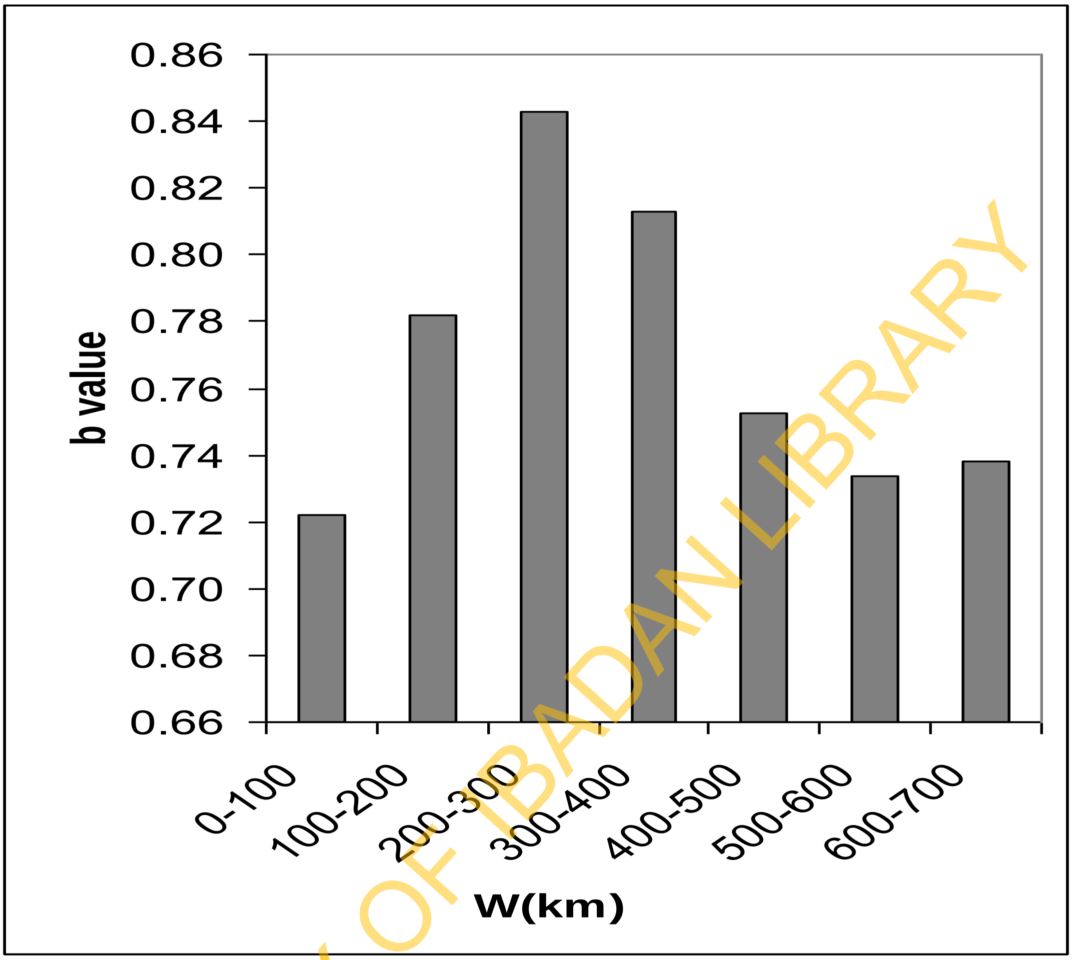

Fig. 4.4: Graphical representation of spatial variation of b-values for Region 2

Table 4.5: Temporal variation of b-values (1960-2009) for Region 3

T(yr)	b
1960-1964	0.7900
1965-1969	0.8800
1970-1974	0.8800
1975-1979	0.9630
1980-1984	0.8600
1985-1989	0.9503
1990-1994	0.8369
1995-1999	0.9630
2000-2004	0.9130
2005-2009	0.9700

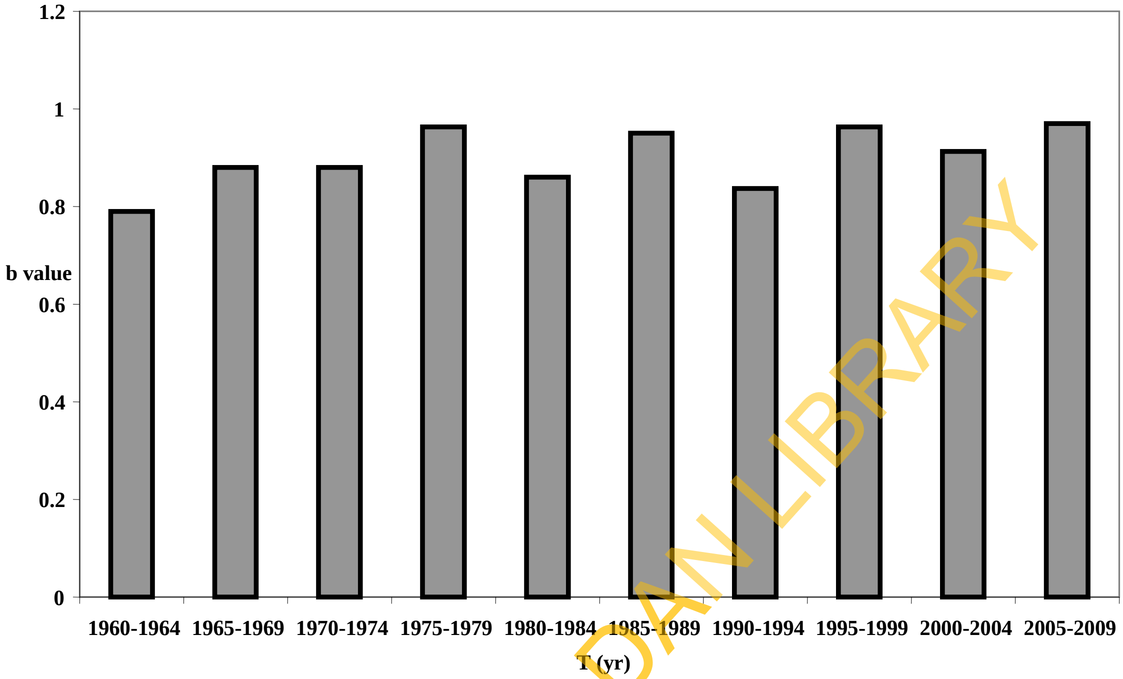

Fig. 4.5: Graphical representation of temporal variation of b-values for Region 3

Table 4.6 shows the b values extracted from the Gutenberg-Richter Distribution between 1963 and 1978. This volume is sandwiched between two large earthquakes of 1963 and 1978, the b values ranges from 0.7120 to 1.0528 the lowest was obtained in the period 1971 to 1972 and the highest was obtained in 1975 to 1976. The time interval for this volume is 2 years. The highest value is slightly different from that of 1965 to 1966 (1.0457). The graphical presentation of Table 4.6 is shown in Figure 4.6.

Table 4.7 showed the temporal variation of b values on a 2.5 years interval from 1978 to 2003. This period (1978 - 2003) is between two large earthquakes of 1978 and 2003. The lowest value of 0.8291 was obtained within the period 2001 to 2003 while the highest value 1.1258 was obtained in 1996 to 1998.The graphical presentation in Figure 4.7 showed a non linear variation of b value.

One of the most important parameters to characterize seismicity is the b-value, defined as the slope of the frequency-magnitude distribution of earthquakes. A high b-value is assumed to showed a relative abundance of smaller events compare to larger ones.

Extensive laboratory and field studies suggested that an increased material heterogeneity correspond to a higher b value (Mogi, 1962) or a high thermal gradient can cause an increase in b-value (Warren and Lathan, 1970)

Many researchers have mapped spatially the b values in several volcanic regions in the Circum Pacific Zone (Wiemer and Wyss, 1997, Wiemer et al., 1998) and found a high value of b, probably associated with the cracking produced by magma intrusion or the presence of a magma chamber. These studies suggest that the b-value may be a useful tool for studying and tracing the magma-related processes and also for volcanic hazard assessment.

Other researchers have also mapped zones of low b values, An inverse correlation is also assumed between the magnitude of observed b and the level of stress accumulated in and around the source volume, which implies that high and low stresses cause earthquake series with low and high b-values (Scholz,1968; Wyss, 1973; Kulhanek, 2005).

The zones of low b – values in the region indicated higher stress. The possible explanations for the variation of b-values include heterogeneity, temperature and stress conditions. Such anomalies were reported in several volcanic areas, sometimes occurring during earthquake swarms (Katsumata et al, 1995).

The long temporal variation employed in this research shows a pattern of b values that is repeatedly wavy or undulating but not periodic. There is no general or consistent correlation between b values and the occurrence of earthquake. Increase in b values (mountain - shaped) was observed at some period while a seismic quiescence or a decrease (valley - shaped) b values were observed at other instance Figures 4.6 and 4.7.

Table 4.6: Temporal variation of b-values in Region 3 from 1963 to 1978

T (yr)	b
1963-1964	0.8190
1965-1966	1.0457
1967-1968	0.8854
1969-1970	0.8661
1971-1972	0.7120
1973-1974	0.8967
1975-1976	1.0528
1977-1978	0.8850

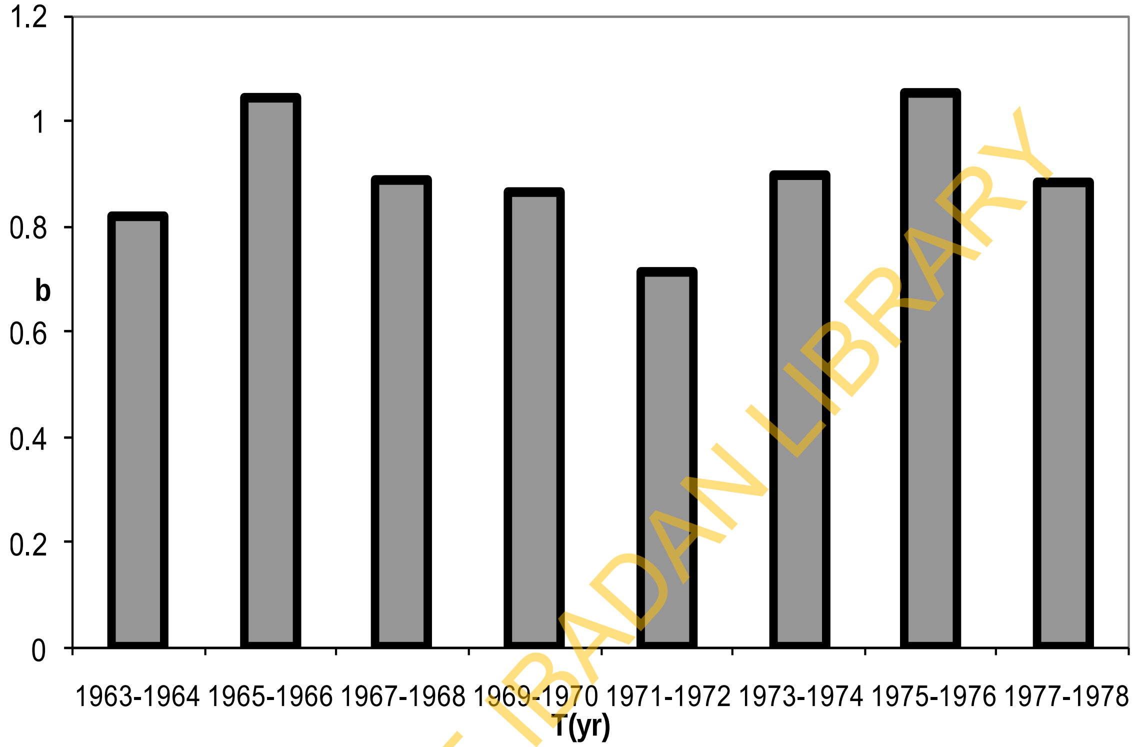

Fig. 4.6: Graphical representation of temporal variation of b-values for Region 3, 1963 to 1978.

Tab 4.7; Temporal variation of b-values (1978 to 2003) for Region 3

T(yr)	b
1978-1981	0.9431
1981-1983	0.8424
1984-1986	0.8358
1986-1988	1.0119
1989-1991	1.0337
1991-1993	0.9263
1994-1996	0.8295
1996-1998	1.1258
1999-2001	0.8462
2001-2003	0.8291

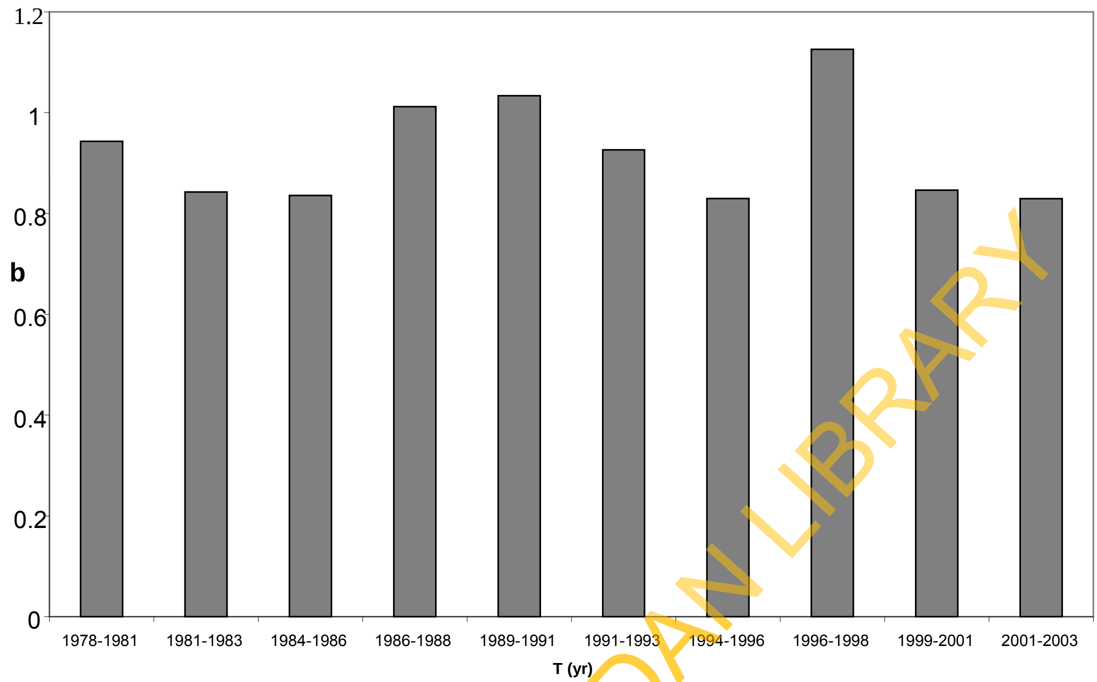

Fig. 4.7: Graphical representation of temporal variation of b-values for Region 3 1978 to 2003

Table 4.8 is the result for temporal variation of b values for Region 4. It showed a least value of 0.6705 in 1985 to 1989 period and highest value of 1.0045 in 2005 to 2009 period. The spatial variation (Table 4.9), has the least value of 0.55719 for the volume within 0 - 100 annular width and the highest value of 0.70314 within annular width 200 to 300km annular width. Fig. 4.8 is the graphical presentation of the temporal variation in Table 4.8 while Fig. 4.9 is the graphical presentation of Table 4.9 for the spatial variation.

The result for temporal variation of b values for Region 5 is showed in Table 4.10. It showed an increase from 0.55137 in 1960 to 1969 period to 0.84018 in 2000 to 2009 period, while the spatial variation in Table 4.11 has the least value of 0.50516 for the volume within 600 - 700km annular width and the highest value of 0.76027 within 200 to 300km annular width. Fig.4.10 is the graphical presentation of the temporal variation in Table 4.10 while Fig. 4.11 is the graphical presentation of Table 4.11 for the spatial variation. These reveals an undulating pattern for the temporal and spatial variation of b values, it also shows that the b value varies temporally and spatially.

One of the very important parameters for b value analysis is the magnitude of completeness. Observations showed that the magnitude of completeness varies from one region to another. In Region 1, which is North America area, the magnitude of completeness (Mc) is about 2 while in Region 4, Peru – Chile region, Mc is about 4. There is a direct relation between Mc and the density of earthquakes in the regions. Mc can be described as the magnitude, where the Gutenberg – Richter distribution curve is bending for incremental distribution or for cumulative distribution (Fig. 3.4a and Fig. 3.4b). This deviation is due to limitation of the observation system in terms of numbers and spread of the seismometers.

Table 4.8; Temporal variation of b-values (1960-2009) for Region 4

T(yr)	**b**
1960-1964	0.9587
1965-1969	0.7229
1970-1974	0.7105
1975-1979	0.7632
1980-1984	0.6827
1985-1989	0.6705
1990-1994	0.9753
1995-1999	0.8163
2000-2004	0.7478
2005-2009	1.0045

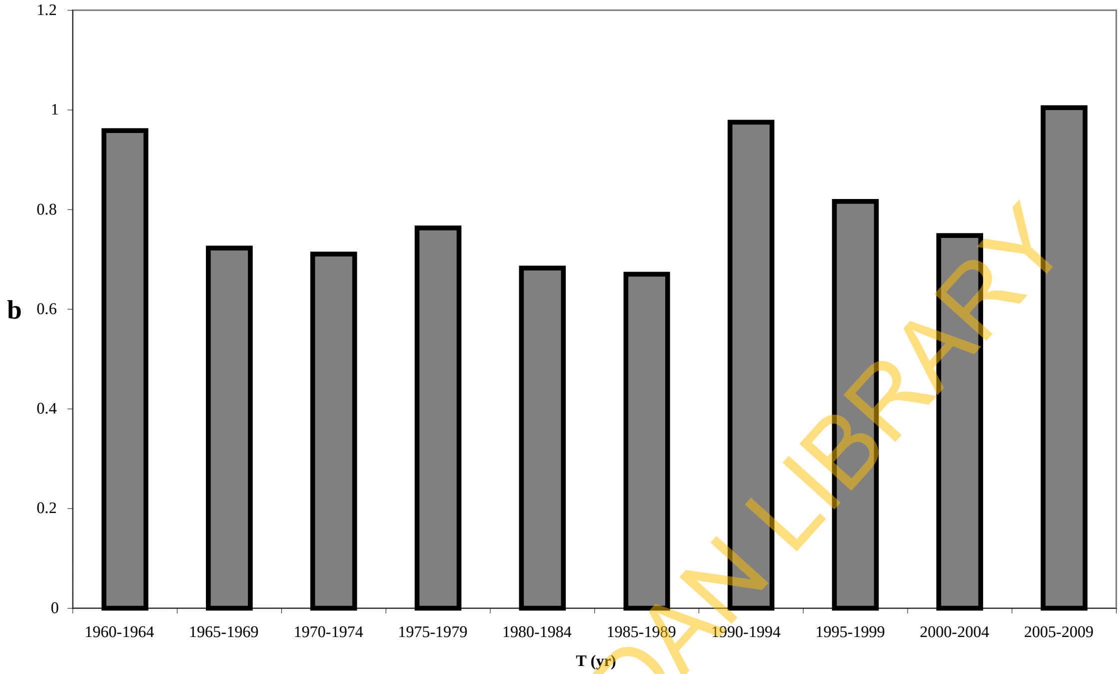

Fig. 4.8: Graphical Representation of temporal variation of b-values for Region 4

Table 4.9: Spatial variation of b-values in Region 4

W(km)	b
0-100	0.55719
100-200	0.65463
200-300	0.70314
300-400	0.64399
400-500	0.67588
500-600	0.65178
600-700	0.69887

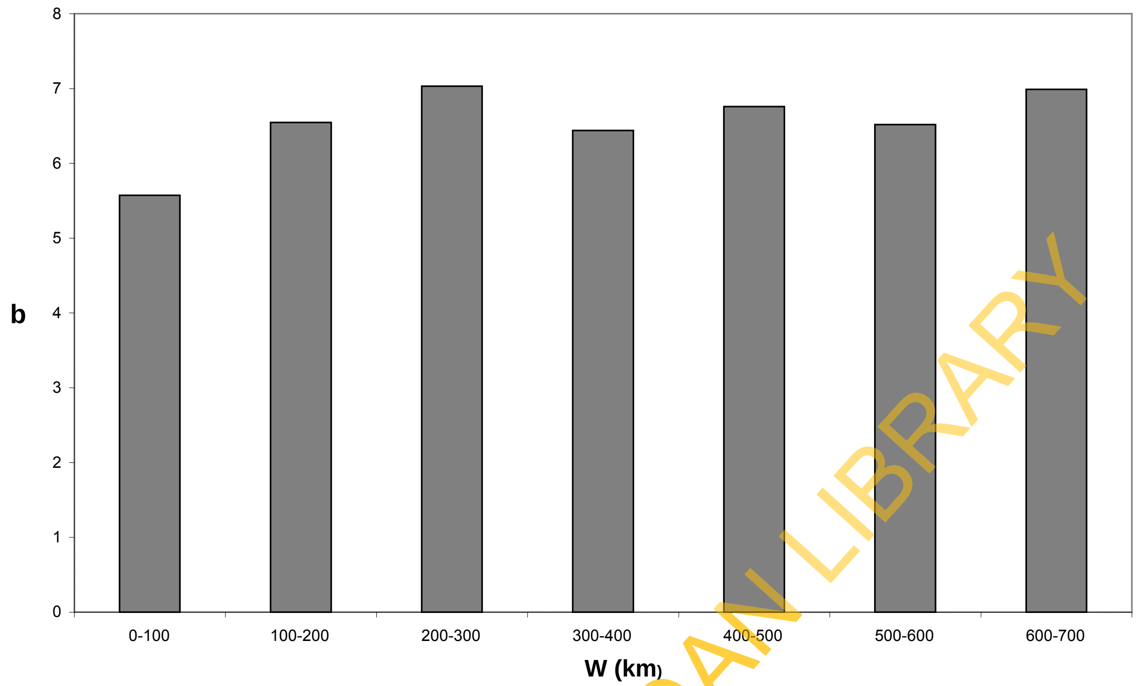

Fig. 4.9; Graphical representation of spatial variation of b-values for Region 4

Table 4.10 Temporal variation of b-values in Region 5

T(yr)	**b**
1960-1969	0.55137
1970-1979	0.57661
1980-1989	0.58334
1990-1999	0.78882
2000-2009	0.84018

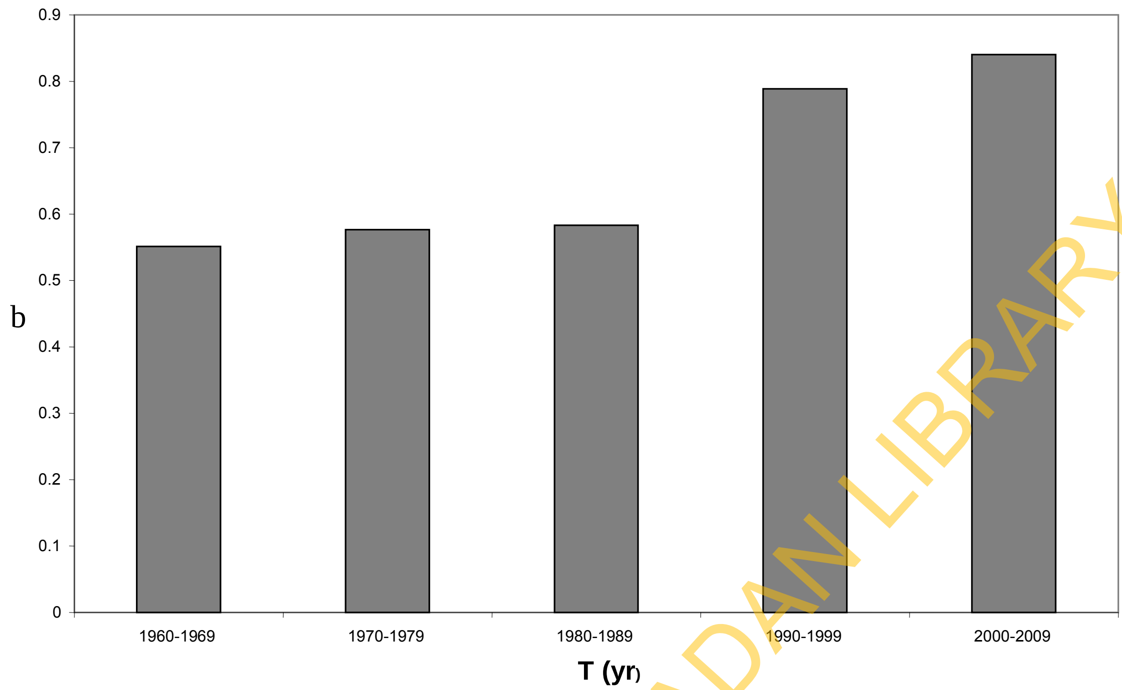

Fig. 4.10; Graphical representation for temporal variation of b values for Region 5

Table 4.11; Spatial variation of b-values in Region 5

W(km)	b
0-100	0.62189
100-200	0.68390
200-300	0.76027
300-400	0.63649
400-500	0.62571
500-600	0.57340
600-700	0.50516

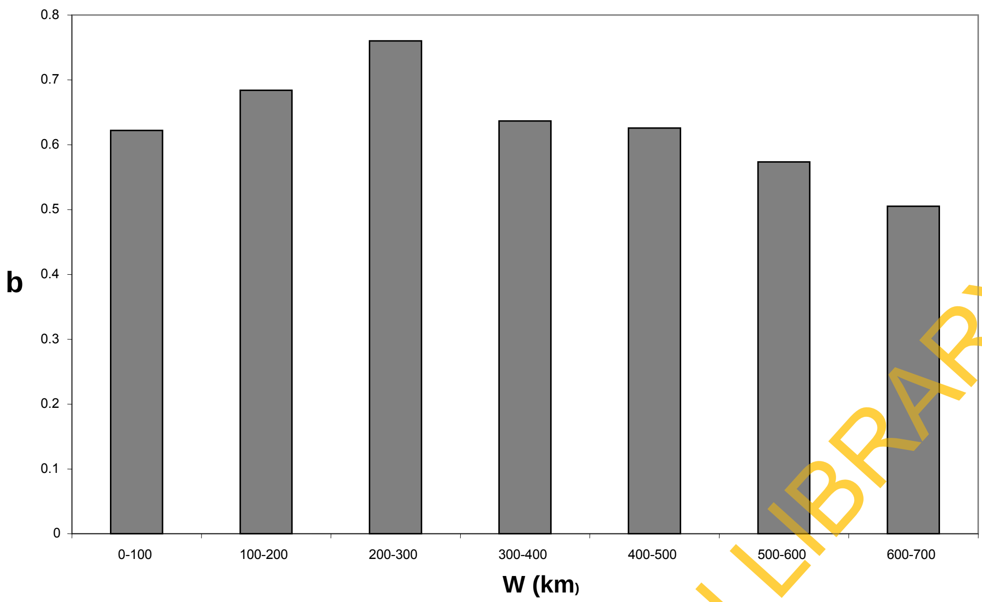

Fig. 4.11; Graphical representation of spatial variation of b values for Region 5

4.2 Propagation of Maximum Seismic Energy

Figure 4.12 a and b showed a snapshot of the typical visualization output window of the program/software. The frequencies of earthquake distribution were recorded on the snapshot as 2-dimensional intensity with different colour code depicting the high, moderate and low level of activities. The red colour indicated zones of the highest frequency of occurrence of earthquakes. The yellow colour indicates zones of moderate activities while the blue colour indicates zones of low activities.

The red colour indicated locations at which high amount of energy released was concentrated, while the yellow and the blue colours indicated zones of moderate and low seismic energy respectively. The zones and locations where maximum seismic energies were released were identified. These locations are areas of probable future earthquakes.

Table 4.12 showed the result of the locations of maximum or highest seismic energy. The 2-dimensional weighted sum of energy counts showed that between 1960 and 1964, the largest amount of energies were released at Latitude 61.58^0 and Longitude $-147.02^{0.}$; For 1965 to 1969, 1970 to 1974, 1975 to 1979, 1980 to 1984, 1985 to 1989, 1990 to 1994, 1995 to 1999, 2000 to 2004 and 2005 to 2009 periods, the maximum energy was released at Latitude 65.38^0 and Longitude -149.97^0; Latitude 59.79^0 and Longitude -142.46^0; Latitude 60.75^0 and Longitude -141.46^0; Latitude 61.02^0 Longitude -147.26^0; Latitude 56.86^0 and Longitude -142.91^0 ; Latitude 62.46^0 and Longitude-154.27^0 ; Latitude 57.34^0 Longitude -154.21^0 ; Latitude 63.44^0 and Longitude -147.43^0 ; Latitude 55.89^0 and Longitude -153.43^0 respectively.

Table 4.13 showed the propagation of seismic energy obtained or extracted from Table 4.12, using equation 3.4 where X and Y are the latitude and longitude of the reference large earthquake in the region (Table 3.1 and Figure 3.3), while Xi and Yi are the latitude and longitude of the location of the maximum seismic energy released in each temporal volume in the region respectively. Figure 4.13 showed the pattern of propagation of maximum seismic energy obtained from Table 4.12.

Table 4.14 showed the locations with the highest frequency of occurrence of earthquakes from 1960 to 2009 for region 1, while its propagation is shown in table 4.15. The pattern of propagation is shown in Figure 4.14.

(a)

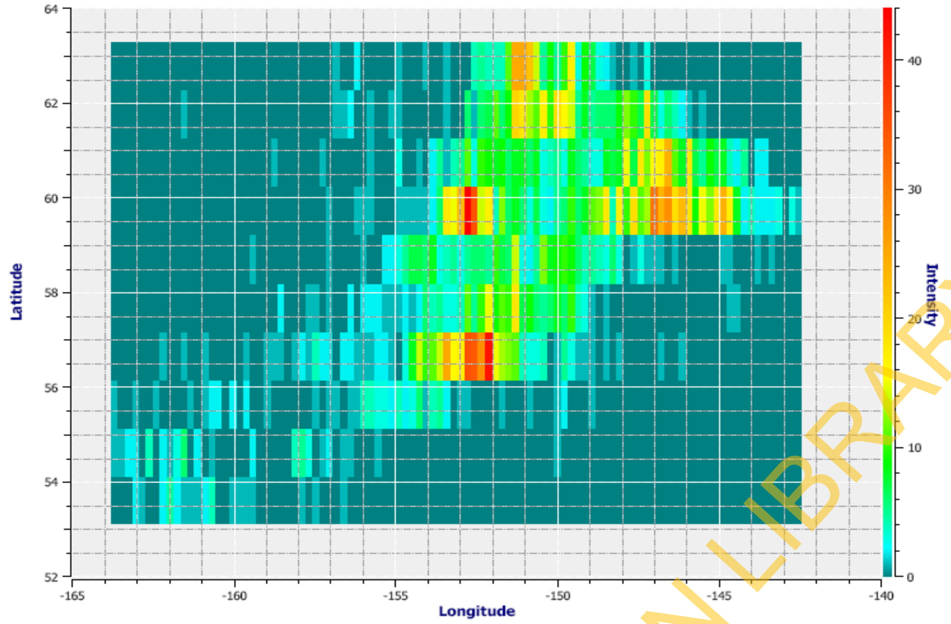

(b)

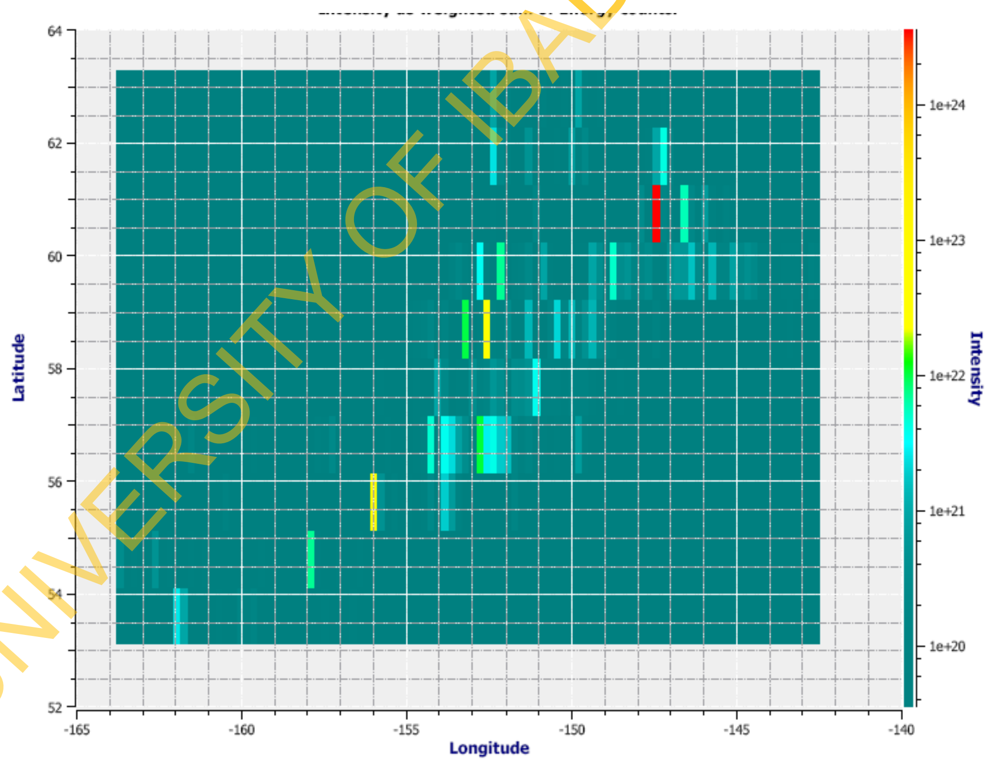

Fig 4.12 a and b; A snapshot of the typical visualization output window of the CompiCat program/software.

Table 4.12; Locations of maximum seismic energy for Region 1

Period (yr)	Latitude (^{o})	Longitude(^{o})	Energy(J)
1960-1964	61.58	-147.02	3.981E+31
1965-1969	65.38	-149.97	2.398E+26
1970-1974	59.79	-142.46	1.800E+25
1975-1979	60.75	-141.46	3.199E+27
1980-1984	61.02	-147.26	5.880E+23
1985-1989	56.86	-142.91	1.798E+25
1990-1994	62.46	-154.27	1.396E+24
1995-1999	57.34	-154.21	1.799E+25
2000-2004	63.44	-147.43	2.317E+29
2005-2009	55.89	-153.43	1.863E+22

Table 4.13 Pattern of propagation of maximum Seismic energy for Region 1

Period (yr)	**R**
1960-1964	0.7017834
1965-1969	4.9948974
1970-1974	5.1776524
1975-1979	6.0272727
1980-1984	0.2220360
1985-1989	6.2000806
1990-1994	6.9348540
1995-1999	7.6839795
2000-2004	2.3905230
2005-2009	7.8757920

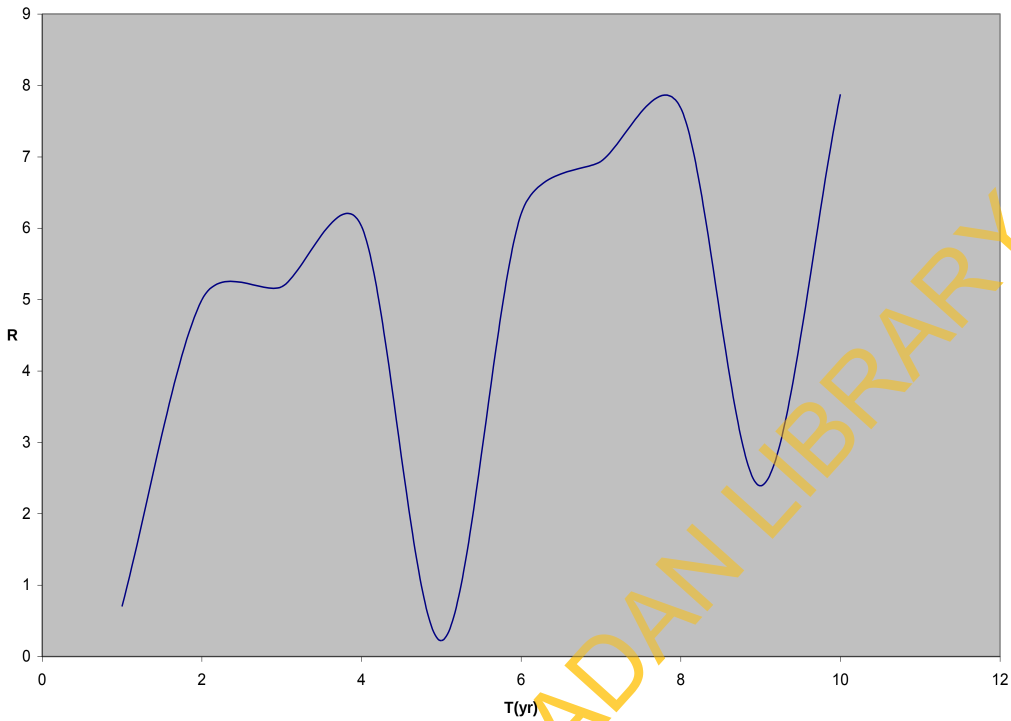

Fig. 4.13; Pattern of propagation of maximum Seismic energy for Region 1

Table 4.14; Location of highest frequency of earthquakes for Region 1

Period (yr)	Latitude (^{o})	Longitude (^{o})	Frequency
1960-1964	56.58	-152.02	10
1965-1969	65.38	-149.97	32
1970-1974	60.00	-152.83	12
1975-1979	64.82	-147.36	95
1980-1984	60.98	-147.15	50
1985-1989	66.21	-149.96	75
1990-1994	63.22	-151.03	200
1995-1999	57.96	-156.65	309
2000-2004	63.47	-147.50	417
2005-2009	60.04	-152.84	147

Table 4.15: Pattern of propagation of highest frequency of earthquakes for Region 1

Period (yr)	**R**
1960-1964	6.3712244
1965-1969	4.9958947
1970-1974	5.4510826
1975-1979	3.7719093
1980-1984	0.3414396
1985-1989	5.7250328
1990-1994	4.1572847
1995-1999	9.6706060
2000-2004	2.4200826
2005-2009	5.4543286

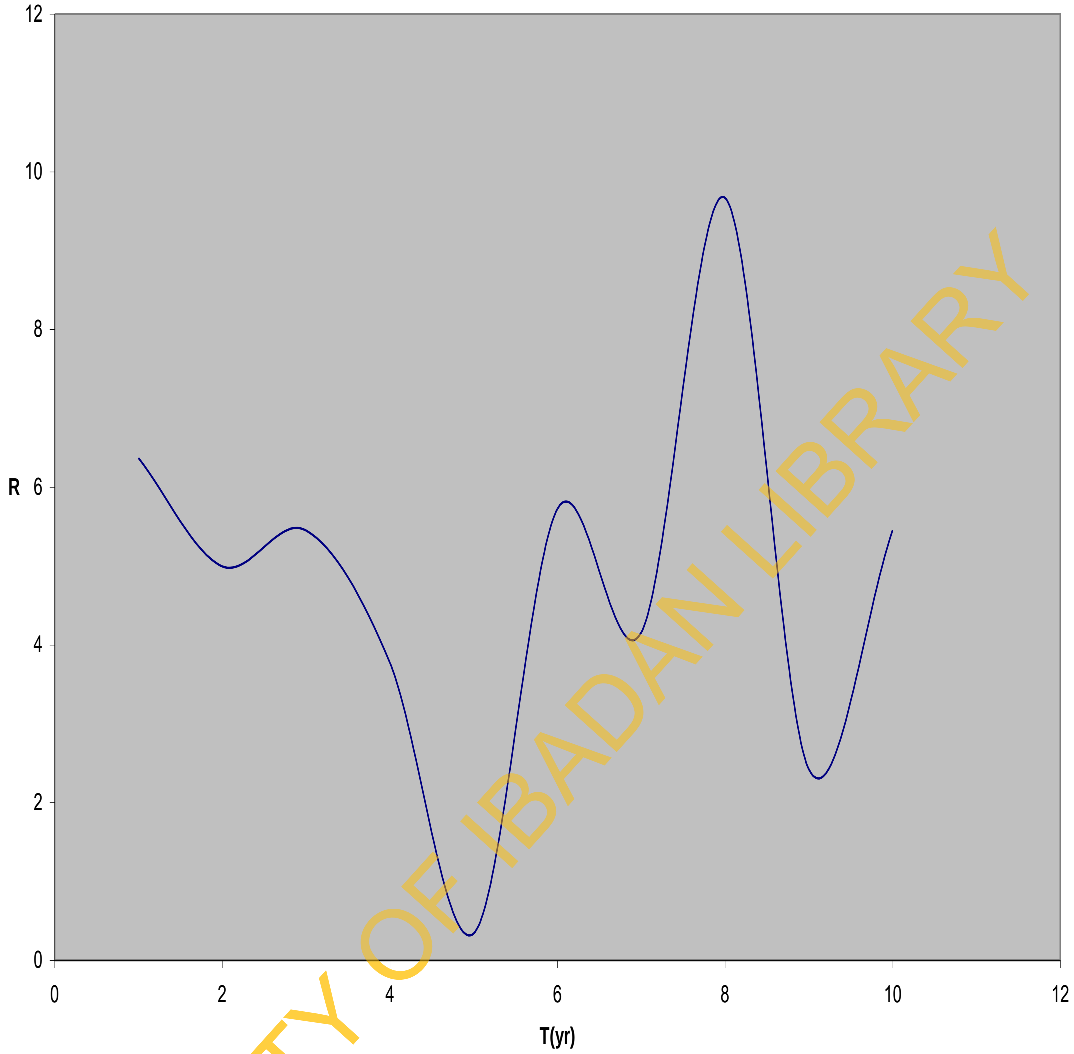

Fig. 4.14: Pattern of propagation of highest frequency of earthquakes for Region 1

The results showed that for almost all the temporal distribution considered, the temporal volume at which the largest amount of seismic energy was released does not coincide with the most active zone or the highest frequency of occurrence of earthquake because of the ten folds magnitude increase and the thirty two folds energy increase since large earthquake (M greater than or equal to M8 are less frequent than smaller earthquake) but the energy released is enormous (Table 4.12). The location at which the largest amount of seismic energy was released between 1960 and 1964 which is within the first annular grid (0-100km) is the epicentre of the 1964 great Alaska earthquake of magnitude Mw 9.2. Observation shows that this point of maximum energy almost coincide with the most active zone, this is because of the many aftershocks associated with this earthquake.

Tables 4.16 to 4.24 are the results for the locations where maximum seismic energy were released in the regions 2, 3, 4 and 5 respectively, while Figures 4.15 to 4.19 shows the pattern of propagation of the maximum seismic energy for the regions respectively. The pattern of energy propagation was not linear but flapping. It was undulating but not periodic. A periodic pattern will imply that the location of the next seismic energy is predictable. This predictable location will be assumed to be the location of the next earthquake. Figure 4.20 a and b are the pattern of propagation of seismic energy for temporal volume of ten years and five years respectively, it appear to be geometrically fractal i.e. self similarity. Fractal is as an object which appears self-similar under varying degrees of magnification. It possesses symmetry across scale, with each small part of the object replicating the structure of the whole.

Table 4.16; Location of maximum seismic energy for Region 2

Period (yr)	**Latitude (^{o})**	**Longitude (^{o})**
1960-1964	34.76	145.54
1965-1969	40.34	142.19
1970-1974	41.37	142.65
1975-1979	43.38	147.67
1980-1984	40.61	139.44
1985-1989	33.25	146.90
1990-1994	43.35	147.77
1995-1999	43.25	146.90
2000-2004	41.85	142.77
2005-2009	34.07	136.01

Table 4.17 Pattern of propagation of maximum seismic energy for Region 2

Period (yr)	R
1960-1964	7.239577
1965-1969	3.116807
1970-1974	4.152438
1975-1979	8.140182
1980-1984	4.455644
1985-1989	6.046367
1990-1994	8.177429
1995-1999	7.553579
2000-2004	4.638312
2005-2009	7.073579

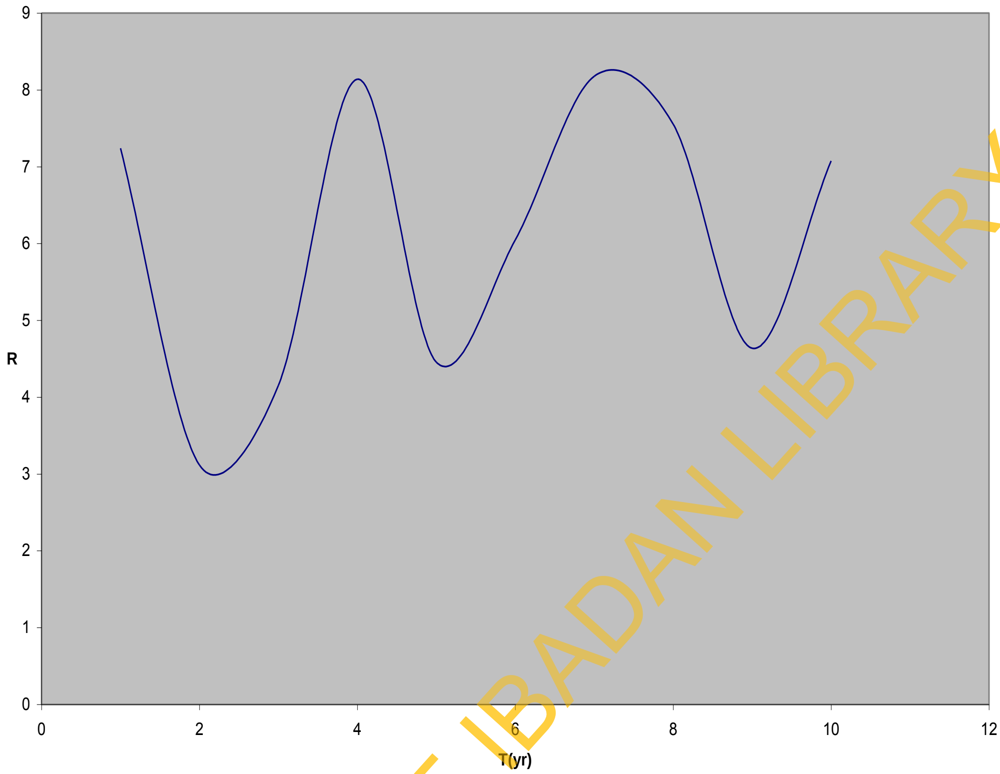

Figure 4.15: Pattern of propagation maximum seismic energy for Region 2

Table 4.18; Epicentres of maximum seismic energy for Region 3

Period (yr)	Latitude (^{o})	Longitude (^{o})	Energy (J)
1963-1964	44.73	149.52	4.68E+30
1965-1966	44.18	145.26	1.05E+23
1967-1968	40.78	143.31	2.32E+29
1969-1970	43.53	147.35	9.77E+28
1971-1972	46.53	141.24	2.40E+26
1973-1974	43.25	141.82	4.12E+28
1975-1976	43.05	147.69	1.01E+26
1977-1978	44.26	148.86	1.74E+28

Table 4.19: Pattern of propagation of maximum seismic energy for Region 3 (1963-1978)

Period (yr)	**R**
1963-1964	6.388606
1965-1966	2.257762
1967-1968	2.124625
1969-1970	3.997290
1971-1972	4.218895
1973-1974	1.620125
1975-1976	4.295523
1977-1978	5.626100

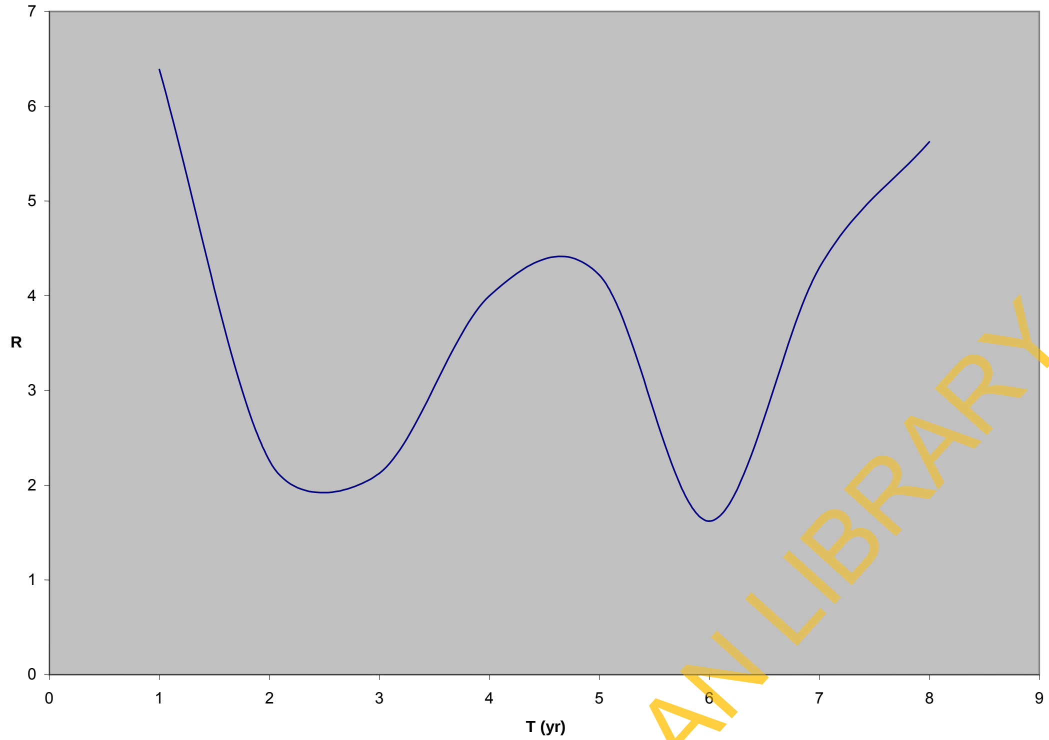

Fig. 4.16 Pattern of propagation of maximum seismic energy for Region 3(1963- 1978)

Table 4.20; Epicentres of maximum seismic energy for Region 3 1978-2003

Period(yr)	Latitude (°)	Longitude (°)	Energy(J)
1978-1981	43.47	146.81	1.01E+26
1981-1983	44.72	151.13	4.27E+25
1984-1985	44.13	148.24	6.33E+23
1986-1988	42.59	142.85	3.20E+24
1989-1991	48.22	154.39	2.49E+23
1991-1993	45.50	151.09	3.20E+27
1994-1996	43.76	147.42	1.30E+30
1996-1998	43.82	149.25	3.20E+24
1999-2001	43.03	146.92	1.80E+25
2001-2003	47.85	146.15	1.35E+27

Table 4.21: Pattern of propagation of maximum seismic energy for Region 3 (1978 – 2003)

Period (yr)	**R**
1978-1981	1.144142
1981-1983	4.554799
1984-1985	1.716991
1986-1988	4.237401
1989-1991	8.612606
1991-1993	4.594832
1994-1996	1.187454
1996-1998	2.780273
1999-2001	1.593692
2001-2003	3.283018

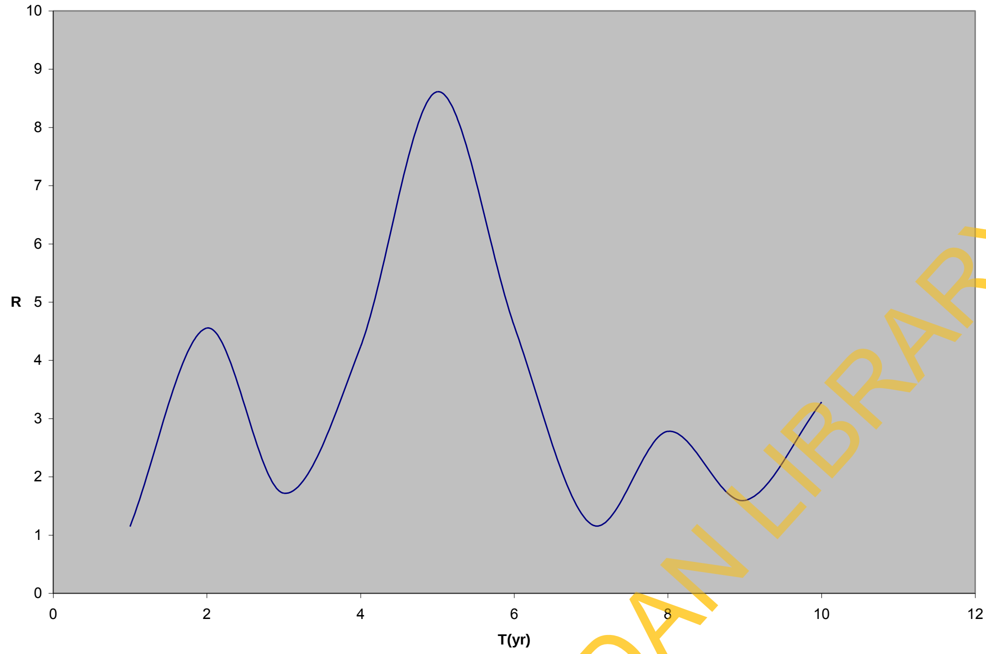

Fig. 4.17: Pattern of propagation of maximum seismic energy for Region 3 (1978 -2003)

Table 4.22; Epicentres of maximum seismic energy for Region 4

Period (yr)	Latitude (°)	Longitude (°)	Energy (J)
1965-1969	-32.31	-71.20	3.055E+26
1970-1974	-38.50	-73.46	2.399E+26
1975-1979	-38.25	-73.21	4.121E+28
1980-1984	-30.71	-71.18	2.483E+23
1985-1989	-33.18	-71.87	9.773E+28
1990-1994	-31.30	-71.98	1.396E+24
1995-1999	-30.95	-71.12	2.399E+26
2000-2004	-30.64	-71.58	1.799E+25
2005-2009	-31.24	-71.34	5.888E+23

Table 4.23 Pattern of propagation of maximum seismic energy for Region 4

Period (yr)	**R**
1965-1969	4.1739192
1970-1974	2.4418857
1975-1979	2.1471333
1980-1984	5.6781395
1985-1989	3.1188149
1990-1994	4.9046855
1995-1999	5.4711458
2000-2004	5.6364545
2005-2009	5.1276287

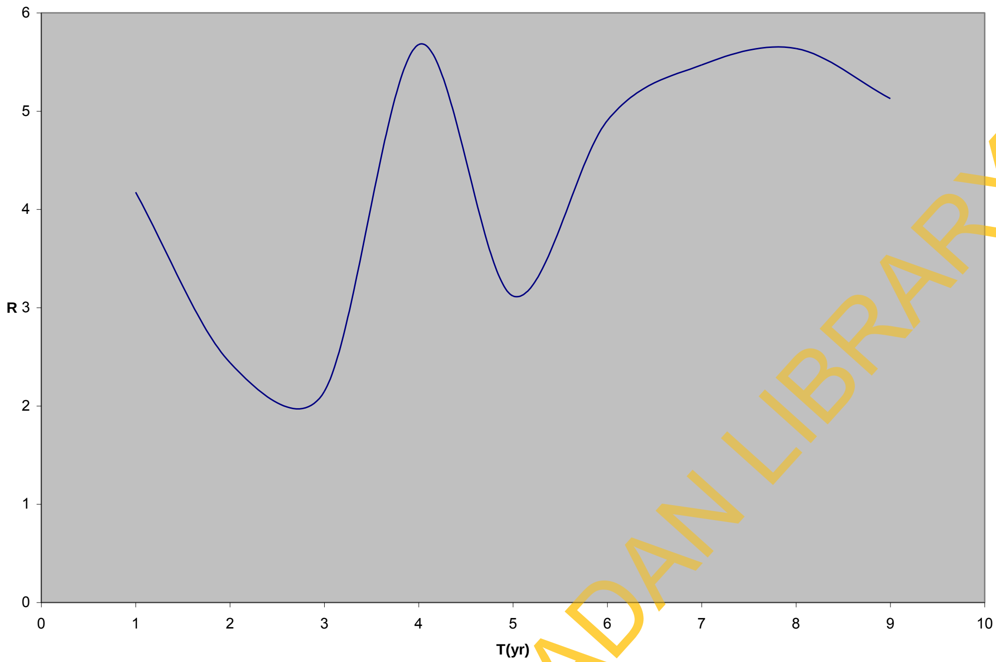

Fig. 4.18; Pattern of propagation of maximum seismic energy for Region 4

Table 4.24: Pattern of propagation of maximum seismic energy for Region 5

Period (yr)	**R**
1960-1964	2.5382502
1965-1969	3.9786186
1970-1974	5.5204635
1975-1979	3.3524847
1980-1984	7.7506008
1985-1989	0.4022002
1990-1994	4.1830553
1995-1999	1.2566499
2000-2004	4.5995367
2005-2009	8.0158129

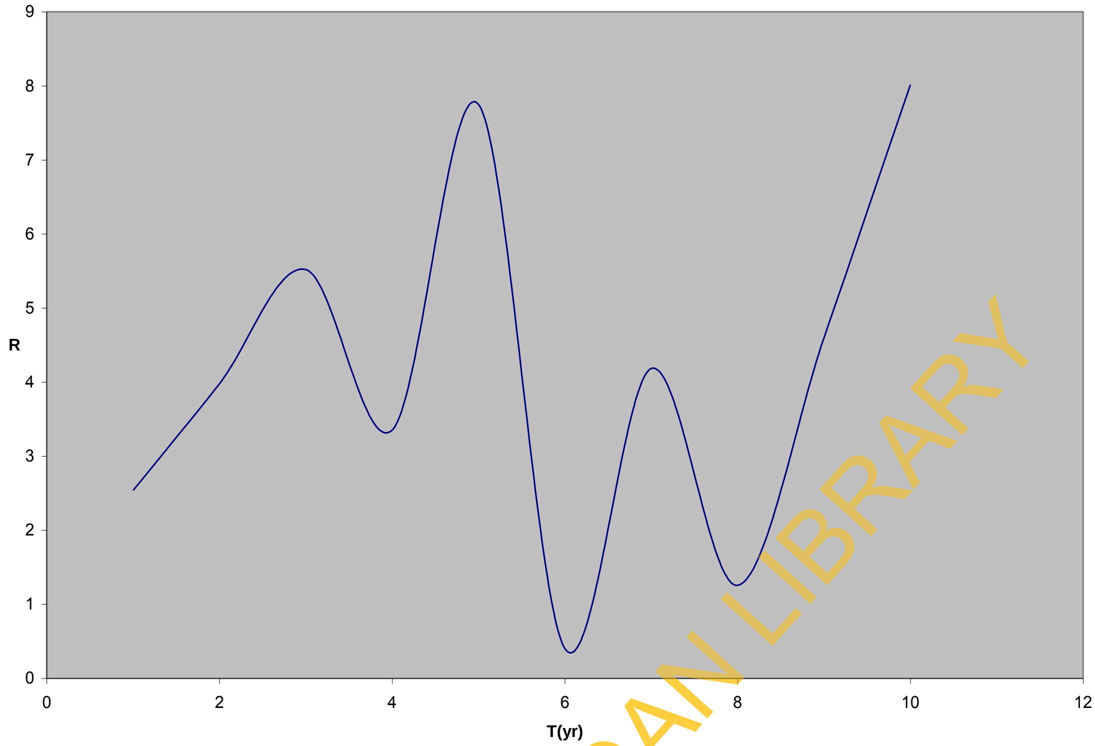

Fig. 4.19; Pattern of propagation of maximum seismic energy for Region 5.

(a)

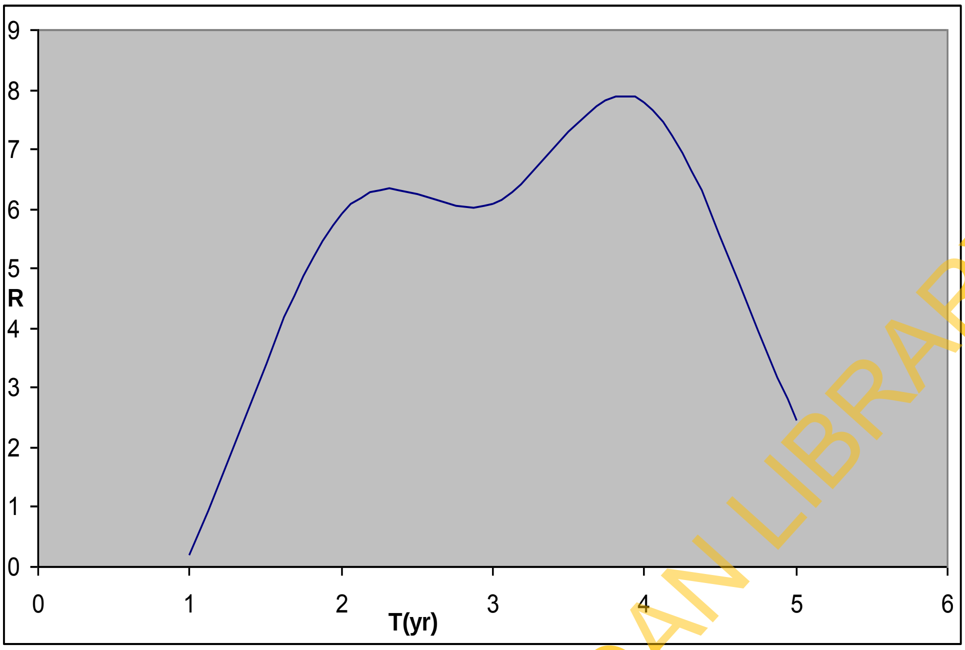

(b)

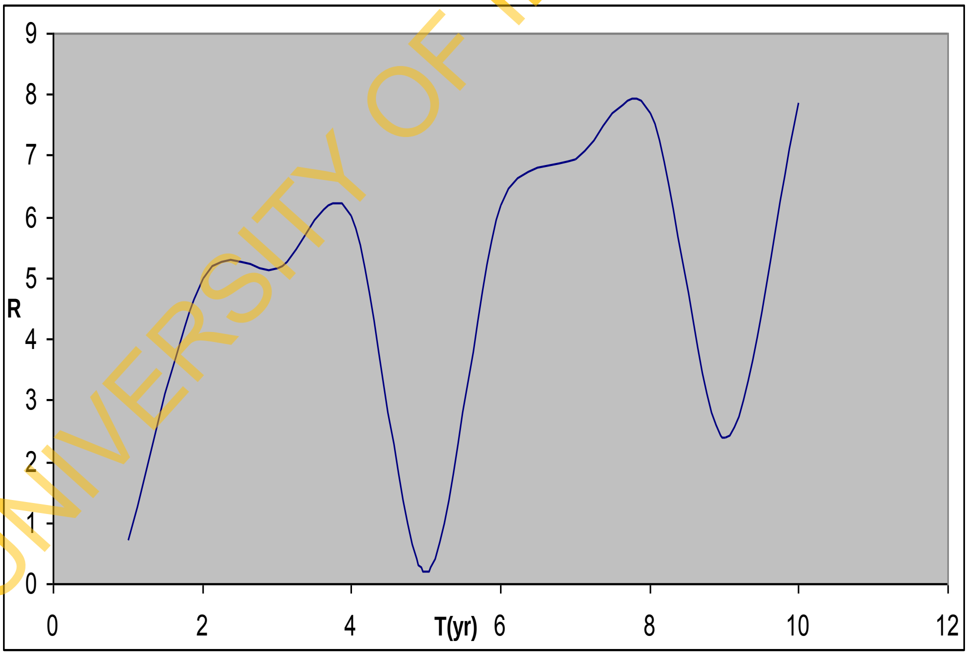

Fig. 4.20: A symptom of fractal geometry;
(a) seismic energy propagation pattern for 10 years
(b) seismic energy propagation pattern for 5 years

4.3: Phase Space Trajectory

Phase space is the collection of possible states of a dynamical system. It is the representations of the trajectories of a dynamical system. The state variable of a system can exhibit periodic, quasi periodic and chaotic behaviour. The phase-space trajectory of a dynamical system gives hints about the system. It can be used as an indicator to determine whether the motion of that system is chaotic or not.

Experimental data usually consist of discrete measurements of a single observable hence there is a need to reconstruct phase space. If the position vector of an object in 2 - dimensional is given as $r = xi + yj$, the phase space plot is r' vs r , where r' and r are given by equation 3.5 and equation 3.6.

Figure 4. 21 is the phase space plot of the seismic activities associated with the large earthquakes in Region 1. It showed that phase space was densely filled with scattered points in a manner that appears to be random. The occurrence of dense orbits is a fundamental property of chaos (Ozer and Akin, 2005).

Figures 4.22 to 4.25 show the phase space plot for Regions 2 to 5 respectively. Each of the region phase space was densely filled with scattered points known as Chaos Sea, which indicate that the trajectory of the earthquake is chaotic.

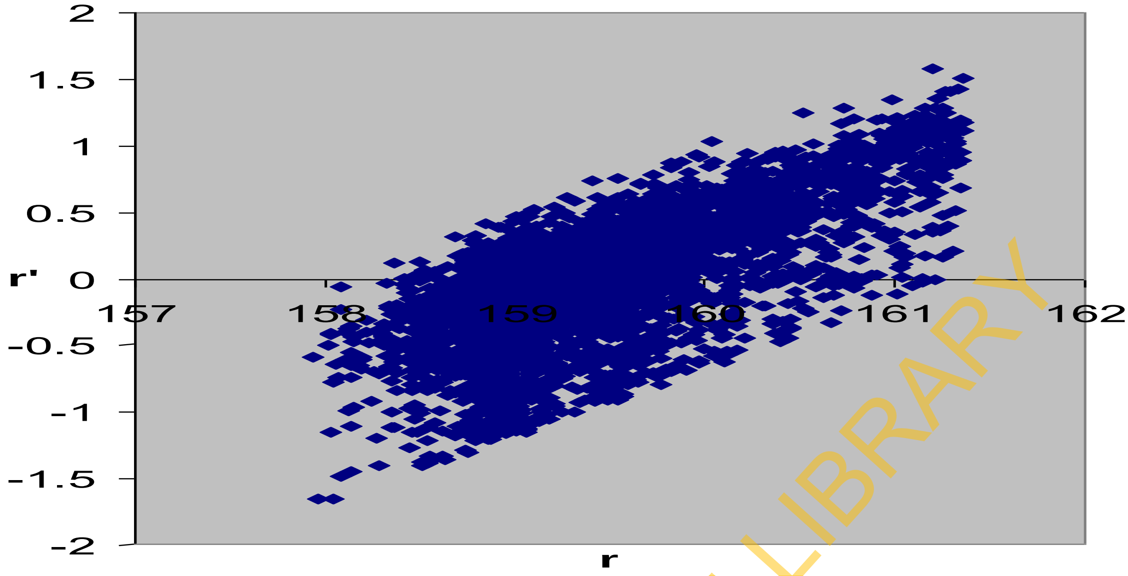

Fig. 4.21: Phase space plot for region 1.

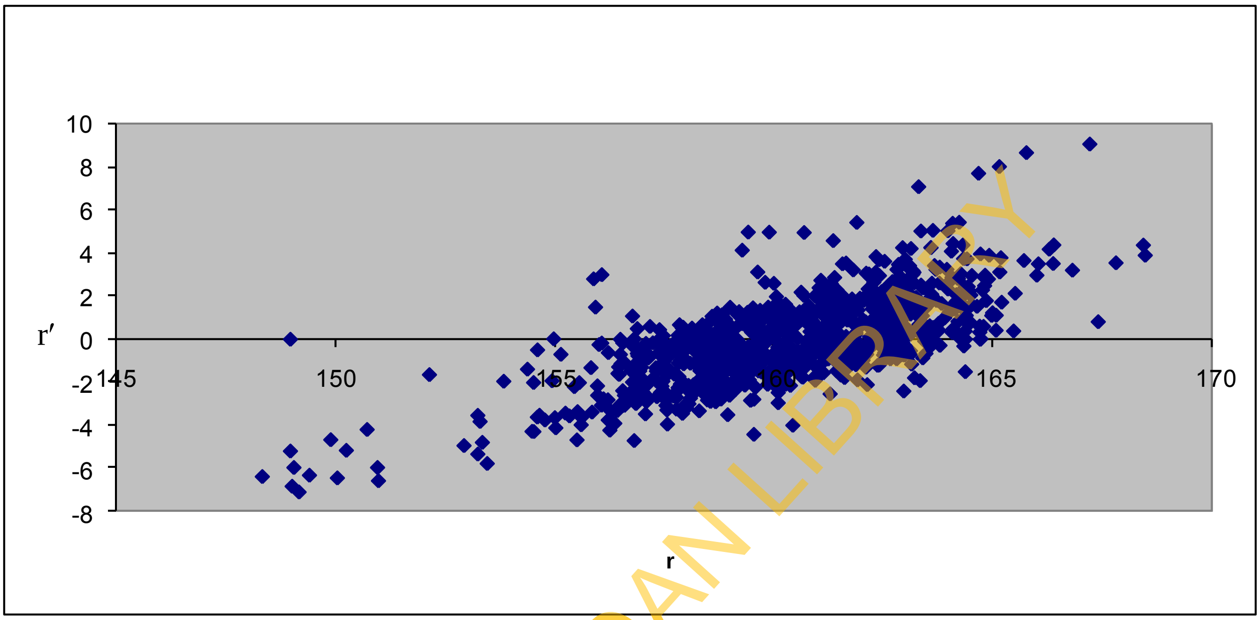

Fig. 4.22: Phase space plot for region 2.

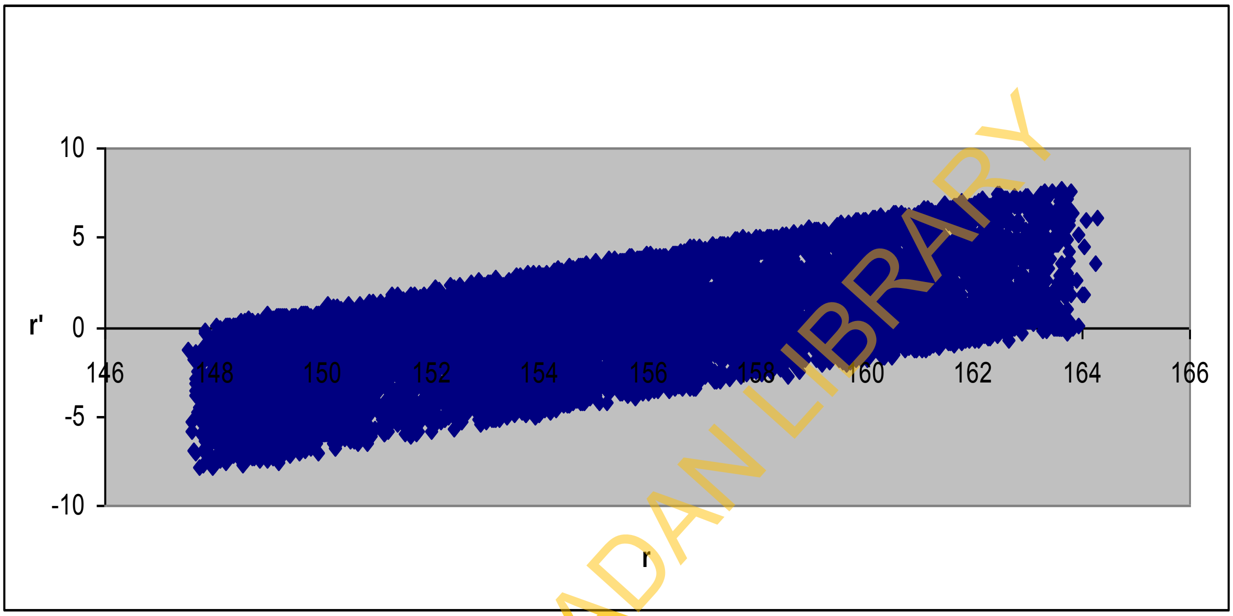

Fig. 4.23: Phase space plot region 3.

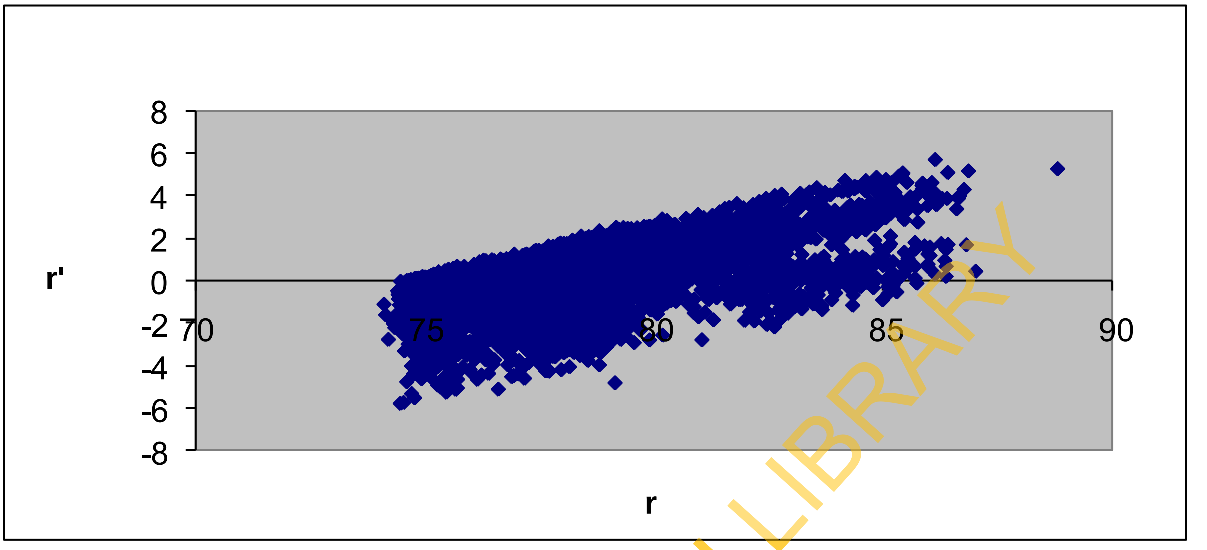

Fig. 2.24: Phase space for region 4.

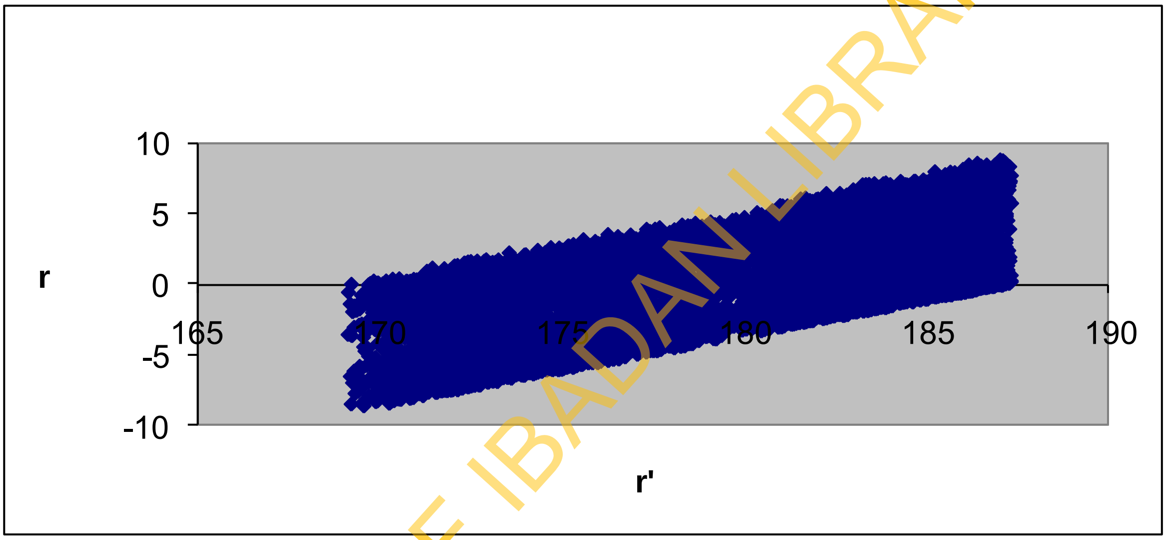

Fig. 4.25: Phase space plot for region 5.

Figure 4.25; phase space plot for region 5

4.4 Lyapunov exponent and Spectrum

Table 4.25 showed the result of the Lyapunov exponent computed for the all the regions. The value of the Lyapunov exponent is positive for each of the region but its magnitude varies from one region to another. The lowest value of 0.688 was obtained in Region 4 while the highest value of 2.688 was obtained in Region 3.

The Lyapunov exponents quantify the exponential divergence of initially close state-space trajectories and estimate the amount of chaos in a system (Rosenstein et al, 1992). It is a basic indicator of deterministic chaos (Sano and Sawada, 1985).

The Lyapunov exponent is positive when neighbouring trajectories diverge from each other at large n, which corresponds to chaos. However, if the trajectories converge to a fixed point or limit cycle, they will get closer together, which corresponds to negative Lyapunov exponents. Hence we can determine whether or not the system is chaotic by the sign of the Lyapunov exponent. It is a way of distinguishing between a stochastic process and a deterministic system (Lacasa and Toral, 2010).

Figure 4.26 showed the spectrum of the Lyapunov exponent for region 1, Observation showed that the Lyapunov exponent is very sensitive to discontinuity in the catalogue and exhibits an asymptotic behaviour before the occurrence of a large earthquake. Lyapunov exponent spectrum for regions 2, 3, 4 and region 5 are shown in Figure 4.27 to 4.30 respectively, the Lyapunov exponent spectrum exhibit an asymptotic behaviour in all the regions.

Table 4.25: the Lyapunov exponents for the five regions

Region	LE
1	1.757
2	2.528
3	2.688
4	0.688
5	1.523

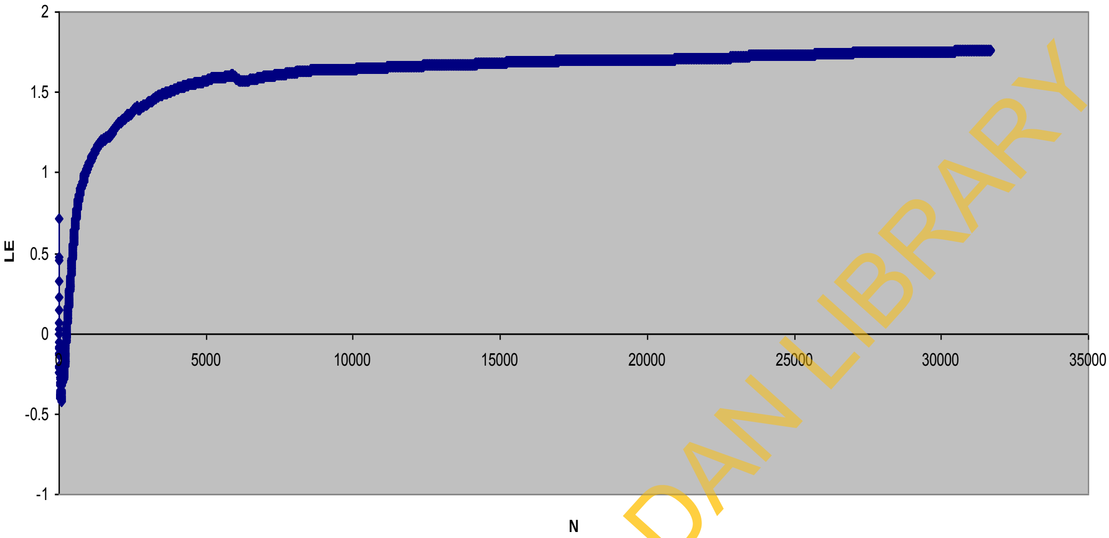

Fig. 4.26; Lyapunov exponent spectrum for regions 1.

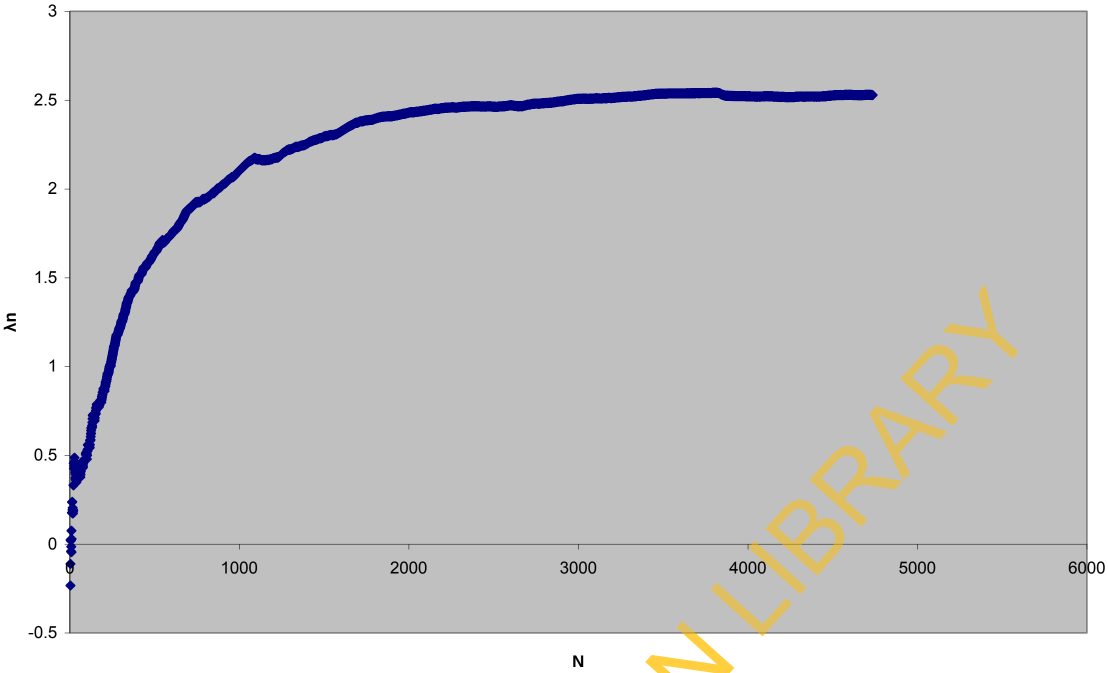

Fig. 4.27: Lyapunov exponent spectrum for regions 2

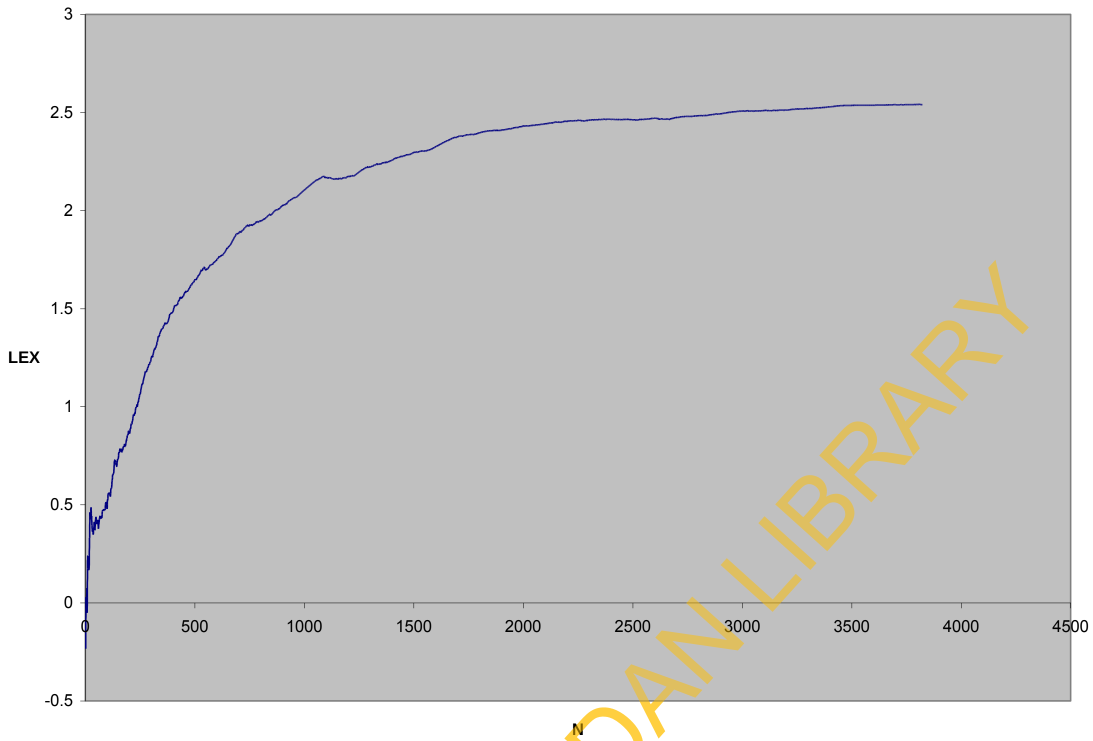

Fig. 4.28: Lyapunov exponent spectrum for regions 3.

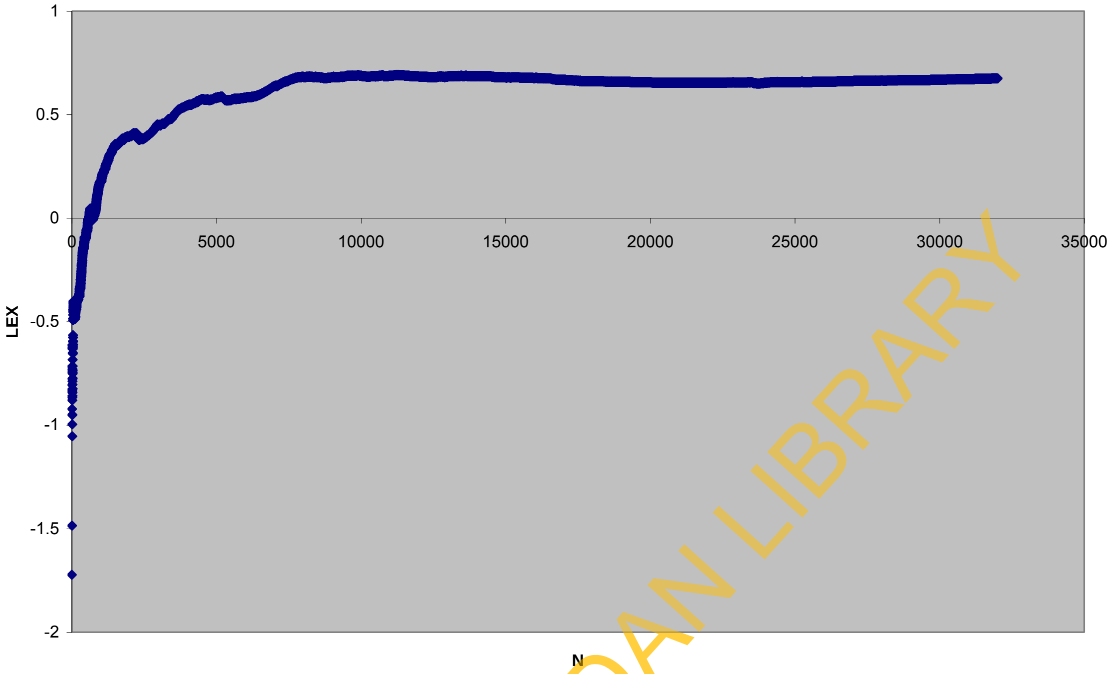

Fig. 4.29: Lyapunov exponent spectrum for regions 4.

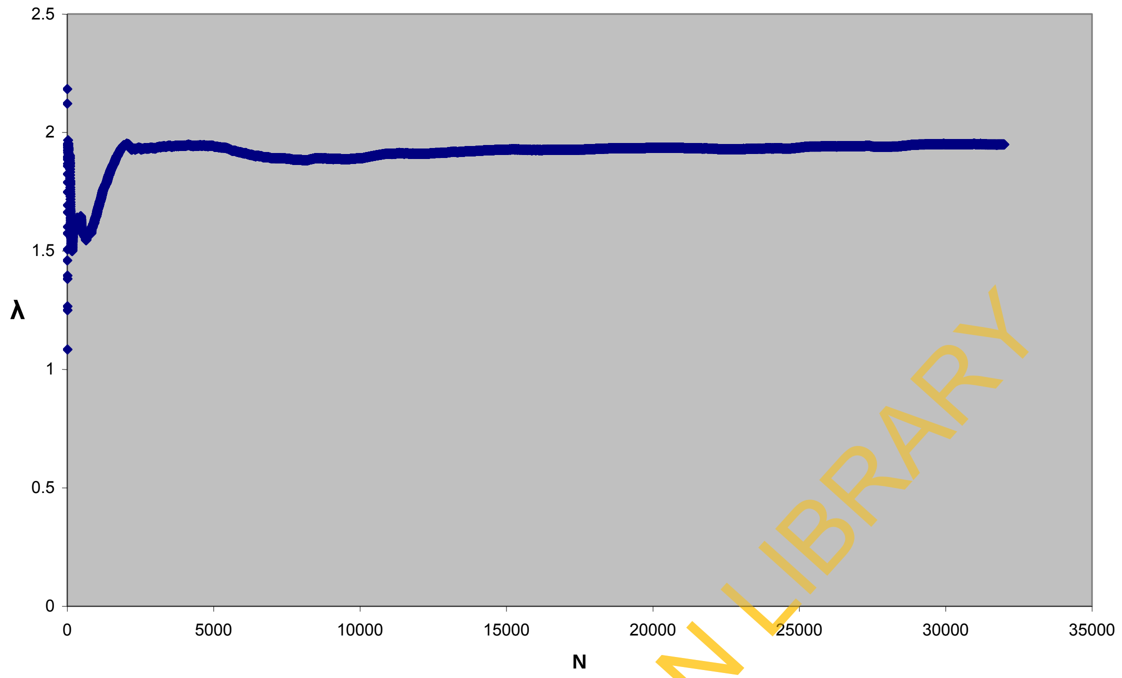

Fig. 4.30: Lyapunov exponent spectrum for regions 5.

CHAPTER FIVE

CONCLUSION AND RECOMMENDATION

5.1 Summary and Conclusion

The entire large earthquakes occur at plate boundaries (Figure 3.3) in support of the plate tectonic theory. Greater percentage of the large earthquake (Table 3.1) occurred at subduction zones possibly because they can support large stresses, and so large-magnitude earthquakes are also found there. This occurs irrespective of the trajectory or rate of motion of the subducting lithospheric plate into the mantle.

The temporal and spatial variations of the b-values for all the regions were non - linear, oscillatory but not periodic, indicating a pattern that is unreliable for prediction. The pattern of propagation of the maximum seismic energy was non-linear and geometrically fractal. The most active zone in term of the highest frequency of occurrence of earthquake differs from the zone at which the largest amount of seismic energy was released, which implies that the most active zone does not necessarily produce large earthquakes.

The phase space was densely filled with scattered points similar to chaos sea which implies chaotic trajectory hence the occurrence of earthquakes had chaotic characteristics. The Lyapunov exponent was positive for all the regions, also indicating the chaotic nature of the earthquakes occurrence. This was highest for Region 3 (2.688) and lowest for Region 4 (0.688). The Lyapunov exponent spectrum behaved asymptotically prior to the occurrence of the large earthquake, these can serve as a precursor for earthquake forecasting in hazard management.

5.2 Recommendations

It is recommended that chaos theory should be incorporated into Pattern Recognition method and that the spectrum of the lyapunov exponent, which behaves asymptotically prior to the next earthquake, could be used as a precursor in seismic hazard management.

REFERENCES

Aki, K. 1965. Maximum likelihood estimate of b-value in the formula logN=a-bM and its confidence limits. *Bulletin of Earthquake Research Institute, University of Tokyo.* 43, 237-239pp.

Ambraseys, N. and Bommer, J. 1990. Uniform magnitude re-evaluation for strong motion database of Europe and adjacent areas. *European earthquake, Engineering*. 2, 3 –16.

Ayele, A. and Kulhanek, O. 1997. Spatial and temporal variation of seismicity in the horn of Africa from 1960 to 1993. *Geophysical Journal International*. 130, 805-810.

Barrell, J. 1914. The strength of the Earth's crust. *Journal of Geology*. 22, 425-433, 441-468, 655-683.

Baskoutas, I. Panopoulou, G. and Papadopoulos, G. 2004. Long Temporal Variation of Seismic Parameters for Patterns Identification in Greece. *Bulletin of the Geological Society of Greece* vol. XXXV1.

Bayrak, Y. and Ozturk S. 2004. Spatial and temporal variation of the aftershock sequence of the 1999 Izmit and Duzce earthquakes. *Earth Planets and Space*, 56, 933-944.

Bayrak, Y. Özturk, S.; Cinar H.; George C and Tsapanos T. M. 2009. Earthquake Hazard assessment for different Regions in and around Turkey based on Gutenberg-Richter Parameters by the Least Square Method. *Journal of Applied Functional Analysis*, Vol. 4, No. 2, 286-299.

Bender, B. 1983. Maximum likelihood estimation of b-values for magnitude grouped data. *Bulletin of Seismological Society of America*. 73, 831–851.

Biagi, P. F. 1999. *Nature Debate*, Nature© Macmillan Publishers Ltd 1999 Registered No. 785998 England.

Brandstäter, A and Swinney, H. L. 1987. Strange attractors in weakly turbulent Couette–Taylor flow. *Physics Review*. A 35, 2207–20.

Brandstäter, A. Swift, J. Swinney, H. L. Wolf, A. Farmer, J. D. Jen, E. and Crutchfield, P. J. 1983. Low-dimensional chaos in a hydrodynamic system. *Physics Review Letter* 51, 1442–5

Broomhead, D.S., King, G.P. 1985. Extracting Qualitative Dynamics from Experimental Data. *Physica* 20D, 217- 236.

Bryant, P. Brown, R. and Abarbanel, H. D. I. 1990. Lyapunov exponents from observed time series. *Physics Review Letter*. 65, 1523–6.

Campbell, W.H. 1998. A misuse of public funds: UN support for geomagnetic forecasting of earthquakes and meteorological disasters. *Eos Trans. Am. Geophys. Union* 79, 463-465.

Chen, L. and Talwani, P. 1998 Seismicity in China, *Pure and Applied Geophysics*. 153, 133-149.

Coffman, J. L. and Carl, A.V. 1982. Earthquake History of the United States. *United States Department of Commerce*, Colorado.

Comninakis, P.E., 1975. Contribution to the study of the seismicity of Greece. PhD, Thesis, Univ. of Athens, 110pp.

Daly, R. 1940. *Strength and structure of the Earth*. New York: Prentice-Hall.

Darbyshire, A G and Broomhead, D S 1996. Robust estimation of tangent maps and Liapunov spectra . *Physica.* D 89, 287–305.

Davison, C. 1978. *The Founders of Seismology*. Arno Press, New York.

Defant, M. J. 1998. *Voyage of Discovery: From the Big Bang to the Ice Age*, Mancorp, and 325p. doi: 10.1029/2002JB002276.

Deissler, R. J. and Kaneko, K. 1987. Velocity-dependent Lyapunov exponents as a measure of chaos for open-flow systems. *Physics Letter.* 119A, 397–402

Doyle, H. 1995. *Seismology*. John Wiley and Sons: New York.

Eckmann, J.P. Kamphorst, S. O. Ruelle, D. and Ciliberto, S. 1986. Lyapunov exponents from time series *Physics Review*. A 34, 4971–9.

Eijsa, V. R. Muldersa, F.M. Nepveua, M. Kenterb, C.J. and Scheffers, B.C. 2006. Correlation between hydrocarbon reservoir properties and induced seismicity in the Netherlands. *Engineering Geology*, 84, 99-111.

Enescu, B. and Ito, K. 2002. Spatial analysis of the frequency-magnitude distribution and decay rate of aftershock activity of the 2000 Western Tottori earthquake. *Earth, Planets and Space*. Vol. 54.

Enescu, B and Ito, K. 2004. Temporal and Spatial Variations of Seismicity during the 1998 Hida Mountain Earthquake Swarms, Central Honshu, Japan, *Bulletin of the Seismological Society of America*. Vol. 94; no. 2; p. 430-438.

ESZ 2013. Earth Science Zone, *Earth Science for School.* Moorland School, Clitheroe, Lancashire, BB7 2AJ England.

Fedotov, S. A. 1968. The seismic cycle, quantitative seismic zoning, and long-term seismic forecasting. In *Seismic Zoning of the USSR* (Ed. Medvedev, S.) (Idatel'stvo ''Nauka'', Moscow) pp. 133–166.

Frohlich, C. and Davis, S. 1993. Teleseismic b-values: or, much ado about 1.0, *Journal of Geophysical Research*. 98, 631–644.

Froyland, J and Alfsen, K. H. 1984. Lyapunov-exponent spectra for the Lorenz model. *Physics Review*. A 29, 2928–31.

Geller, R.J. 1976. Scaling relation for earthquake source parameters and magnitude. *Bulletin of the Seismological Society of America*. 66, 1501-1523.

Geller, R. J. 1997 Earthquake prediction: A critical review. *Geophysical Journal International*. 131, 425–450, doi:10.1111/j.1365-246X.1997.tb06588.x.

Geller, R. J. Jackson, D. D. Kagan, Y. Y. and Mulargia, F. 1997 Earthquakes cannot be predicted. *Science*. 275, 1616–1617.

Geller R.J. 1999 Earthquake Prediction: What should we be debating? *Nature Debate,* Nature© Macmillan Publishers Ltd 1999 Registered No. 785998 England.

Geography.about.com. 2010. *Ring of Fire - Pacific Ring of Fire*". Geography.about.com.,http://geography.about.com/cs/earthquakes/a/ringoffire.htm. Retrieved 2010-11-01

Geophysics.ou.edu. 2011. *Global seismicity*. http://geophysics.ou.edu/solid_earth/notes/seismicity/global/global_seismicity.html

Geology.com 2011. *Plate boundary* http://geology.com/nsta/plate-boundary.shtml Retrieved 2011-02-26.

Geo.mtu.edu. 2010. *Earthquakes magnitude scale and classes* http://www.geo.mtu.edu/UPSeis/magnitude.html Retrieved 2011-02-26

Gerstenberger, M. Wiemer, S. and Giardini, D. 2001. A systematic test of the hypothesis that the b value varies with depth in California, *Geophysical Research Letter*, Vol. 28, No. 1, pages 57-60.

Gibowicz, S. J. and Lasocki, S. 2001. Seismicity induced by mining: Ten years later. In: Dmowska, R. and Saltzman, B. (Eds.), *Advances in Geophysics*, 44, Academic Press, 39-181.

Gibson, D. D. and Byrd, G.V. 2007. *Birds of the Aleutian Islands, Alaska*. Cambridge, Mass: Nuttall Ornthological Club, ISBN 9780943610733.

Goldstein, H. Poole, C. and Safko, J. 2002. *Classical Mechanics*. Pearson Education, Inc., publishing as Addison Wesley. ISBN; 0321-188977.

Grunthal, G. Hurtig, E. and Ruge, E. 1982. Time dependence of statistical parameters: the aftershock sequence of the Friuli, Northern Italy, 1976 earthquake and a section of the

Montenegro, Yugoslavia, earthquake series 1979. *Earthquake Prediction Research*. 2, 275-285.

Gutenberg, B. and Richter, C.F. 1942. Earthquake magnitude, intensity, energy and acceleration. *Bulletin of the Seismological Society of America*. 32, 163-191.

Gutenberg, B. and Richter, C.F. 1965, *Seismicity of the Earth and Associated Phenomenon* Hafner Publishing Company.

Hanks, T. C. 1979. b Values and γ Seismic Models: Implications for Tectonic Stress Variations Along Active Crustal Fault Zones and the Estimation of High-Frequency Strong Ground Motion. *Journal of Geophysical Research*. Vol. 84, No. B5.

Hanks, T.C. and Kanamori, H. 1979. A moment magnitude scale. *Journal of Geophysical Research*. 84, 2348-2350.

Hazen, A. 1920. Transactions of the American Society of Civil Engineers 83: 1717–1745

Herndon, J. M. 1980. The chemical composition of the interior shells of the Earth. *Proc. R. Soc. Lond*, A372, 149-154.

Herndon, J. M. 2005. Scientific basis of knowledge on Earth's composition. *Curr. Sci*. 88(7), 1034-1037.

Holmes, A. 1978. *Principles of Physical Geology* (3rd ed.). Wiley. pp. 640–641.

Huffaker, R. 2010. *Phase Space Reconstruction from Time Series Data: Where History Meets Theory*, Food and Resource Economics Department, University of Florida, USA.

Hurtig, E. and Stiller, H. 1984. *Erdbeben und Erdbebengefährdung*. Akademie Verlag

Hyndman, D. and Hyndman, D. 2009. "Chapter 3: Earthquakes and their causes". Natural Hazards and Disasters (2nd edition). Brooks/Cole: Cengage Learning. ISBN 0495316679.

IASPEI, 1994; International Association of Seismology and Physics of the Earth's Interior, *Preliminary list of Significant Precursors*.

Isacks, B. L. Oliver, J. and Sykes, L. R. 1968 Seismology and the new global tectonics. *Journal of Geophysical Research*, 73, 5855–900.

Ishimoto, M and Iida, K. 1939. Observations sur les seismes enregistres par le microsismographe construit dernierement (1). *Bulletin of Earthquake Research Institute University of Tokyo* 17; 443-478. (in Japanese with French abstract).

Jefferies, M. and Been, K. 2006. *Soil Liquefaction: A Critical State Approach*. Taylor & Francis. ISBN 978-0-419-16170-7.

Jordan, T. H. 1978. Composition and development of the continental tectosphere. *Nature* 274, 544-548.

Jordan, T. H. 1979. "Structural Geology of the Earth's Interior", *Proceedings of the National Academy of Science*, 76(9): 4192–4200

Kagan, Y. 1999. The universality of the frequency-magnitude relationship. *Pure and Applied Geophysics*. 155: 537-574.

Kamland.Standford.edu. 2014. *Structure of the earth*. http://www. Kamland.Standford.edu/GeoNeutrinos.html. Retrieved 2014-28-05.

Kanamori, H. 1977. The energy release in great earthquakes. *Journal of Geophysical Research.* 82, 2981 – 2877.

Kanamori, H. 1983. Magnitude scale and quantification of earthquakes. *Tectonophysics* Volume 93, Issues 3-4, 10 April 1983, Pages 185-199.

Kanamori, H. and Brodsky, E. 2004. The physics of earthquakes. *Rep. Prog. Phys*. 67, 1429–1496.

Kaplan, J. L. and Yorke, J. A. 1979. Chaotic Behaviour of Multidimensional Difference Equations (Lecture Notes in Mathematics) (Berlin: *Springer*) pp 204–27.

Katsumata, K. 2006. Imaging the high b-value anomalies within the subducting Pacific plate in the Hokkaido corner. *Institute of Seismology and Volcanology*, Hokkaido University.

Kearey, P. and Vine, F. J. 1996. *Global tectonics*. Blackwell Science, Oxford.

Keilis-Borok, V.K. and Soloview, A. 2009. *Pattern recognition methods and algorithms.* Advance school of Non –Linear Dynamics and Earthquake prediction. Trieste, Italy.

Keilis-Borok, V.I. Shebalin, P.N. and Zaliapin, I.V. 2002. Premonitory patterns of seismicity months before a large earthquake: five case histories in Southern California. *Proceedings of the National Academy of Science*. 99 (26), 16562–16567.

Keilis-Borok, V.I., Soloviev, A.A. 2003. *Nonlinear Dynamics of the Lithosphere and Earthquake Prediction*. Springer–Verlag, Heidelberg, 335 pp.

Kiekeben, F. 1999. *Does Determinism Imply Absolute Predictability?* http://www.franzkiekeben.com/home.html Retrieved 2012-07-07.

Kisslinger, C 1976. "A review of theories of mechanisms of induced seismicity". *Engineering Geology*. 10 (2-4): 85–98. doi:10.1016/0013-7952(76)90014-4. ISSN 00137952.

Kossobokov, V.G. and Carlson, J.M. 1995. Active zone size vs. activity: a study of different seismicity patterns in the context of the prediction algorithm M8. *Journal of Geophysical Research*. 100, 6431–6441.

Kossobokov, V. and Shebalin, P. 2003. Earthquake prediction. In: Keilis-Borok, V.I., Soloviev, A. A. (Eds.), *Nonlinear Dynamics of the Lithosphere and Earthquake Prediction.* Springer–Verlag, Heidelberg, pp. 141–207

Kossobokov, V. 2009. *Practise of predicting large earthquake on global and regional scales.* Advance School of Non –Linear Dynamics and Earthquake prediction. Trieste, Italy.

Kot, M. Schaffer, W. Truty, G. Graser, D. and Olsen, L. 1988. Changing Criteria for Imposing Order. *Ecological Modelling*. 43: 75 - 110.

Kulhanek, O. 2005. *Seminar on b-value*. Department of Geophysics, Charles University, Prague.

Lacasa, L. and Toral, R. 2010. Description of stochastic and chaotic series using visibility graphs, *Physical Review*, DOI: 10.1103/PhysRevE.82.036120.

Liu, Z. Zhu, X. H. Hu, W. and Jiang, F. 2007. Principles of chaotic signal radar. *International Journal of Bifurcation and Chao*s 17, 1735-1739.

Main, I. 1996. Statistical physics, seismogenesis and seismic hazard, Rev. Geophys. 34, 433-462.

Main, I. 1999 Is the reliable prediction of individual earthquakes a realistic scientific goal? *Nature Debate*, Nature© Macmillan Publishers Ltd 1999 Registered No. 785998 England.

McBride, N. and Gilmour, I. 2004. An Introduction to the Solar System; Cambridge University Press.

McGarr, A. 1984. Some application of seismic source mechanism studies to assessing underground hazard. In: N.C. Gay and E.H. Wainwright (Eds.), *Proceeding of 1st International Congress on Rockbursts and Seismicity in Mines*. SAIM Johannesburg, pp. 199-208.

McNally, K.C. 1989. Earthquakes and seismicity. In: D.E James (Ed.) *The Encyclopaedia of Solid Earth Geophysics*, pp. 308-315.

Mehra, V. and Ramaswamy, R. 1996. Maximal Lyapunov exponent at crises. *Physics Review* E 53 3420–4.

Michael, A. 1999a. How well can we predict earthquakes? United States Geological Survey, Menlo Park, California, USA. *Nature Debate*, Nature© Macmillan Publishers Ltd 1999 Registered No. 785998 England.

Michael, A. 1999b. Realistic predictions: are they worthwhile? United States Geological Survey, Menlo Park, California, USA *Nature Debate*, Nature© Macmillan Publishers Ltd 1999 Registered No. 785998 England.

Mogi, K. 1962. Magnitude-frequency relationship for elastic shocks accompanying fractures of various materials and some related problems in earthquakes. *Bulletin of Earthquake Research Institute, University of Tokyo*. 40, 831-883.

Mogi, K. 1967 "Regional variation of aftershock activity", *Bulletin of Earthquake Research Institute, University of Tokyo*. 46, 175-203.

Mogi, K. 1969, Some Features of Recent Seismic Activity in and near Japan (2). Activity before and after Great Earthquakes, *Bulletin of Earthquake Research Institute, University of Tokyo.* 47, 395–417.

Mogi, K. 1979. Two Kinds of Seismic Gaps, *Pure Applied Geophysics.* 117, 1172–1186.

Mogi, K. 1980. Seismic Actitity: Earthquake Prediction in and around the Tokyo Metropolitan Area, *Bull. Reg. Coord. Comm. Earthquake Prediction* 2, 20–21

Mogi, K. 1981. *Seismicity in western Japan and long-term earthquake forecasting. In Earthquake Prediction, An International Review* (eds. Simpson, D. W., and Richards, P.G.) (AGU, Washington, D.C.) pp. 43–51.

Mogi, K. 1985. *Earthquake Prediction* Tokyo. Academic Press.

Monterroso, D. and Kulhanek, O. 2003. Spatial variations of b-values in the subduction zone of Central America. *Geofisica Inter*. 42: 1-13.

Monterroso, D. 2003. Seismic precursory potential of temporal variation of b-value: five case studies in Central America. *Comprehensive Summaries of Uppsala Dissertations from the Faculty of Science and Technology*. 897, 17 pp.

Moores, E. M. 1995. *Volcanoes and Earthquakes*. Time Life Books: Australia.

Mori, J. and Abercrombie, R.E. 1997. Depth dependence of earthquake frequency-magnitude distributions in California: Implications for rupture initiation, *Journal of Geophysical Research*. Vol. 102, No. B7, pages 15,081-15,090

NASA. 1998. *Tectonic Map of the Earth*. National Aeronautics and Space Administration http://denali.gsfc.nasa. gov/dtam/gtam Retrieved 2009-06-23

Natural Resources Canada Classes of Earthquake Magnitude v www.nrcan.gc.ca Retrieved 2011-02-26.

NOAA. 2009. National Oceanic and Atmospheric Administration. *The Great Alaskan Earthquake and Tsunamis of 1964.* Accessed 2009-06-23.

Noson, L. J. Qamar, A. and Thorsen, G. W. 1988. *Washington State Earthquake Hazards*. Washington Division of Geology and Earth Resources Information Circular 85. Pacific rim used books.

Nuannin, P., Kulhanek, O., Persson, L. and Tillman, K., (2002). Forecasting of increasing induced seismicity in the Zinkgruvan mine, Sweden, by using temporal variations of b-values. *Acta Montana*. Series A, 21: 13-25.

Nuannin, P. Kulhanek, O. and Persson, L. 2005. Spatial and temporal b value anomalies preceding the devastating off coast of NW Sumatra earthquake of December 26, 2004. *Geophysics Research Letter*. 32, L11307.

Okal, E.A and Romanowicz, B.A. 1994. On the variation of b-values with earthquake size. *Physics of the Earth and Planetary Interiors*. 87, 55-76 Elsevier.

O'Reilly, S. Y. 2009. Ultradeep continental roots and their oceanic remnants: A solution to the geochemical mantle reservoir problem? *LITHOS* doi:10.1016/j.lithos. 2009.04.028.

Oreskes, N. 2003. *Plate Tectonics: An Insider's History of the Modern Theory of the Earth. Westview*. ISBN 0813341329.

Ozer, B and Akin, E. 2005. *Tools for detecting chaos*. SAÜ Fen Bilimleri Enstitüsü Dergisi 9.Cilt, 1.Sayõ

Paige Sellers. 1997. Poseidon. *Encyclopaedia Mythica*. http://www.pantheon .org/articles/p/poseidon.html. Retrieved 2008-09-02.

Papadopoulos, G.A. and Baskoutas, I. 2009. New tool for the spatio-temporal variation analysis of seismic parameters. *Nat. Hazards Earth Syst. Sci*. 9, 859-864.

Papazachos, C. 1999. An alternative method for a reliable estimation of seismicity with an application in Greece and the surrounding area. *Bulletin of the Seismological Society of America*. Vol. 89, no. 1, p. 111-119.

Parlitz, U. 1992. Identification of true and spurious Lyapunov exponents from time series. *International Journal of Bifurcation and Chaos*. 2 155–65

Peresan, A. Vorobieva, I. Soloviev, A. and Panza G. F. 2007. Simulation of Seismicity in the Block-structure Model of Italy and its Surroundings. *Pure and Applied Geophysics*. 164 2193–2234.

Plate Tectonic.com. 2010. *Plate Tectonics* http://www.plate tectonic .com/book Retrieved 2011-01-24.

Plate Tectonic.com. 2010. *Plate Boundaries* http://www.plate tectonic .com/book Retrieved 2011-01-24.

Redmayne, D.W. 1988. Mining induced seismicity in UK coalfields identified on the BGS National Seismograph Network. Geological Society, London, *Engineering Geology Special Publications*; vol. 5; pp. 405-413.

Reid, H. F. 1910. The Mechanics of the Earthquake. The California Earthquake of April 18, 1906: *Report of the State Earthquake Investigation Commission*, Vol. 2. Carnegie Institution of Washington, Washington, D.C.

Rikitake, T. 1975. Earthquake precursor. *Bulletin of Seismological Society of America*. 65, 1133-1162.

Riper, V and Bowdoin, A. 2002. *Science in popular culture: a reference guide*. Westport: Greenwood Press p. 60. ISBN 0313318220.

Robinson, A. 1993. *Earth Shock: Hurricanes, Volcanoes, Earthquakes, Tornadoes and Other Forces of Nature*. Thames and Hudson: London.

Roeloffs, E. and Quilty, E. 1997. Water level and strain changes preceding and following the August 4, 1985 Kettleman-Hills California earthquake. *Pure and Applied Geophysics*. 149, 21-60.

Roeloffs, E. and Langbein, J. 1994. The earthquake prediction experiment at Parkfield, California, *Reviews of Geophysics*. 32, 315-335.

Rosenstein, M. T. Collins, J. and. De Luca, C. J. 1993. A practical method for calculating largest Lyapunov exponents from small data sets, *Physica* D 65 (1993) 117-134 North-Holland SDI: 0167-2789(92)00033-6

Ruppert, N.A. and Hansen, R.A. 2010. Temporal and Spatial Variations of Local Magnitudes in Alaska and Aleutians and Comparison with Body-Wave and Moment Magnitudes, *Bulletin of the Seismological Society of America*; June 2010; v. 100; no. 3; p.1174-1183; Nature 199: 947–949.

Saegusa, A. 1999. Japan tries to understand quakes, not predict them, *Nature* 397, 284

Sano, M. and Sawada, Y. 1985. Measurement of the Lyapunov spectrum from a chaotic time series. *Physics Review Letter*. 55 1082-5.

Saskia, G. 2003. Seismotektonik – seismotectonics Lecture notes

Sauber, J. and Dmowska, R. 1999. Introduction Seismogenic and Tsunamigenic Processes in Shallow Subduction Zones. *Pure and Applied Geophysics*. 154; 405–407.

Schaffer, W. and Kot, M. 1985. Nearly One Dimensional Dynamics in an Epidemic. *Journal of Theoretical Biology*. 112: 403 - 427.

Shaw, R. 1984. *The Dripping Faucet as a Model Chaotic System*. Santa Cruz, CA: Aerial.

Schorlemmer, D. Gerstenberger, M. C. Wiemer, S. Jackson, D. D. and Rhoades, D. A. 2007. Earthquake Likelihood Model Testing. *Seismology Research Letter*. 78, 17.

Scholz, C. H. 1968. The frequency-magnitude relation of microfracturing in rock and its relation to earthquakes. *Bulletin of the Seismological Society of America*. 58, 399-415.

Scholz, C.H. Sykes, L.R. Aggarwal, Y.P. 1973. Earthquake prediction: A physical basis. *Science*. 181 (4102), 803-810.

Scholz, C.H. 1990. *The Mechanics of Earthquakes and Faulting*. Cambridge University Press.

Schubert, G. Turcotte, D.L. and Olson, P. 2001. *Mantle Convection in the Earth and Planets.* Cambridge University Press. ISBN 052135367X.

Scordilis E.M. 2006. Empirical global relations converting MS and mb to moment magnitude *Journal of Seismology* 10: 225–236 DOI: 10.1007/s10950-006-9012-4 C

Shebalin, P. Zaliapin, I. and Keilis-Borok, V.I. 2000. Premonitory rise of the earthquakes' correlation range: lesser Antilles. *Physics Earth and Planetary Int*. 122 (3-4), 241–249.

Shearer, P. M. 2009. *Introduction to Seismology* (Second ed.). Cambridge University Press. ISBN 978-0521708425.

Skinner, B.J. and Porter, S.C. 1987. *Physical Geology*. The Earth: Inside and Out. John Wiley & Sons, ISBN 0-471-05668-5, pg 17.

Sprott, J.C. 2003. *Chaos and time-series analysis*. Oxford University Press. ISBN 0-19-850839-5.

Stanley, S. M. 1999. *Earth System History*. W.H. Freeman. pp. 211–228. ISBN 0716728826.

Stein, S. and Wysession, M. 2003. *An Introduction to Seismology, Earthquakes and Earth Structure*. Blackwell Publishing, Ltd.

Suyehiro, S. Asada, T. and Ohtake, M. 1964. Foreshocks and aftershocks accopmpanying a perceptible earthquake in central Japan: On the peculiar nature of foreshocks. *Pap. Meteorol. Geophys*, 19: 427-435.

Talwani, P. 1997. On the Nature of Reservoir-induced Seismicity. *Pure and Applied Geophysics* 150 (3-4): 473–492. doi:10.1007/s000240050089. ISSN 0033-4553.

Tarbuck, E. J. and Frederick K. L. 1996. *Earth: An Introduction to Physical Geology*. Prentice Hall: New Jersey.

Tester, J. W. 2006. *The Future of Geothermal Energy - Impact of Enhanced Geothermal Systems (EGS) on the United States in the 21st Century*. Idaho Falls: Idaho National Laboratory. pp. 4–10. ISBN 0-615-13438-6.

Thompson, G. R. and Turk, J. 1991. *Modern Physical Geology*. Saunders College Publishing. ISBN 0030253985.

Tobin, G. A. and Burrell E. M. 1997. *Natural Hazards: Explanation and Integration.* The Guilford Press: New York.

Toshiro, T. and Thorne, L. 2000. Mantle dynamics and seismic tomography. *Proceedings of the National Academy of Science* 97: 12409.

Tsapanos, T. M. 1988. The seismicity of Greece in comparison with the seismicity of other seismogenic countries of the world. *Proceeding 1st Symposium On recent trends in Seismology and Applied Geophysics*, Thessaloniki 1-3 July 1988, 186-193

Turcotte, D. L and Schubert, G. 2002. *Geodynamics*; Second Edition. New York: John Wiley & Sons. ISBN 0521666244.

Turcotte, D.L. 1991. *Fractals and Chaos in Geology and Geophysics*. Cambridge University Press.

Turcotte, D.L. and Schubert, G. 2001. Geodynamics, 2nd ed., Cambridge University Press

UCSB (2012); The University of California, Santa Barbara, http://www.library.ucbs.edu/

Udias, A. and Mezcua, J. 1997. *Fundamentos de Geofisica*. Alianza Universidad Textos, 476 pp.

USGS 2010. United States Geological Survey, Menlo Park, California, *United States Geological Survey report on the earthquake*, *Earthquakes and Plate Tectonics*. National Earthquake Information Centre.

Utsu, T. 1965. A method for determining the value of b in the formula logN=a-bM showing the magnitude-frequency relation for earthquakes. *Geophysical Bulletin Hokkaido University*. 13: 99-103.

Wakita, H. Nakamurai, Y. K. Notsu, K. Noguchi, M. and Asada, T. 1980. Radon Anomaly: A Possible Precursor of the 1978 Izu-Oshima-kinkai Earthquake. *Science* Vol. 207 no. 4433 pp. 882-883

Wang, Q. and Jackson, D. D. 2008. Spatial variation of seismic parameters and seismic properties in California. *American Geophysical Union*. Fall Meeting 2008.

Warren, N.W. and Latham, G.V. 1970. An experiment study of thermal induced microfracturing and its relation to volcanic seismicity. *Journal of Geophysical Research*. 75: 4455-4464.

Wegener, A. 1966. *The origin of continents and oceans*. Courier Dover. pp. 246. ISBN 0486617084.

Wiemer, S. and Benoit, J. 1996. Mapping the b-value anomaly at 100 km depth in the Alaska and New Zealand subduction zones. *Geophysics Research Letter*. 23: 1557-1560.

Wiemer, S. and Wyss, M. 1997. Mapping the frequency-magnitude distribution in asperities: An improved technique to calculate recurrence times? *Journal of Geophysical Research*. 102, 15115-15128.

Wiemer, S. McNutt, S.R. and Wyss, M. 1998. Temporal and three-dimensional spatial analyses of the frequency-magnitude distribution near Long Valley Caldera, California. *Geophysical Journal International*. 134: 409-421.

Wiemer S. and Wyss M. 2002. Spatial and temporal variability of the b-value in seismogenic volumes: An overview. *Advances in Geophysics*. 45, 259-302.

Williams, G. 1997. *Chaos Theory Tamed* Joseph Henry Press, Washington D.C. Chapter 19.

Wolf, A. Swift, J. B. Swinney, H.L. and Vastano, J.A. 1985. Determining Lyapunov exponents from a time series, *Physica* D 16, 285.

Worth, R. 2005. *The San Francisco Earthquake*. Facts On File Incorporated (Environmental Disasters) New York, ISBN 0-8160-5756-7, pg 70-72.

Wyss, M. 1973. Towards a physical understanding of the earthquake frequency distribution. *Geophys. J.R. astr. Soc.*, 31: 341-359.

Wyss, M. 1991. Second round of evaluation of proposed earthquake precursors, Pure and Applied Geophysics 149, 3-16

Wyss, M. 1997a. Cannot earthquakes be predicted? *Science*, 278, 487-488.

Wyss, M. 1997b. Not yet, but eventually, Geophysical Institute, University of Alaska, Fairbanks, Alaska, USA. *Nature Debate*, Nature© Macmillan Publishers Ltd 1999 Registered No. 785998 England.

Yang, W. Ding, E.J. and Ding, M. 1996. Universal scaling law for the largest Lyapunov exponent in coupled map lattices. *Physics Review Letter*. 76 1808–11.

Yeats, R. S. Kerry, S. and Clarence, R. A. 1997. *The Geology of Earthquakes.* Oxford University Press: Oxford.

Yegulalp, T. M. and Kuo, J. T. 1974. Statistical prediction of occurrence of maximum magnitude earthquake. *Bulletin of Seismological Society of America*. 64, 393-414.

Yenier1, E. Erdoğan1, Ö. and Akkar, S. 2008 Empirical relationships for magnitude and source to site distance conversions using recently compiled Turkish strong- ground motion database. *The 14th World Conference on Earthquake Engineering*. October 12-17, 2008, Beijing, China.

Zeni, A. R. and Gallas, J. A. 1995. Lyapunov exponents for a Duffing oscillator. *Physica* D 89 71–82

APPENDIX

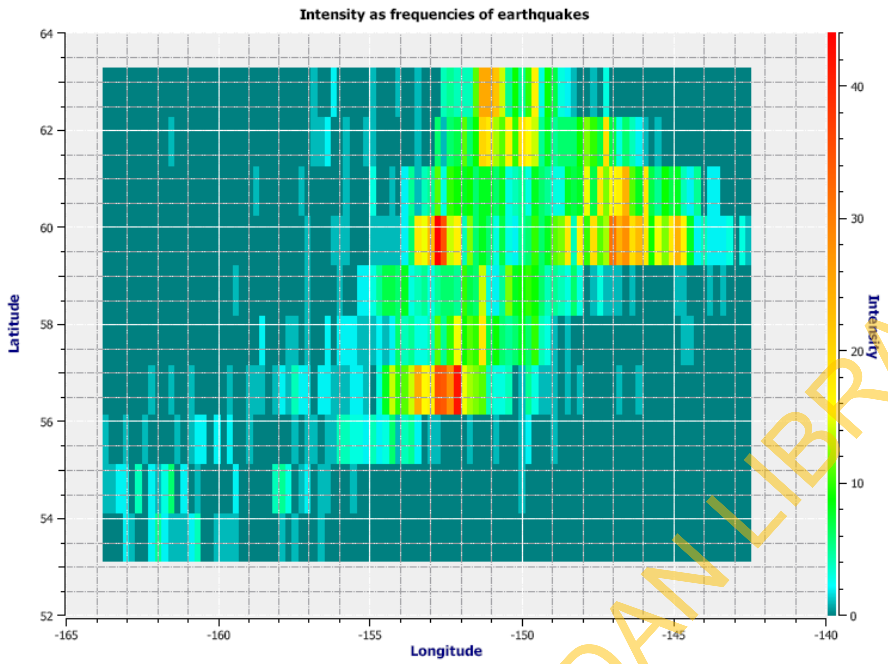

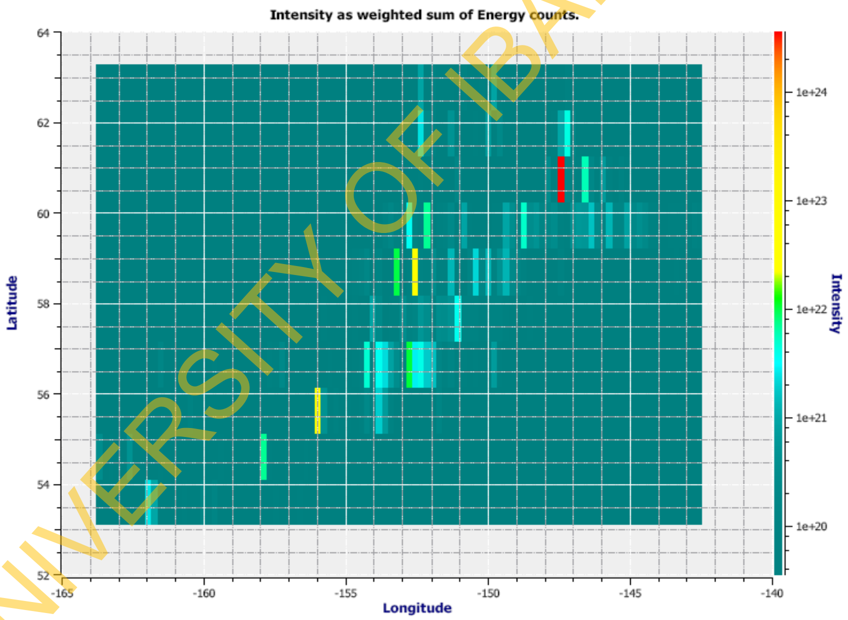

Fig 1; Temporal distribution between 1960 and 1969

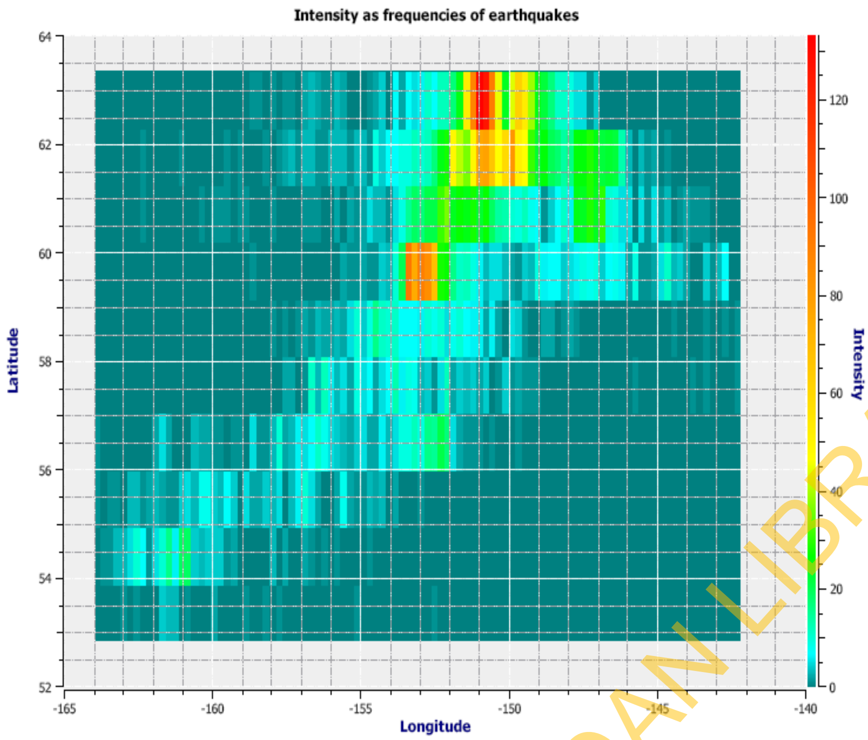

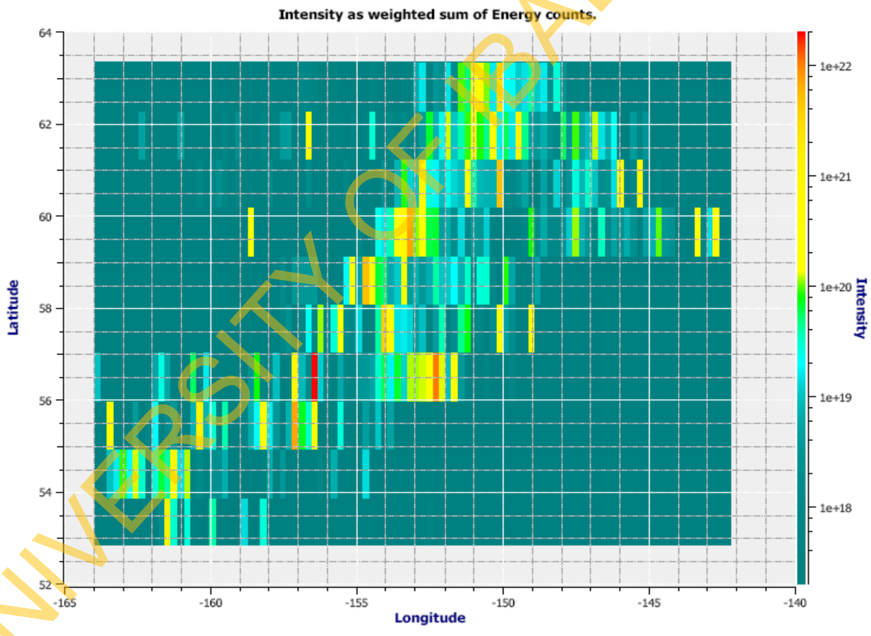

Fig 2: Temporal distribution between 1970 and 1979

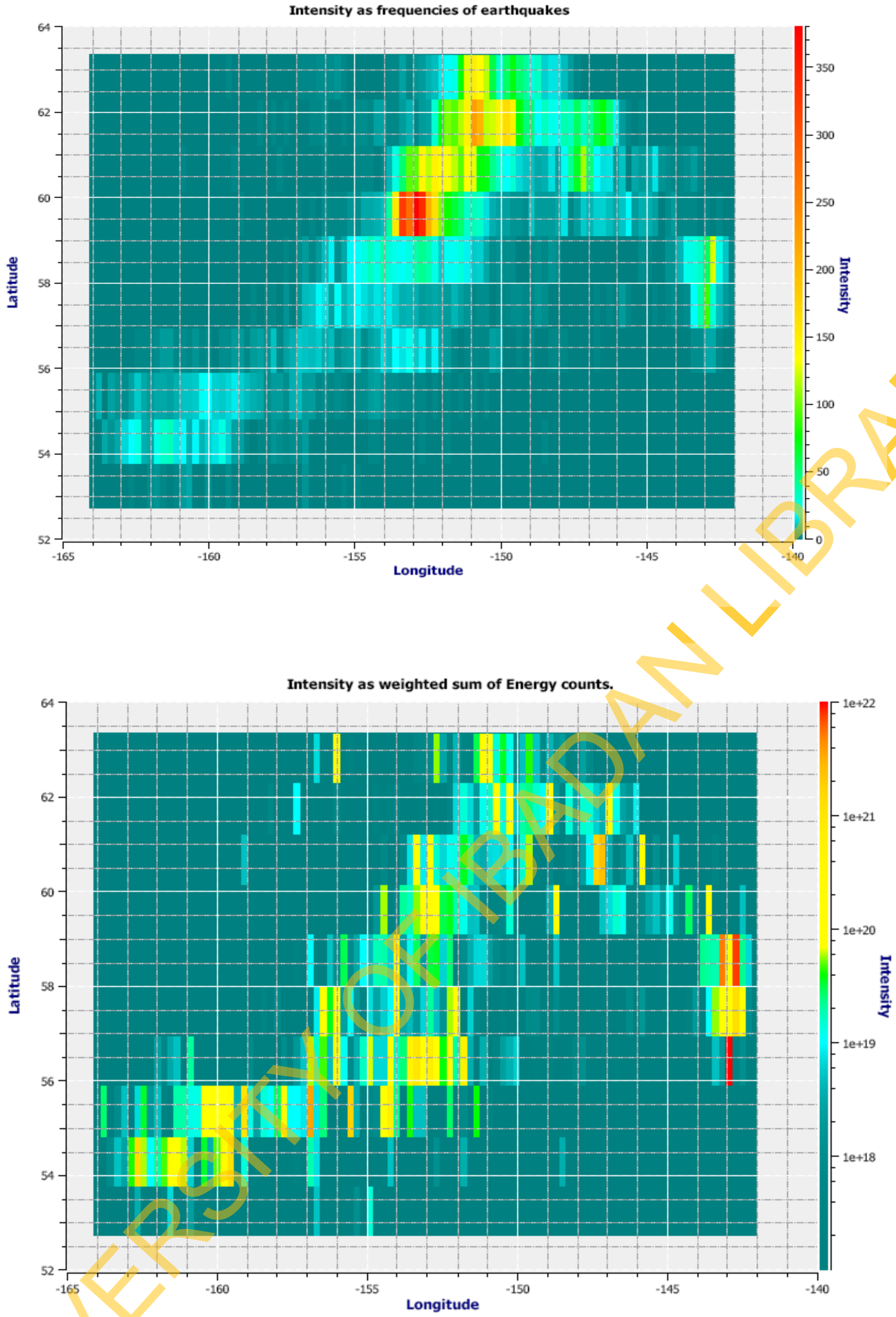

Fig 3: Temporal distribution between 1980 and 1989

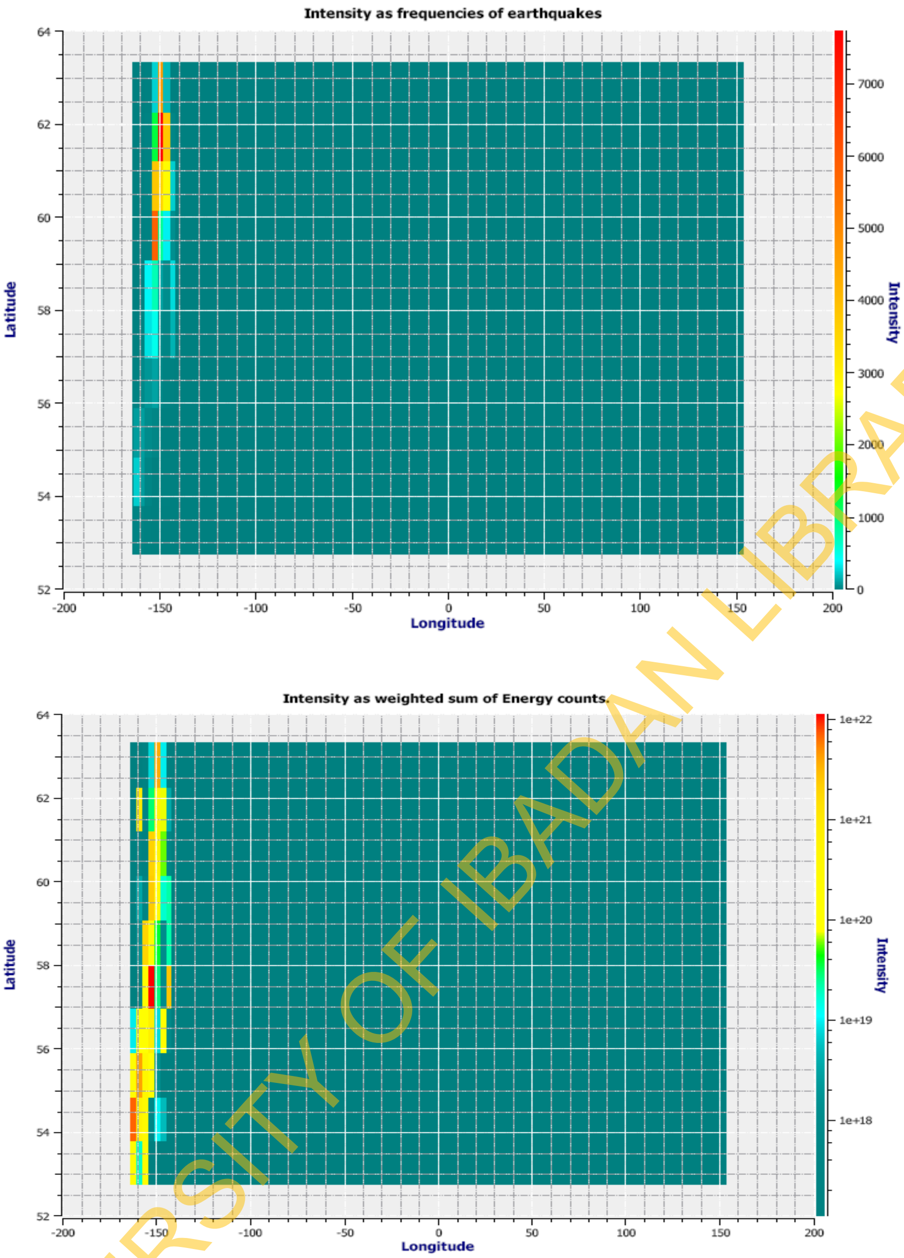

Fig 4; Temporal distribution between 1990 and 1999

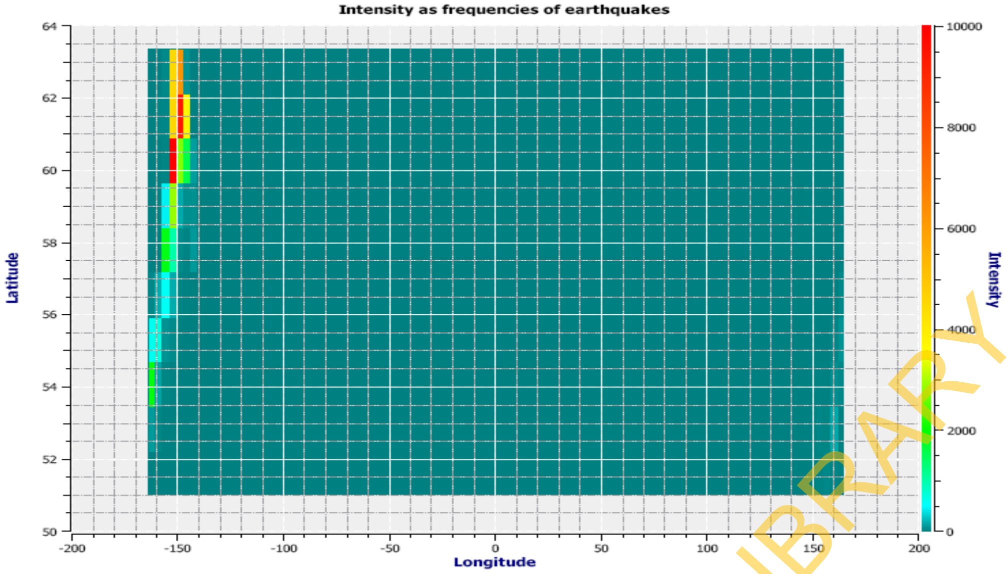

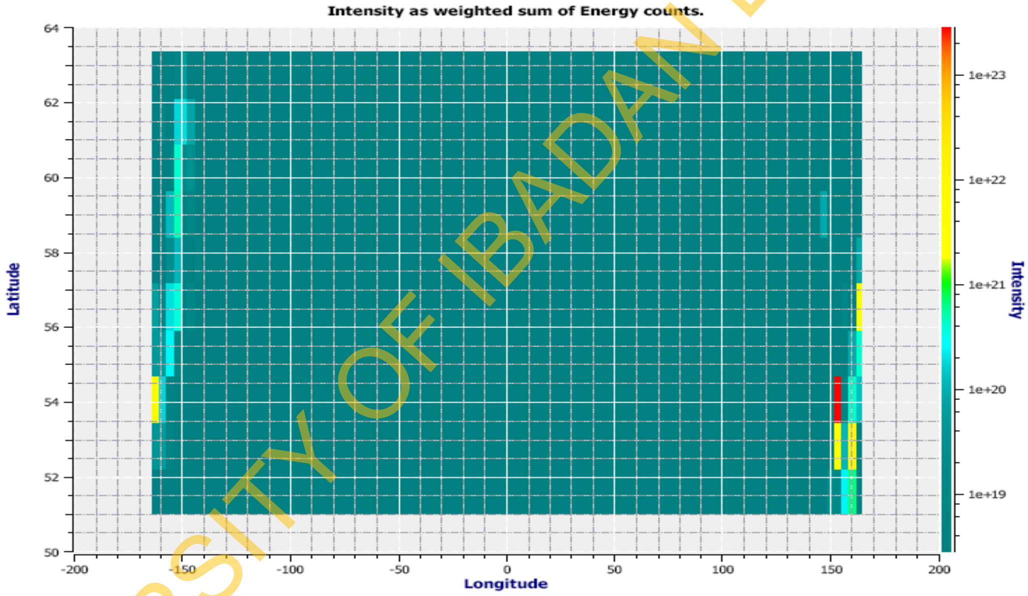

Fig 5: Temporal distribution between 2000 and 2009

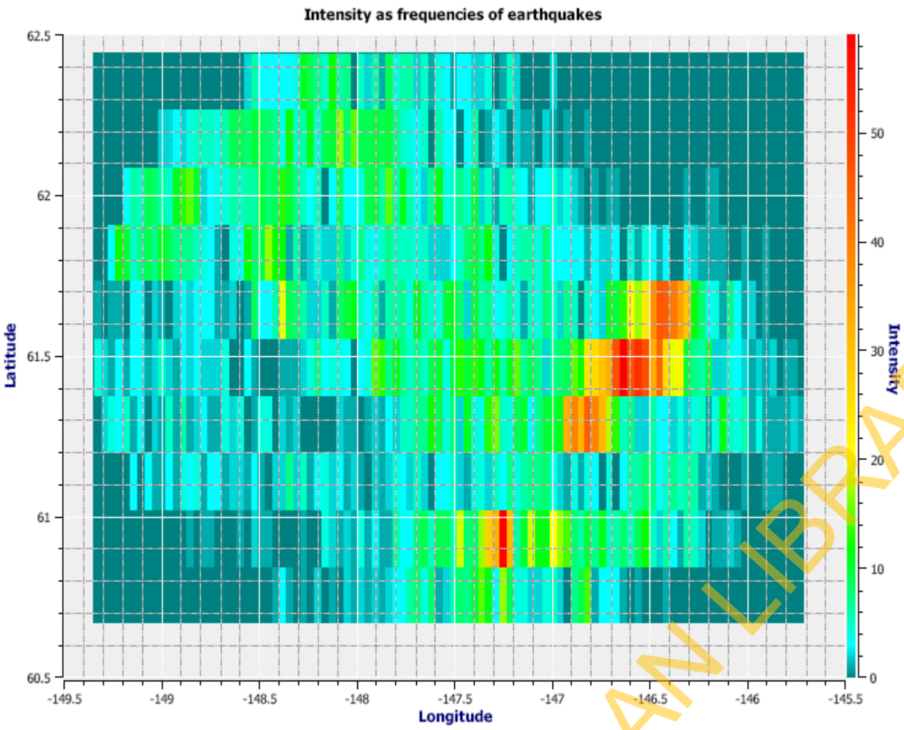

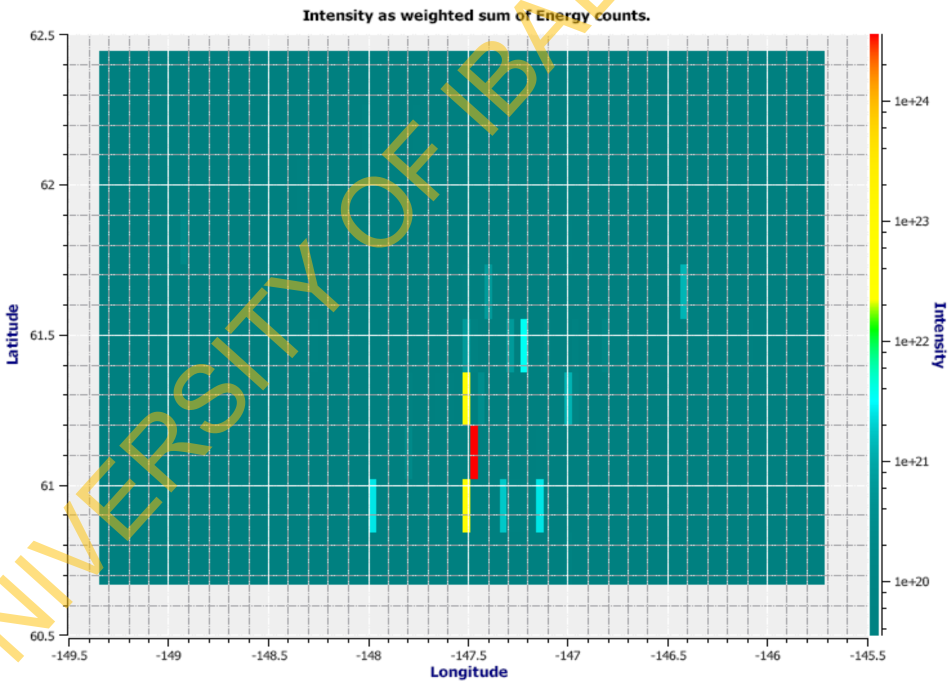

Fig. 6; Spatial distribution for annular grid 0-100km from the epicenter

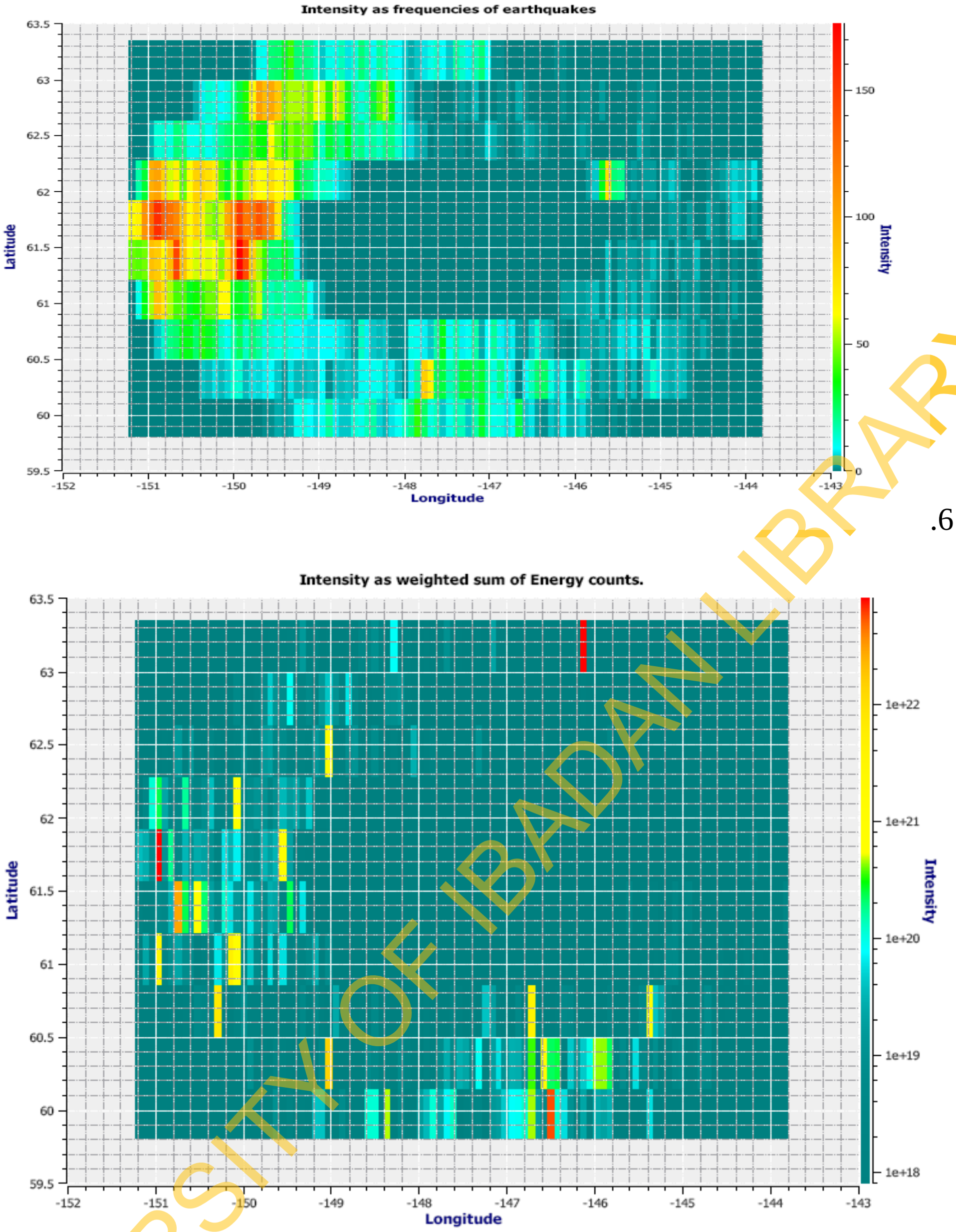

.6

Fig 7; Spatial distribution for annular grid 100-200km from the epicentre

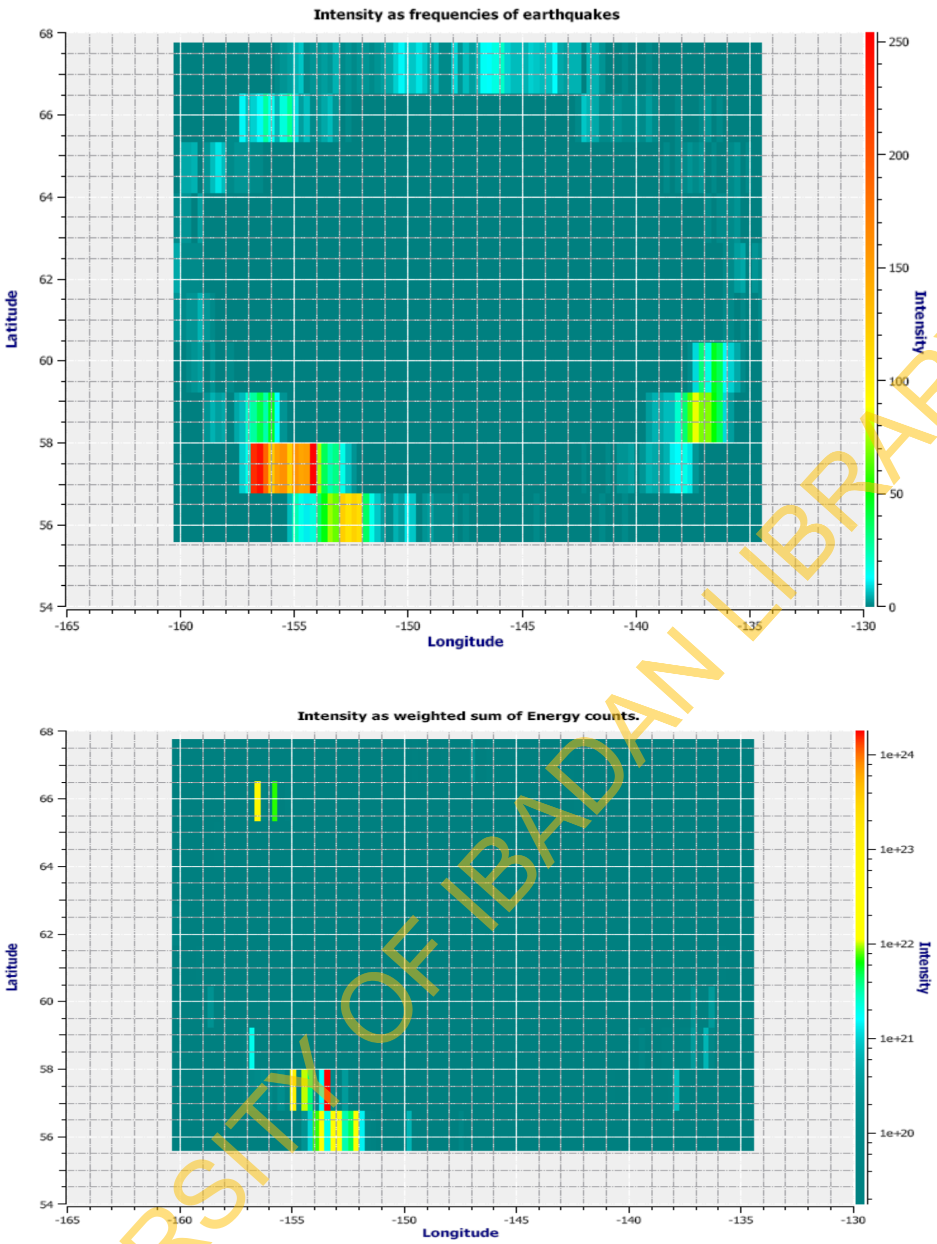

Fig 8: Spatial distribution for annular grid 600-700km from the epicentre